CHMC

ORIGIN AND CONTROLS OF DEPOSITION OF THE WHEAL HUGHES AND POONA COPPER DEPOSITS, MOONTA, SOUTH AUSTRALIA.

MARK R. HAFER, B.Sc.

Thesis submitted as partial fulfilment for the Honours Degree of Bachelor of Science

NOVEMBER, 1991

Department of Geology and Geophysics
The University of Adelaide

NATIONAL GRID REFERENCE: MAITLAND SHEET I- 53 / 12 (1: 253 440)

CONTENTS

ABSTRACT

1. INTRODUCTION

1.1 Location and physiography 1
1.2 History of mining 1
1.3 Previous investigations 2
1.4 Aims of the study 3
1.5 Methods 3

2. GEOLOGICAL SETTING

2.1 Regional geology 5
2.2 Lithological descriptions 7
2.2.1 Moonta Porphyry 7
2.2.2 Blue Range Beds 9
2.2.3 Pegmatites 10
2.2.4 Silcrete 10
2.2.5 Calcrete 10

3. STRUCTURE AND METAMORPHISM

3.1 Regional 11
3.1.1 Deformation 11
3.1.2 Structural controls of mineralisation 11
3.2 Wheal Hughes 12
3.3 Discussion 13
3.4 Metamorphism 15

4. MAJOR AND TRACE ELEMENT GEOCHEMISTRY

4.1 Geochemical discrimination 16
4.2 Tectonic setting 16

5. MINERALISATION

5.1 Mineralogy 17
5.2 Wheal Hughes 17
5.2.1 Morphology of mineralisation 17
5.2.2 Mineralogy and textures of primary assemblages 17
5.2.3 Wallrock alteration 18
5.2.4 Oxidised and supergene assemblages 19
5.2.5 Paragenesis 20
5.3 Poona 20
5.3.1 Morphology of mineralisation 20
5.3.2 Mineralogy and textures of primary assemblages 20
5.3.3 Wallrock alteration 21
5.3.4 Oxidised and supergene assemblages 21
5.3.5 Paragenesis 22

6. FLUID INCLUSION STUDY

6.1 Introduction 23
6.2 Sample petrography 23
6.3 Microthermometry- cooling 24

6.4 Microthermometry- heating 25
6.5 Depth and pressure calculations 25

7. SULPHUR ISOTOPE ANALYSES

7.1 Introduction 27
7.2 Sulphur geothermometry 27
7.3 Results 28

8. ELECTRON MICROPROBE ANALYSIS

8.1 Chlorite 29
8.2 Sericite 29
8.3 Tourmaline 30

9. GEOCHEMISTRY OF THE MINERALISING FLUID

9.1 Geochemical modelling 32
9.2 Source for the sulphur 34
9.3 Gold solubility 35

10. GENESIS OF MINERALISATION

10.1 Introduction 36
10.2 Metal/ligand source 36
10.2 Metal transport 37
10.3 Heat source 37
10.4 Metal deposition 38

11. CONCLUSIONS 39

ACKNOWLEDGEMENTS

REFERENCES

APPENDICES:

1. Moonta-Wallaroo lode distribution.
2. Thin section section descriptions.
3. Polished thin section descriptions.
4. Polished block descriptions.
5. Wheal Hughes cross-sections.
6. XRF-Whole rock analyses.
7. XRD-Alteration assemblages.
8. Fluid inclusion analyses.
9. Sulphur isotope analyses.
10. Electron microprobe - chlorite.
11. Electron microprobe - sericite.
12. Electron microprobe - tourmaline.
13. Thermodynamic Equations.
14 Wheal Hughes open pit plan- R.L. 14.7 to 15.9
15 Wheal Hughes open pit plan- R.L. 15.7 to 19.7

FIGURES:

1. Locality map
2. Regional map
3. Cross-section of the porphyry
4. Geochemical discrimination plot - Nb/Y vs SiO_2

5. Geochemical discrimination plot - Zr/TiO_2 vs SiO_2
6. Tectonic setting plot - Y+Nb vs Rb
7. Tectonic setting plot - Y vs Nb
8. Paragenetic sequence
9. Fluid inclusion - Frequency vs T_m
10. Fluid inclusion - Frequency vs T_{fm}
11. Fluid inclusion - Frequency vs T_{hom}
12. Fluid inclusion - T_{hom} vs T_{fm}
13. Sulphur isotope - Wheal Hughes
14. Sulphur isotope - Poona
15. Tourmaline - Ca-Fe(tot)-Mg
16. Tourmaline - Al-Fe(tot)-Mg
17. Tourmaline - CaO-FeO-MgO and Na_2O-Fe)-MgO
18. Tourmaline - $Na_2O/(Na_2O+CaO+K_2O)$ vs $FeO/(FeO+MgO+MnO)$
19 Geochemical plots (a-f).

TABLES:

1. Fluid inclusion classification scheme
2. Chlorite data table

PLATES:

1. Typical Moonta Porpyry (M.P.)
2. M.P. displaying ignimbrite texture
3. Relic primary texture-flattened pumice
4. Relic primary texture-vesicle infill
5. Blue Range Beds overlying the M.P.
6. Pegmatite intrusion into Corunna equivalents, Port Hughes
7. Leighton's lode
8. Minor crenulations
9. Curviplanar "roll" feature
10. Slickenside lineations
11. Boudinage
12. Chalcopyrite and hematite, relic hematite
13. Fractured pyrite and replacements
14. Association of marcasite and carrollite
15. Marcasite contact with pyrite
16. Gold
17. Chlorite association with mineralisation
18. Tourmaline association with mineralisation
19. Hematite network
20. Bornite
21. Carrollite
22. Digenite alteration

ABSTRACT

The Wheal Hughes and Poona mines are situated within the Moonta-Wallaroo copper district on the NW region of Yorke Peninsula approximately 150 km NW of Adelaide, S.A. . Copper mineralisation is hosted by the Moonta Porphyry, a rhyolite/rhyodacite feldspar porphyry of Early Proterozoic age.

The Wheal Hughes and Poona lodes are structurally controlled tabular, en échelon and sheeted fissure veins, which strike 040-050 and have a 45° to 60° westerly dip. Two distinct groups of mineralisation are found to occur at Wheal Hughes: (1) the NE Leighton's lode which closely resembles Poona and is typical of Moonta lodes, and (2) the SW Wheal Hughes lode which is unique to the region, in consisting of a series of parallel veins in close proximity and having extensive wallrock alteration. Mineralisation consists predominantly of chalcopyrite and pyrite with minor components of magnetite, hematite, bornite, marcasite, carrollite, molybdenite and gold.

A genetic model for the mineralisation at Wheal Hughes and Poona is proposed from fluid inclusion and petrographic studies, and sulphur isotope, chlorite and sericite analyses together with thermodynamic modelling. Magmatic hydrothermal fluids enriched in metals migrated towards the surface via fractures, which were possibly formed from the emplacement and subsequent cooling of underlying Proterozoic granites. These fractures provided pathways for the migration of hydrothermal fluids as well as sites for the deposition of the ore bodies. Metal deposition occurred as a consequence of a two step boiling process during fluid ascent along fracture conduits, which involved the separation of gases (+ steam) from the liquid phase. Condensation and oxidation of the gas phase produced acid waters that triggered argillic alteration of the country rocks.

Two possible heat mechanisms generated the hydrothermal system in the Moonta district; the disruption of the geothermal gradient by the intrusion of an igneous body at depth or a dilatancy/fluid diffusion process. In either case, the heat source generated a hydrothermal system which focussed mineralising fluids into dilatant fractures, effectively localising the mineralisation.

FIGURE 1: LOCATION MAP

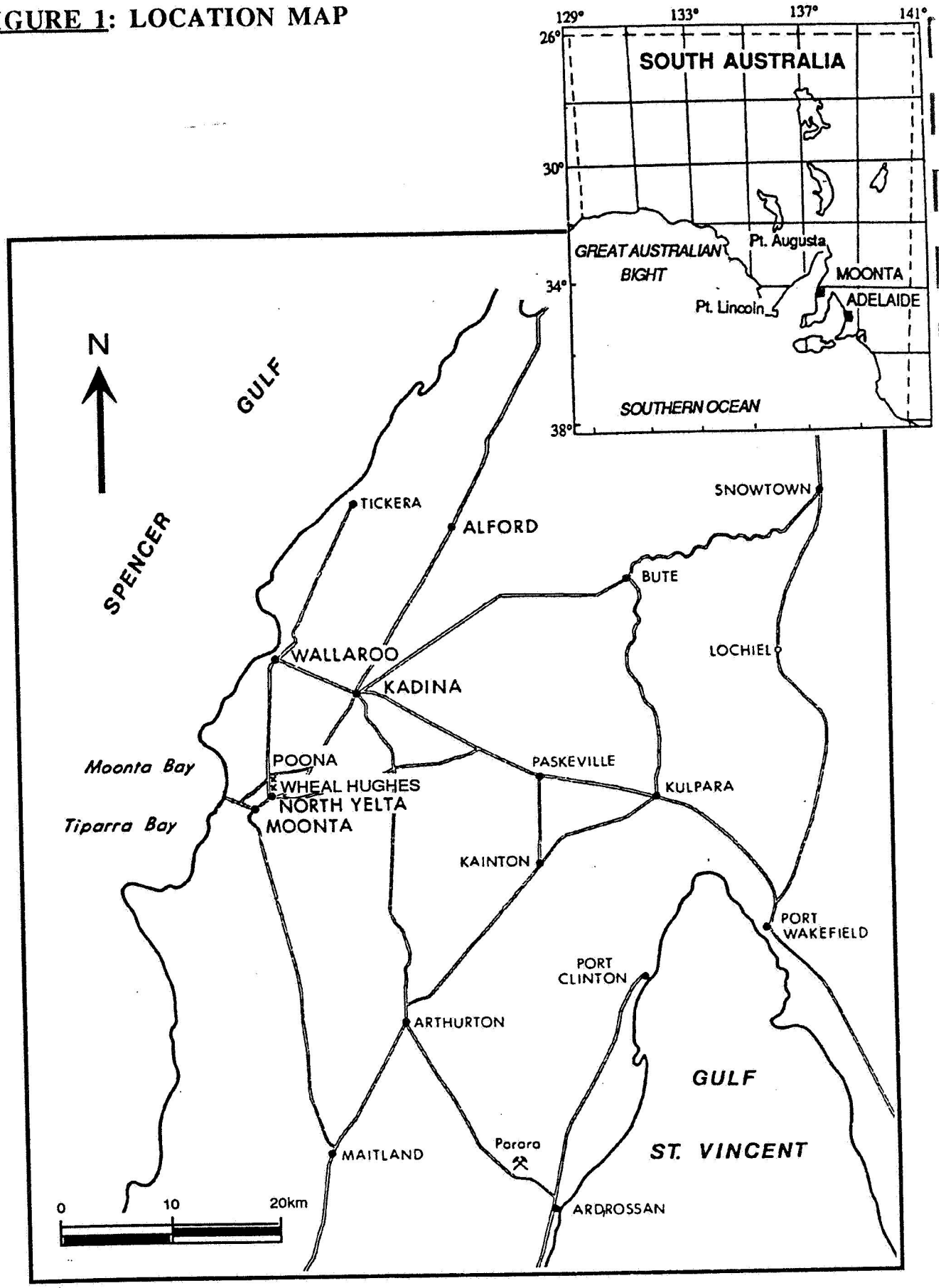

1. INTRODUCTION

1.1 LOCATION & PHYSIOGRAPHY

The Wheal Hughes and Poona mines are situated within the Moonta-Wallaroo copper district (in the hundred of Wallaroo, county of Daly) on the NW region of Yorke Peninsula approximately 150 km NW of Adelaide, South Australia (Figure 1). Wheal Hughes is located immediately north of North Yelta adjacent to the now abandoned Moonta-Wallaroo railway, 3 km NE of Moonta at latitude 34°37'30", longitude 137°02'00" within the Maitland 1:250 000 geological sheet. The Poona mine is located 1.5 km north of Wheal Hughes.

The topography consists of a flat to gently undulating region covered by Cambrian and Tertiary sedimentary units. The plains have an average elevation of 50 to 100m above sea-level and lack any evidence of a surface drainage system.

The temperature averages 18°C with a rainfall of 300 to 400 mm per annum. Native vegetation has been cleared from the region, the land presently being utilized for pastoral and agricultural purposes.

1.2 HISTORY OF MINING

Mining was undertaken by the Moonta Mining Co. within the Moonta district in 1861, with copper production commencing in 1862, following the discovery of copper carbonate on a mound of earth raised by a native wombat. Production of copper at the Wallaroo mines commenced in 1861 by the Wallaroo Mining and Smelting Co., following their discovery late in 1859 under similar circumstances (Pryor, 1962). Falling copper prices resulted in the amalgamation of the principal companies of the two districts in 1889, to create the Wallaroo and Moonta Mining and Smelting Ltd., which in turn absorbed smaller syndicates during its 34 year existence.

The Moonta-Wallaroo district was the most productive copper mining field in South Australia. From the periods of their discovery until 1923, the mines were worked continuously, producing 6,250,000 tonnes of ore yielding 336,000 tonnes of copper, valued at over £20 million (Plimer, 1980). Production ceased in 1923 due to exhaustion of the higher grade ores, decreasing size of the orebodies at depth, expense of mining at depths of nearly 1000 m and the post-war fall in the price of copper (Dickinson, 1953).

Spasmodic exploration was carried out between 1923 and the mid-1950's by the South Australian Department of Mines, Enterprise Exploration and small syndicates which produced 55,327 tonnes of ore, slimes and tailings yielding 2,947 tonnes of copper (Plimer, 1980). In 1959 Western Mining Corporation (WMC) acquired the title to the Wallaroo-Moonta district and from the early 1960's until 1987 they carried out exploration as a joint venture with North Broken Hill Limited.

The Poona and Wheal Hughes deposits were discovered in 1985 and 1986 respectively, the Poona lode being an extension of the original Poona Mine discovered in 1866, and the Wheal Hughes mine situated within the original Wheal Hughes leases on which 3 shafts (Andrew's, Colley's and Cooper's) had been sunk near the eastern boundary during the late 1860's (Rowe, 1963). The leases to these small but economic lodes were sold, and consequently acquired in 1987 by the present operators, Moonta Mining NL, a joint venture between Melita Mining NL and Amalgamated Syndicate NL (WMC, 1987). Open-cut mining commenced at Poona in 1988 (from 1988-1990 16,426.3 tonnes of concentrate were produced with 29.9% copper and 10.2 g/t gold) and was subsequently developed into an underground operation in 1990, whereas the Wheal Hughes open-cut operations began early 1991.

1.3 PREVIOUS INVESTIGATIONS

The underlying geology in the Moonta-Wallaroo district is almost wholly masked by travertine. Because of the sparseness of outcrops very few detailed geological investigations have

been carried out and investigations have been limited to "the evidence afforded by scattered workings and occasional field stones" (Jack, 1917).

The only comprehensive geological survey of the Moonta and Wallaroo district was published by Jack (1917). Dickinson (1942) attempted to construct a structural model from the observed relationships of the lode structures and Dickinson (1953) collated all the existing knowledge available for a treatise on Australian ore deposits.

More recent studies within the Moonta-Wallaroo province include:

McBriar (1962)- Copper mineralisation at Moonta & Wallaroo.

Lemar (1975)- Origin of the Moonta Porphyry.

Lynch (1982)- Interpretation of the geology and mineralisation.

Gerdes (1983)- Geophysical and geological interpretation.

Janz (1990)- Mineralogy and paragenesis of the Poona mine

1.4 AIMS OF THE STUDY

The main aims of this study were:

(1) to map two different levels of the Wheal Hughes open-cut at 1:500 scale as mining of the deposit proceeded.

(2) to investigate the mineralisation by means of mineralogical and petrological studies, fluid inclusion measurements, mineral analyses and sulphur isotope analysis.

(3) to propose a model for the origin and depositional constraints of the ore.

1.5 METHODS

The methods of this study have included:

Field studies:

(1) Detailed plan-mapping at 1:500 scale of the Wheal Hughes open-cut.

(2) Examination of diamond drill core.

(3) Collection and examination of samples from the Wheal Hughes open-cut and Poona underground mines.

Laboratory Studies:

(1) Petrographic examination of polished-thin sections, normal thin sections and polished blocks.

(2) Electron microprobe analysis of polished thin-sections to determine the composition of chlorite, sericite and tourmaline.

(3) Sulphur isotope analysis of 25 samples of chalcopyrite, 9 samples of pyrite and 1 sample of bornite.

(4) Fluid inclusion measurements of 12 quartz samples.

(5) XRF and XRD analyses of the Moonta Porphyry and its associated alteration, from samples obtained from the Poona and Wheal Hughes mines.

(6) Thermodynamic calculations to model the conditions of mineralisation.

2. GEOLOGICAL SETTING

2.1 REGIONAL GEOLOGY

The regional geology of northern Yorke Peninsula is largely interpreted from geophysical and drill-hole data, due to the paucity of outcrop (Figure 2).

The Moonta-Wallaroo district is situated within the Moonta Subdomain of the Gawler Craton. Geological evolution of the Gawler Craton extended from Late Archaean to the present, experiencing three major megacycles (Parker, 1990). Copper mineralisation is associated with the third of these megacycles and is hosted by the Moonta Porphyry and the Doora Schist, at Moonta and Wallaroo respectively. Though the Moonta Porphyry and Doora Schist are the oldest basement rocks identified in the Moonta-Wallaroo district, Parker (in Plimer, 1980) inferred a regional basement consisting of the Hutchinson Group sediments and plutonic Lincoln Complex, unconformably overlain by metasediments (Doora Schists) and intruded by the Moonta Porphyry (Figure 3).

The Moonta Porphyry is a porphyritic, felsic composite rock whilst the Doora Schist is a schist-gneiss-quartzite-amphibolite sequence (Parker, 1990). The Moonta Porphyry and the Doora Schist have been correlated with the Wardang Volcanics (30km south of Moonta), as they exhibit similar textural and fabric characteristics (Webb et al., 1986). A zircon age of 1741 ± 9 Ma (Fanning et al., 1988) for the Moonta Porphyry, and similarities in texture and fabrics have resulted in the Myola Volcanics and the McGregor Volcanics of Eyre Peninsula being considered as Early Proterozoic equivalents (Parker, 1990).

Sedimentation late in the Early Proterozoic deposited the Wandearah Metasiltstone unconformably upon the basement. The Wandearah Metasiltstone unit is a deformed and recrystallised sequence of hematitic siltstones, interbedded with the basic Willamulka Volcanics on the northern Yorke Peninsula (Parker, 1986). Rb-Sr dating produced a metamorphic age of 1561 ± 30Ma (Webb et al., 1986).

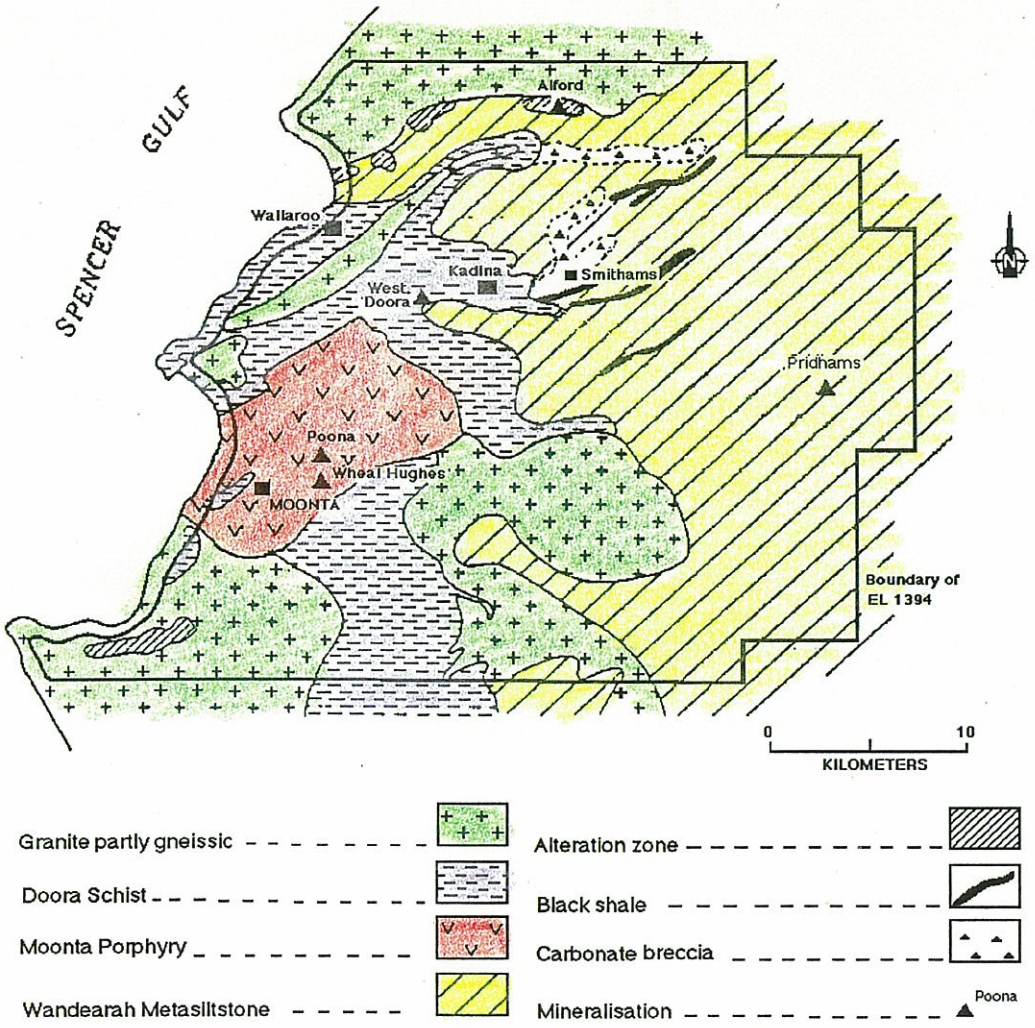

Figure 2: Regional geology map, after WMC (1987)

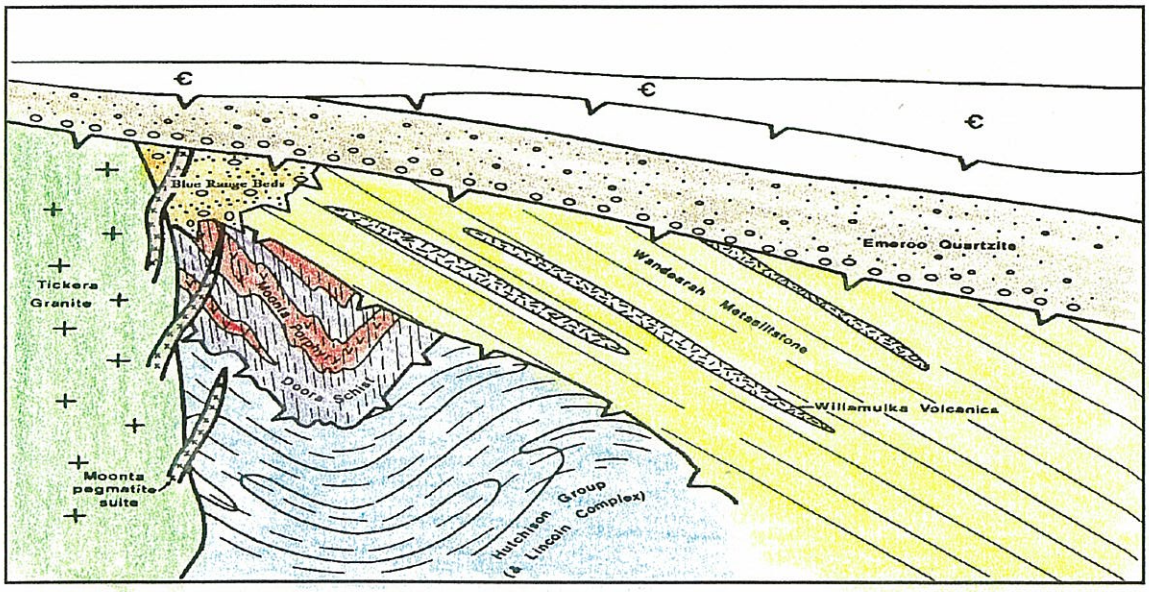

Figure 3: Schematic diagram of rock relationships of the Moonta Subdomain, modified after Parker (in Plimer, 1980).

An unmetamorphosed conglomeratic unit within the Moonta-Wallaroo district, interpreted as Corunna Conglomerate equivalent, the Blue Range Beds (see section 2.2.2), was deposited unconformably upon the Early Proterozoic basement and metasiltstone units. The Blue Range Beds are an intra-continental, shallow water sequence broadly synchronous with the Gawler Range Volcanics (Webb et al., 1986).

Following the Kimban Orogeny (1950-1700Ma) granite plutons of the Tickera and Arthurton suites were emplaced north and south of Moonta, respectively, and are considered to be Middle Proterozoic equivalents of the Hiltaba Suite on Eyre Peninsula. A wide range of ages have been obtained for these suites:

(1) Rb-Sr → Tickera 1215 ± 544 Ma (Webb et al., 1986).

(2) K - Ar → Moonta Area Granites 1470-1530 Ma (Webb, 1979).

(3) U - Pb → Adamellite (Arthurton) 1585 ± 3 Ma (Creaser, 1989).

U-Pb dating by Creaser (1989) has so far been the most reliable technique employed in dating these granites. Therefore, 1585 ± 3 Ma is the most probable representative crystallisation age for the anorogenic granites in the Moonta district. Emplacement and subsequent cooling of a granite batholith has been considered by Jack (1917) to have generated the fractures within the basement rocks, which localised subsequent deformation (faulting and shearing). Creaser (1989) noted several small shear zones transgressing the granites, suggesting either a post-intrusive deformational event related/unrelated to mineralisation or a late intrusive feature. The fractures at Moonta and Wallaroo were subsequently mineralised. Many theories relating to the source of the mineralisation have been proposed, but this remains a controversial issue. The fractures/shears in the Moonta district generally dip 40° to 65°NW and strike NW - SE in concentric arcs parallel to the Moonta Porphyry body extending over 3 km. (Jack, 1917; Dickinson, 1942). The Wallaroo district has three lode shears: (1) striking 090 to 120, dipping 75°S,(2) striking 030 to 045, dipping 70°NW, and (3) striking NW, dipping south westerly (Jack, 1917).

Intrusive throughout the region are numerous pegmatite dykes of Mid-Proterozoic age. Rb-Sr dating suggests an age of ca. 1400-1450 Ma (Webb et al., 1986). These pegmatites are a post or late granitic intrusive feature (Plimer, 1980) and Parker (in Plimer, 1980) suggests that they are a late stage fractionation product of the Mid-Proterozoic granites within the region (Fig. 3). The lodes in the Moonta-Wallaroo district have a pegmatitic and/or quartzose composition, with mineralisation confined to veins and veinlets or disseminated throughout the country rock. According to Dickinson (1953) cupriferous solutions accompanied the intrusions and were subsequently deposited within the shear zones.

Since the Middle Proterozoic the Gawler Craton has not been subjected to any major orogenic event. It has remained relatively stable with thin, widespread, continental sediments being deposited during the Late Proterozoic and Cambrian (Parker, 1990). Subsequent tectonic uplift and gentle folding took place, followed by erosion (Jack, 1917). A marine transgression during the Tertiary resulted in the deposition of marls, sandstone, and clays. A continuous Quaternary sequence, including the Pleistocene laterites and Recent kunkar, dunes and clays (Crawford, 1965), was deposited and effectively conceals the basement units.

2.2 LITHOLOGICAL DESCRIPTIONS

2.2.1 MOONTA PORPHYRY

The Moonta Porphyry is a massive red-brown to pink feldspar porphyry of rhyolite/rhyodacite composition (section 4). Geophysical surveying and drill-hole data has defined a 30 km^2 tear-drop shaped sub-crop, forming the basement in the Moonta district (Fig. 2). Mineralisation is hosted by the porphyry within fissures and associated shear zones (section 3). Brittle deformation resulted in the formation of joints and fissures within the host rock, and these open fractures localised the ductile shears, as evidenced by slickenside lineations and mineral lineations which define a steeply dipping foliation.

The Moonta Porphyry is a composite igneous rock which has been described by Lemar (1975) as a sequence of comagmatic ash flow tuffs and tuff breccias, which have been intruded by microgranitic bodies. Samples of the Moonta Porphyry from Wheal Hughes and Poona display an ignimbrite texture of a welded tuff, closely resembling the ash flow tuff described by Lemar (1975).

Euhedral to subhedral glomeroporphyritic and isolated (possibly resorbed) alkali feldspar phenocrysts comprise up to 10% of the total rock and are randomly distributed throughout an aphanitic groundmass, comprised of quartz intergrown with feldspars (Plate 1). The phenocrysts are relatively pristine and are predominantly sodic in composition. The relatively high potassic content in the whole rock analyses is due to potassic feldspar intergrown with quartz within the groundmass. The groundmass is very fine grained and has been metamorphically recrystallised, suggesting that it was originally extremely fine grained (Lemar, 1975). The red colouration of the porphyry is possibly due to the oxidation of iron within the K-feldspars (K. Stewart, pers. comm.) or ferro-magnesium minerals.

A foliation is defined by green to green/brown laths of chlorite and chloritised biotite. Biotite is a recrystallisation product of primary igneous glass and chloritisation of the biotite is evident from textures, interference colours and compositional data of electron microprobe analyses. Pink to brown phenocrysts and lenticular fragments in sample 953-051 (Plate 2) have an orientated distribution within the groundmass and may represent an ignimbrite texture of a welded tuff. Sub-parallel, linear quartz "stringers" with irregular boundaries are found transgressing the groundmass and wrapping around feldspar phenocrysts (Plate 3); these "stringers" may represent pumice fragments that have been flattened during the consolidation of the tuff. Larger fragments consisting of chlorite clots and coarse quartz and feldspar grains are found distributed in the matrix (Plate 4) and resemble infilled vesicles, which have been subsequently flattened.

Previous workers have proposed a variety of origins for the Moonta Porphyry. Ward and Jack (1912) claimed that there was "no definite evidence to show whether the intrusive or the

extrusive phase of igneous activity is represented...". Jack (1917), Dickinson (1942) and Janz (1990) proposed an intrusive origin for the porphyry. McBriar (1962) concluded that it was extrusive. Callen (1966) described the porphyry as a product of metamorphic differentiation and/or metasomatism of a pre-existing sediment (in Lemar, 1975) and Lemar (1975) and Lynch (1982) interpreted the porphyry as a high level intrusion-extrusion. An extrusive origin for the porphyry in the vicinity of Wheal Hughes and Poona is proposed, based upon the fine grained groundmass, random distribution of granoblastic phenocrysts and the relict primary textures.

2.2.2 BLUE RANGE BEDS

An unmetamorphosed conglomeratic unit interbedded with sandstone is found at Wheal Hughes, unconformably overlying the Moonta Porphyry at the SW and W ends of the open-cut. A quartzite conglomerate unit was first described by Ward and Jack (1912) at Wheal James, which is approximately 1 km north of Wheal Hughes.

At Wheal Hughes the conglomerate is an overlying planar unit with a 6°-10° dip towards the west (Plate 5). It displays jointing and is displaced by a series of shears in the SW face of the open-cut and is intruded by quartz veins. These features suggest that it was deposited prior to the regional shearing of the Moonta Porphyry. Further constraints are established from equivalent sedimentary units cropping out north of the Port Hughes jetty, where pegmatites are intrusive into the sandstone (Plate 6). This relationship requires a Mid-Proterozoic age for the sandstone/conglomerate and it has been correlated with Corunna Conglomerate equivalents (A. J. Parker pers.comm.). The interpretation is based upon the distribution of Corunna Conglomerate equivalents (termed the Blue Range Beds by Flint and Parker, 1981) cropping out across the full width of central Eyre Peninsula, the distribution suggesting an east-west trending basin of deposition. When this trend is extrapolated to northern Yorke Peninsula it correlates with the coastal outcrops found at Port Hughes and at Wheal Hughes.

Sedimentary units at Wheal Hughes have been intensely kaolinised and silicified, effectively concealing the original textures and sedimentary structures. The feldspathic sandstone

is massive, medium to coarse grained with a considerable kaolin component, as a result of alteration of the feldspars. The conglomerate is a massive unit containing rounded to sub-angular quartz clasts (5 - 20 mm) within medium to coarse quartzite and kaolinised feldspathic matrix.

2.2.3 PEGMATITES

Coarse-grained, feldspar-tourmaline-quartz mineralised and unmineralised pegmatite veins and pods are found subvertically transecting Moonta Porphyry. Disseminated iron oxide mineralisation is commonly associated with the potassium feldspar component and minor copper sulphides are intimately associated with the quartz component. Previous investigations in the Wallaroo-Moonta district and observations in the Wheal Hughes open-cut, indicate that the pegmatites and quartzose lodes are separate bodies, with no evidence of mineralised/unmineralised pegmatites transecting the main lode.

2.2.4 SILCRETE

Within the Wheal Hughes open-cut silcrete is observed at the contacts of the Moonta Porphyry and the Blue Range Beds with the overlying clay and calcrete. The silcrete consists of a sub-rounded conglomerate containing quartz clasts within a red/green siliceous cement.

2.2.5 CALCRETE

The calcrete/kunkar horizon in the Moonta district overlies Tertiary clays undifferentiated according to age and origin (Maitland Map; 1:253 440, Sheet I-53/12, 1957). It is well exposed in the Wheal Hughes open-cut where it is overlain by clays and Recent soils (Plate 5).

Plate 1: Typical Moonta Porphyry sample (953-063) from the Wheal Hughes open-pit mine. Pink, subhedral to euhedral feldspar phenocrysts randomly distributed within an aphanitic groundmass.

Plate 2: Moonta Porphyry sample (953-051) from the Wheal Hughes mine, displaying an ignimbrite texture.

Plate 3: Transmitted light photomicrograph of a Moonta Porphyry sample (953-051) from the Wheal Hughes mine. Quartz stringer wrapping around feldspar (F) phenocrysts embayed in a very fine grained matrix, resembling flattened pumice fragments.

Plate 4: Transmitted light photomicrograph of a Moonta Porphyry sample (953-000) from the Wheal Hughes mine. Quartz (Q) and chlorite (Cl) clots within a fine grained feldspar/quartz matrix, resembles infill of a vesicle which has been subsequently flattened.

Plate 5: Blue Range Beds unconformably overlying the Moonta Porphyry at the SW end of the pit, Wheal Hughes. Pit face is approximatey 20m in height.

Plate 6: Light coloured pegmatite intrusion into a fine to medium grained sandstone unit of the Corunna Conglomerate equivalents at Port Hughes.


cm
1

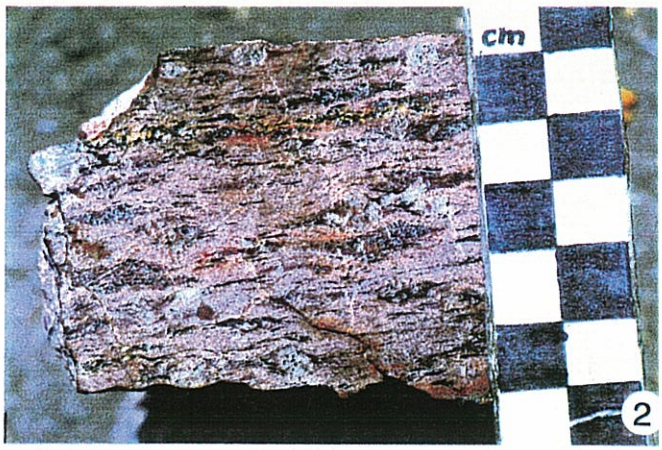
cm
2

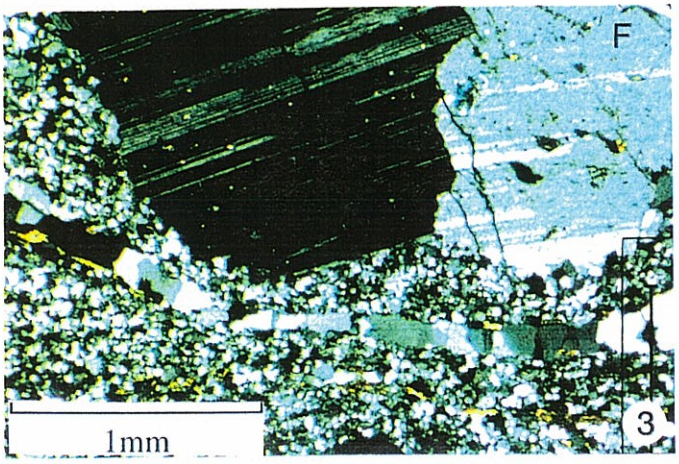
F
1mm
3

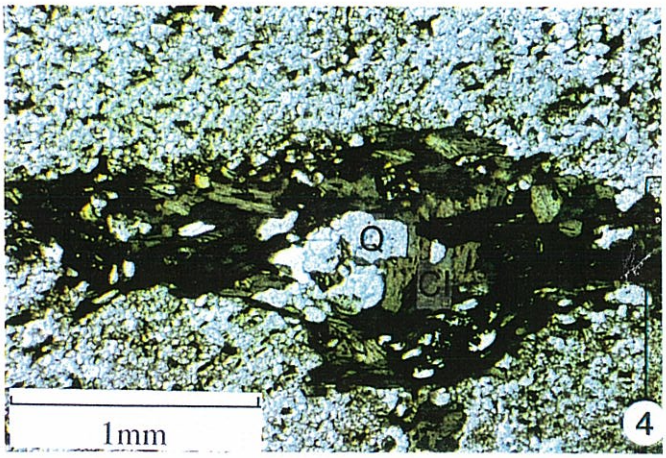
Q
Cl
1mm
4

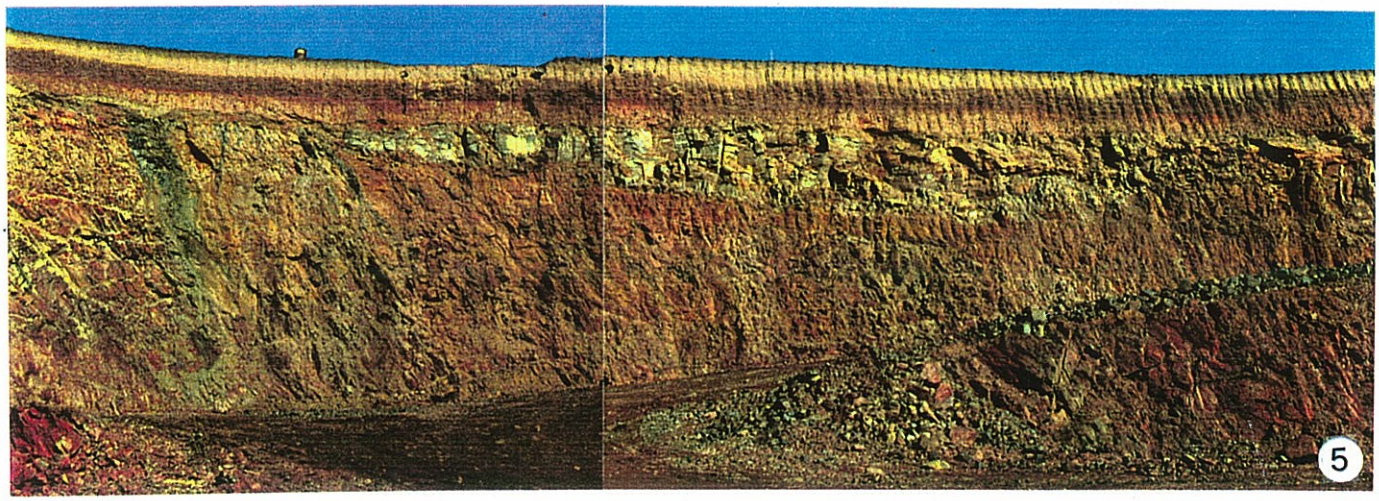
5

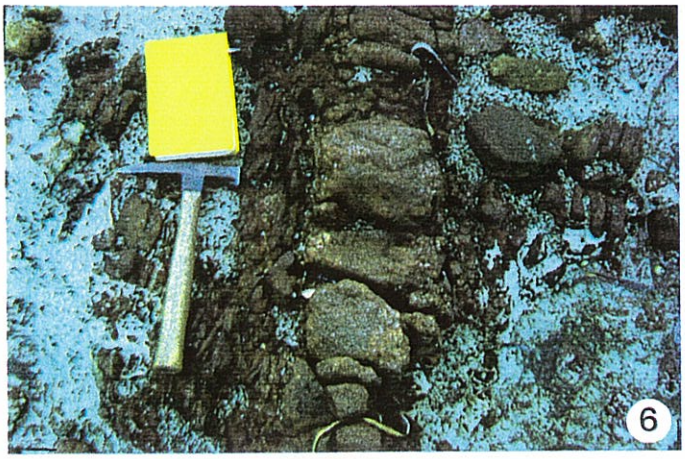
6

3. STRUCTURE AND METAMORPHISM

3.1 REGIONAL

3.1.1 DEFORMATION

Three main phases of deformation have been recognised in the Gawler Craton, viz. D_1 and D_2 dated between 1850 and 1650 Ma and D_3 dated at 1650-1540 Ma (Glen et al., 1977). Deformation in the Moonta Subdomain (Parker, 1990) is characterised by D_3, involving recrystallisation of quartz and feldspar, low grade metamorphism and open, upright folding. D_3 deformation in the Gawler Craton is broadly synchronous with the intrusion of granites (Glen et al., 1977). In the case of the Moonta subdomain, the Arthurton and Tickera granites are synchronous with the D_3 event.

3.1.2 STRUCTURAL CONTROLS OF MINERALISATION

The lodes in the Moonta district are tabular fissure veins hosted by fractures in the competent and brittle Moonta Porphyry. The principle lodes are arranged along three main zones of weakness, in concentric arcs parallel to the length of the Moonta Porphyry (Appendix 1), with a N-S to NE-SW strike and a 40° to 65° westerly dip (Jack, 1917).

Dickinson (1942) had carried out a detailed structural analysis of the lodes and recognised 5 components of the fracture system:

(1) Main Lode Shears- strike 030 and dip 60°W

(2) West Lode Shears- strike 045 and dip 60°W

(3) Strike Faults- strike 030 dipping 45°W

(4) Crosscourses- strike NW and dip SW

(5) E-W Transverse Faults

3.2 WHEAL HUGHES

Since Dr. R. L. Jack's investigation in 1917, no comprehensive studies have been made of the mineralisation and it's association with the country rock. Recent mining operations at Moonta have provided the opportunity to further examine the field relationships of the mineralisation. An investigation of the Wheal Hughes operation in this study expands upon the recent study carried out on the Poona operation by Janz (1990).

The Wheal Hughes lodes are tabular, en échelon, sheeted fissure veins. The lodes strike 040-050 and dip 50°-60°NW. A strike length of 140m has been defined, although the orebody is open along strike with an undetermined persistence with depth.

Two distinct groups of mineralisation are found to occur at Wheal Hughes, the NE Leighton's lode and the SW Wheal Hughes lode. The NE and SW lodes are separated by 5 to 10m of barren, altered country rock (Moonta Porphyry) and differ with respect to the intensity and extent of alteration (hydrothermal and supergene). Leighton's lode is a 40m single, 2 to 3m wide body which thins out to the NE and is offset by 3m by an apparent cross-cutting fault (Appendix 4) (Plate 7). The Wheal Hughes lode is a series of 3 to 4 parallel orebodies which are 2 to 5m wide and have an approximate strike length of 60 to 65m (Appendix 4). Alteration of the wall rocks adjacent to the Leighton's orebody is on the centimetre scale, whilst the alteration associated with the Wheal Hughes lode is more intensive and extensive, and developed up to several metres either side of the lodes (Appendices 14 and 15). The extent of alteration and the close association of a series of parallel veins make Wheal Hughes unique to the Moonta district.

The prominent structural features associated with the ore-bodies are: (1) intense jointing, (2) curviplanar joints and associated chlorite and green biotite lineations (3) episodic fracturing and mineralisation.

Brittle deformation resulted in the formation of dilatant fractures and jointing of the country rock. These dilatant fractures provided a conduit for mineralising fluid, which may have

intensified the fracturing of the wallrock. The lodes are subparallel to the prominent steeply dipping, north easterly striking joint plane, which suggests that this provided the structural control on the mineralisation.

The predominant joint plane, which subparallels the lodes, displays prominent curviplanar features in the form of "undulations and rolls" (more so for the footwall than the hanging wall) (Plate 8, 9). The morphology of the crenulations and en échelon nature of the lodes suggest a dextral shear sense of movement.

Mineral lineations and slickensides are found associated with this curviplanar fracture. Mineral lineations are found to plunge steeply down-dip, subparallel to the joint plane which controls mineralisation. The slip surfaces strike 040-050 and dip moderately to steeply westward. Slickenside lineations are found on these slip surfaces, with the striations plunging steeply westward (Plate 10). The slickensides and the "roll" structure of the curviplanar fracture, prominent in the SW pit-face, suggest an extensional dip-slip movement.

Boudinaged mineralised quartz and feldspar veins are observed in sample 953-133 (DDH 251 - 52.25m). Discontinuous vein pods up to 1.5 x 2.3 cm transgress the country rock and are steeply oriented relative to the core axis and follow the lineations defined by chlorite (Plate 11). Boudins tend to parallel fold axes (McClay, 1987) and in the case of Wheal Hughes the axes are defined by crenulations in the footwall. Crenulation (undulation) axes have azimuths perpendicular to the strike length of the lode and plunge steeply westward.

3.3 DISCUSSION

Veining of dilatant fractures is closely associated with shearing at Wheal Hughes. Though these fractures locally show evidence of shear displacement it is unclear whether they were initiated as extension fractures that were subsequently sheared or formed solely as a result of shearing. Recent work indicates that heterogeneities, in the form of fractures and joints, may pre-

date faulting/shearing and localise subsequent deformations (Hobbs et al., 1976; Segall and Simpson, 1986; Goldstein, 1988; Nicholson, 1991; Olson and Pollard, 1991; Martel, 1991).

A model proposed by Olson and Pollard (1991) suggests that fractures are initiated at points of random heterogeneities and grow perpendicular to the least compressive regional stress. Fluids filling these fractures promote dilation (Simpson, 1986; Gibson, 1990; Nicholson, 1991) and mechanical fracture interaction promotes the growth of en échelon arrays. Recent studies suggest that subsequent deformation is localised at zones of weakness. In the case Wheal Hughes the en échelon vein arrays would have acted as heterogeneities. The migration of fluids into dilatant zones would not only have introduced new mineral species but altered and hydrolytically weakened the host rock, later contributing to the localisation of deformation in the country rocks (Simpson, 1986). Nicholson's (1991) model suggests that en échelon fractures developed synchronously and were linked during development by a ductile shear strain, hence shear strain was a consequence of dilation.

Slip along discontinuous, linked fractures produced dilatancy, allowing the migration of fluids into incipient brittle shear zones (Gibson, 1990). Ore textures indicate that mineralising fluids were introduced episodically into the fissures. This could be explained by the dilatancy/fluid diffusion model of Sibson et al. (1975), whereby pulses of fluid migration are related to dilatancy, and the subsequent fall and rise in fluid pressure.

Textural and structural features of the lode and the adjacent host rock demonstrate that at least four deformational events have influenced the host rock. The first event involved brittle deformation of the Moonta Porphyry and the subsequent migration of the mineralising fluid, which may have intensified fracturing of the host rock. Later deformation was localised at these inhomogeneities in the form of shears. The shears displaced the sedimentary unit overlying the SW lode. Localisation of the sedimentary unit at the SW end of the pit suggests that it was topographically lower relative to the NE end, possibly signifying a tectonic downward displacement or tilting prior to shearing. The dextral strike-slip motion of the shears preceded an

extensional down-dip westerly slip, otherwise the former would have overprinted the less persistent slickenside lineations. The apparent displacement of the NE Leighton's lode is a feature of either a transverse fault, as described by Dickinson (1942), or an en échelon fracture pattern.

3.4 METAMORPHISM

The country rocks in the Wheal Hughes and Poona mines have undergone at least three phases of metamorphism, viz. (1) amphibolite grade metamorphism, which recrystallised the vitric matrix of the Moonta Porphyry and formed large grains of biotite, (2) formation of small linear biotite grains and recrystallisation of felsic minerals around some of the phenocrysts, followed by (3) a retrogressive low grade greenschist facies metamorphism, with retrogression of biotite to chlorite, associated with low grade shear zones (McBriar, 1962; Bone, 1984). Retrogressive mineral assemblages include chlorite at Wheal Hughes and chlorite and epidote at Poona (Janz 1990). Chlorites are typically alteration products of ferro-magnesian minerals (Bates and Jackson, 1984) and at Wheal Hughes chlorite is an alteration product of biotite, occurring as pseudomorphs of biotite and as aligned chlorite fibres.

Plate 7: Steeply dipping lode hosted by the Moonta Porphyry in the NE pit face at Wheal Hughes.

Plate 8: Minor curviplanar fractures, crenulations, on the footwall of the Moonta Porphyry, Wheal Hughes.

Plate 9: "Roll" structure of the Moonta Porpyry, SE end of the Wheal Hughes open-pit.

Plate 10: Slickenside lineations, parallel to the compass, upon a highly chloritised NW dipping joint plane of the footwall, Wheal Hughes.

Plate 11: Drill core sample (DDH 251, sample 953-133) of the Moonta Porphyry. Boudinaged mineralised quartz/feldspar veins with chlorite lineations parallel to the boudin, Wheal Hughes.


7

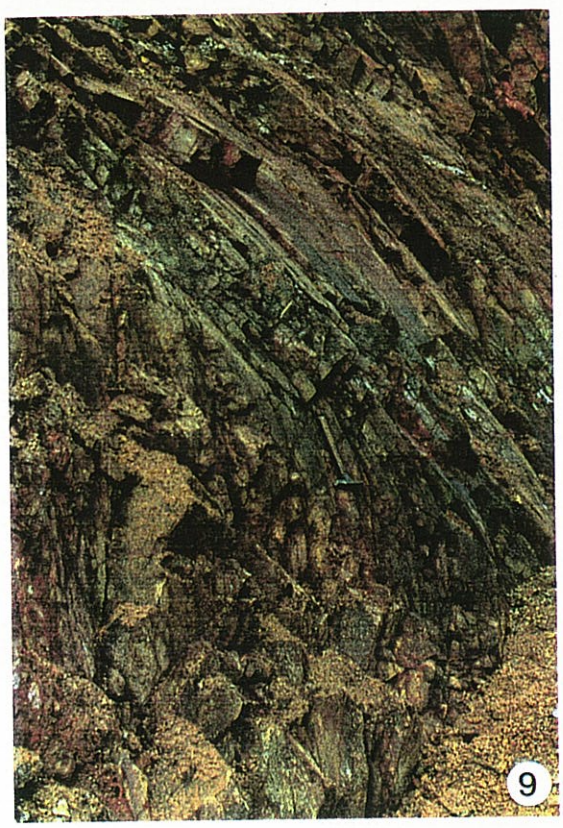
9

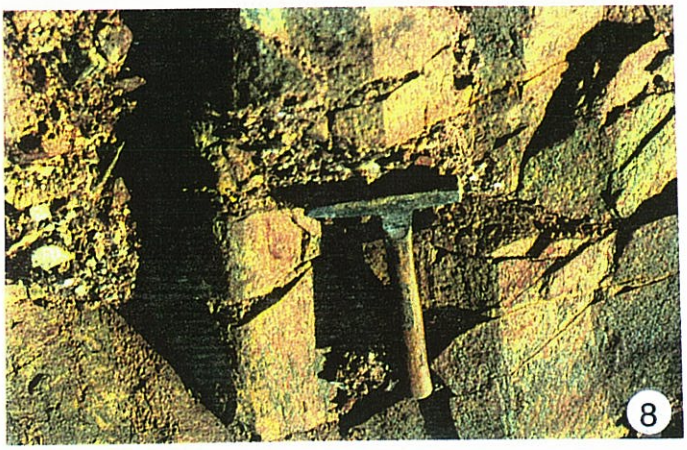
8

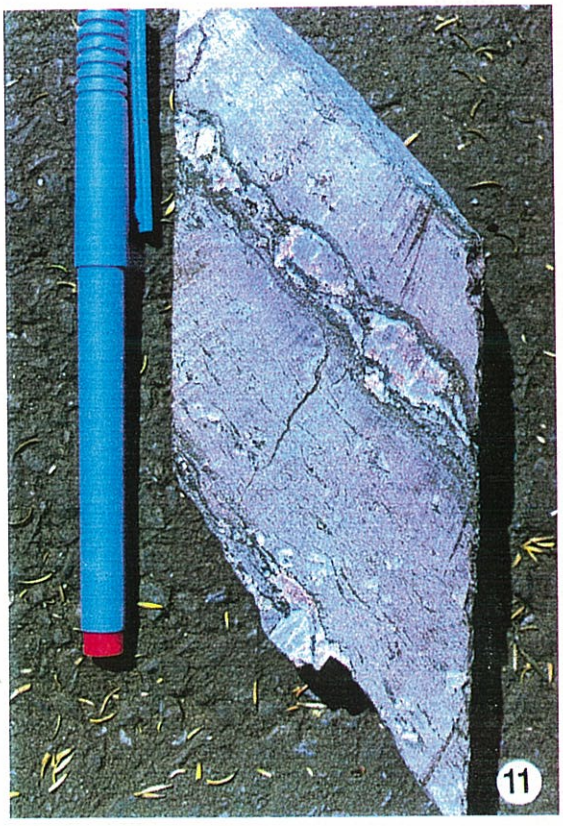
11

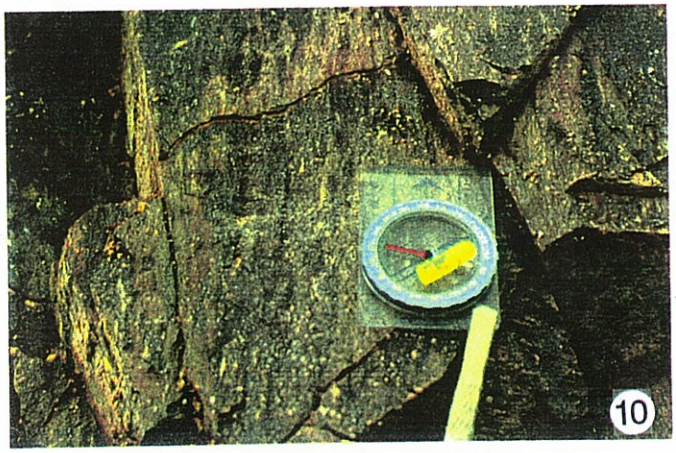
10

4. MAJOR AND TRACE ELEMENT GEOCHEMISTRY

4.1 GEOCHEMICAL DISCRIMINATION

The concentrations and ratios of immobile elements vary systematically with the differentiation of magma series (Winchester and Floyd, 1977), consequently immobile element concentrations and ratios (eg. Nb/Y-SiO_2 and Zr-TiO_2 diagrams) are used to discriminate between tectonic settings.

Moonta Porphyry samples were plotted on Nb/Y-SiO_2 and Zr/TiO_2-SiO_2 diagrams (Figures 4, 5) and were found to plot within the rhyolite and rhyodacite/dacite fields of Winchester and Floyd (1977).

4.2 TECTONIC SETTING

Rb-Y-Nb space and Nb-Y projections of Pearce et al. (1984) discriminate the tectonic settings of Phanerozoic granites. These diagrams define four intrusive settings; (1) ORG- Ocean Ridge Granites, (2) VAG- Volcanic Arc Granites, (3) WPG -Within Plate Granites, (4) COLG- Collisional Granites. The Pearce et al. (1984) discrimination diagrams can only be tentatively used to indicate the tectonic setting of deposition for the Moonta Porphyry, as the models are based upon granites of Phanerozoic age. Although the Moonta Porphyry is apparently largely an extrusive rock of rhyolite/rhyodacite composition and Proterozoic in age, these diagrams provide the only geochemical means of assessing the possible tectonic setting.

The Moonta Porphyry samples plot within the WPG field for both discrimination diagrams (Figures 6, 7). This evidence conflicts with the interpretation of a volcanic arc or subduction complex suggested by Parker (1990).

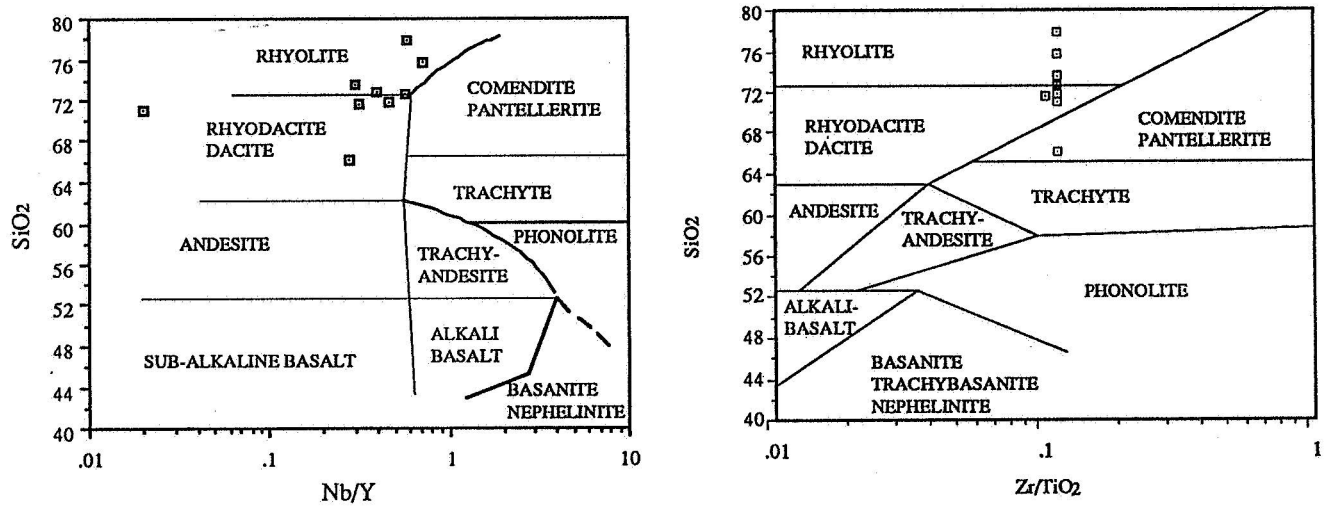

Figures 4 and 5: Geochemical discrimination plot (Winchester and Floyd (1977))

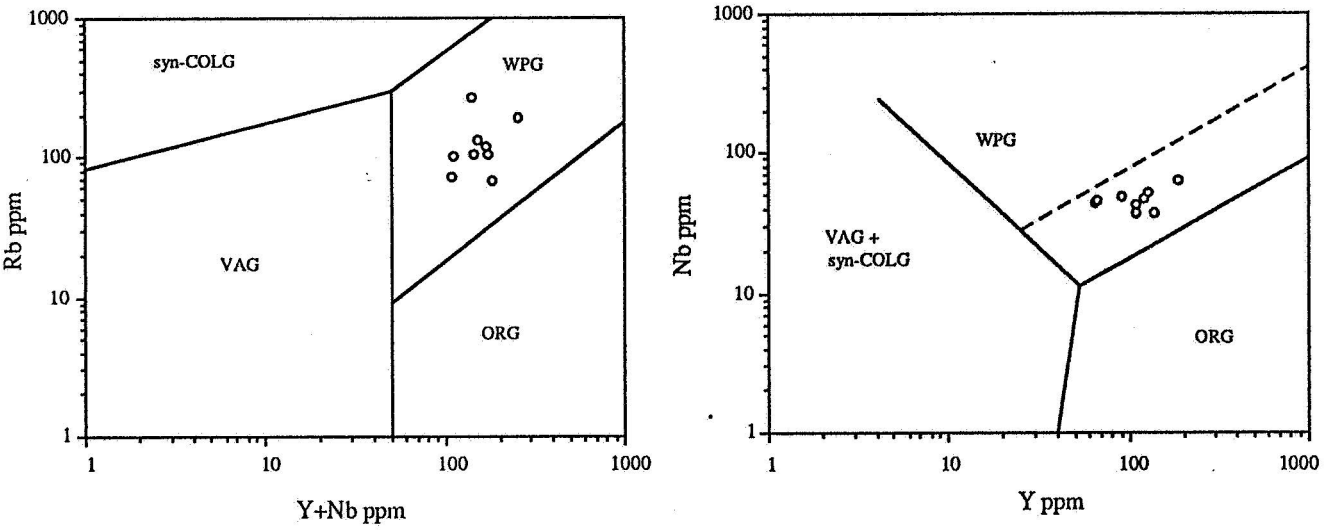

Figures 6 and 7: Tectonic setting plots after Pearce et al. (1984)

5. MINERALISATION

5.1 MINERALOGY

Mineralisation of the Moonta lodes consists primarily of chalcopyrite and bornite, with a minor pyrite and hematite association. Chalcopyrite-rich ores were associated with the more quartzose portions of the lodes, whilst the pegmatitic portions were more bornite-rich (Pring, 1988).

The main ore mineral at Poona and Wheal Hughes is chalcopyrite which is associated with a quartzose fissure-veining system, with minor pods and veins of pegmatites adjacent to the main lodes.

5.2 WHEAL HUGHES

5.2.1 MORPHOLOGY OF MINERALISATION

Mineralisation at Wheal Hughes consists of 3 to 4 parallel orebodies at the SW region and a single orebody at the NE end, respectively known as the Wheal Hughes lode and the Leighton's lode. Leighton's lode is typical of the lodes in the Moonta district, whilst the Wheal Hughes lode is unique to the region as 3 to 4 shears occur in relatively close proximity and also because of the degree of wallrock alteration.

5.2.2 MINERALOGY AND TEXTURES OF PRIMARY ASSEMBLAGES

Primary mineral assemblages at Wheal Hughes consist predominantly of chalcopyrite, pyrite, minor hematite and molybdenite, and traces of magnetite, carrollite, marcasite, gold and magnetite.

Hematite occurs as anhedral grains to euhedral prismatic or tabular crystals. Small magnetite remnants are hosted by the hematite as hydrothermal alteration relics. The hematite grains are fractured and replaced by quartz and chalcopyrite (Plate 12).

Pyrite is found as anhedral to euhedral sulphide grains (up to 1.5mm in size) that have been intensely fractured and the fractures subsequently filled by a later generation of sulphides (Plate 13). Pyrite is found within quartz or chalcopyrite, both as isolated grains and as fragments of massive grains. A mineral identified as marcasite was co-precipitated with pyrite. Though the colour, relative hardness and composition is suited for marcasite it displays unusual anisotropic colours (white/blue to orange/brown), possibly the result of trace elements (Cu?) within its crystal structure (Plate 14, 15).

Chalcopyrite is the principal sulphide mineral and occurs as anhedral grains and as pseudomorphs of pyrite. The pseudomorphous and replacement textures clearly indicate that chalcopyrite followed pyrite in the paragenetic sequence. The chemistry of the fluids and the conditions under which chalcopyrite was precipitated were also conducive for the deposition of carrollite, bornite and gold, as can be seen by the continuous boundary contacts between the respective grains.

Bornite is found to occur as small isolated inclusions within chalcopyrite. Carrollite occurs as anhedral aggregates with a preferential association to marcasite and pyrite. Gold is found as a trace mineral closely associated with chalcopyrite, the bright yellow grains have smooth contacts with the chalcopyrite (Plate 16).

5.2.3 WALLROCK ALTERATION

Emplacement of the ore fluids within the shear-zones hydrothermally altered the surrounding wall-rocks, changing the mineralogy and texture of the adjacent porphyry host. As noted above, alteration associated with the mineralisation is restricted to a narrow zone at Leighton's and is developed up to several metres thick adjacent to the Wheal Hughes lode.

XRD studies of the alteration assemblages revealed the presence of alunite, chlorite, dickite, phlogopite, tourmaline, kaolinite, smectite, illite, siderite, pyrophyllite, muscovite, montmorillonite, hollandite and halloysite (Appendix 6). The feldspar porphyry has been intensely

altered, with complete replacement of the original mineral composition in places but preservation of the original fabric. Extensive pervasive alteration associated with the Wheal Hughes lodes is due to the close proximities of the shears, focussing the hydrothermal fluids within a relatively small area. The alteration was subsequently enhanced by the weathering process, as seen by the extensive supergene kaolinite alteration of the unconformably overlying Blue Range Beds.

Biotite, microcline, K-feldspar, plagioclase and tourmaline have been altered to chlorite and sericite. Sericite is found as a matrix type alteration, replacing the outer rims of K-feldspar grains and altering tourmaline grains. Chlorite is found associated with the ore mineralisation (Plate 17), as pervasive alteration of the host rock and within joint planes. Tourmaline is found as subhedral to euhedral, coarse crystals associated with the primary mineralisation and has a finer texture away from the lode; compositional ternary plots (section 8) suggests tourmaline was a metasomatic alteration product (Plate 18).

5.2.4 OXIDISED AND SUPERGENE ASSEMBLAGES

Patches of atacamite minerals were found at the base of the oxidising zone (B. Kelty, pers. comm.), defining the strike of the underlying lodes. The interpenetration of the oxidised enrichment zone with the underlying supergene zone resulted in the formation of pods of native copper within a zone of supergene enriched mineralisation.

The alteration and subsequent enrichment of ores, by descending ground waters, commences at the redox interface of the water table (Jensen and Bateman, 1981). Supergene enriched assemblages at Wheal Hughes include chalcocite and covellite. The degree of enrichment is more extensive for the Wheal Hughes lodes relative to the Leightons' lode; the oxidation of the ore persists to a greater depth before interpenetrating into the primary ore zone.

Chalcocite occurs as a black 'sooty' sulphide, coating chalcopyrite and as blue/black amorphous clayey pods within zones of pervasive kaolinite alteration. Covellite is an indigo-blue sulphide found coating primary copper ore, and as pods where complete alteration has occurred.

Plate 12: Reflecting light photomicrograph of sample 953-132 from Wheal Hughes. Yellow chalcopyrite filling fractures of hematite (Hm) and magnetite (Mg).

Plate 13: Reflecting light photomicrograph of sample 953-069b from the SW region of Wheal Hughes. Intensely fractured pyrite (Py) which is replaced by later chalcopyrite (Cp), (brown) bornite and (light grey) carrollite.

Plate 14: Reflecting light photomicrograph of sample 953-105b from the Poona underground mine. Blue/white marcasite (Mc) associated with carrollite (Ca) within chalcopyrite.

Plate 15: Reflecting light photomicrograph of sample 953-124 from the Poona underground mine. White marcasite in contact with pyrite (Py). Chalcopyrite (Cp) and carrollite (Ca) infill the fractures of the pyrite fragments.

Plate 16: Reflecting light photomicrograph of sample 953-132 from Wheal Hughes. Bright yellow gold (Au) grains, with smooth grain contacts with the chalcopyrite (Cp).

Plate 17: Transmitting light photomicrograph. Green chlorite (Cl) associated with opaques (Pyrite).

Plate 18: Transmitting light photomicrograph. Anhedral tourmaline (Tm) and its association with the opaques (Chalcopyrite).

Plate 19: Reflecting light photomicrograph of sample 953-114b from Poona. Thin tabular hematite (Hm) lamellae network, with yellow chalcopyrite (Cp) infilling the open lattice voids.

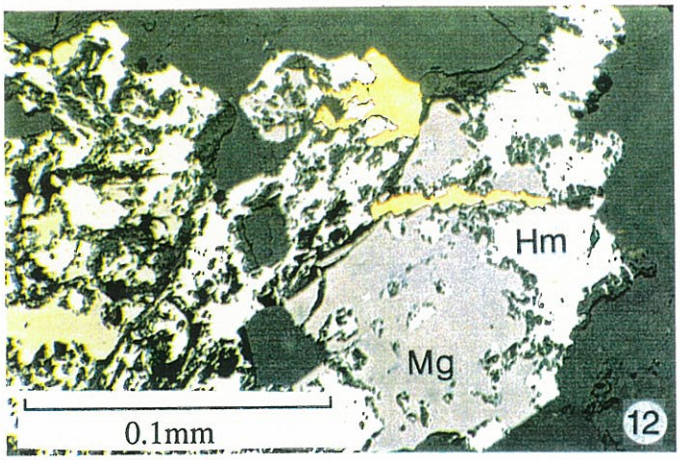
Hm
Mg
0.1mm
12

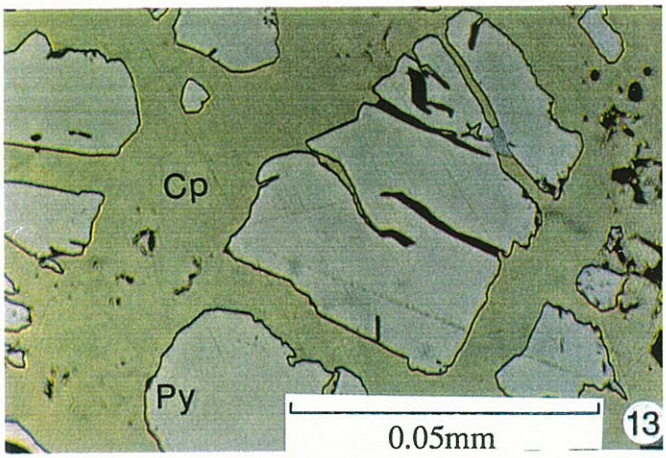
Cp
Py
0.05mm
13

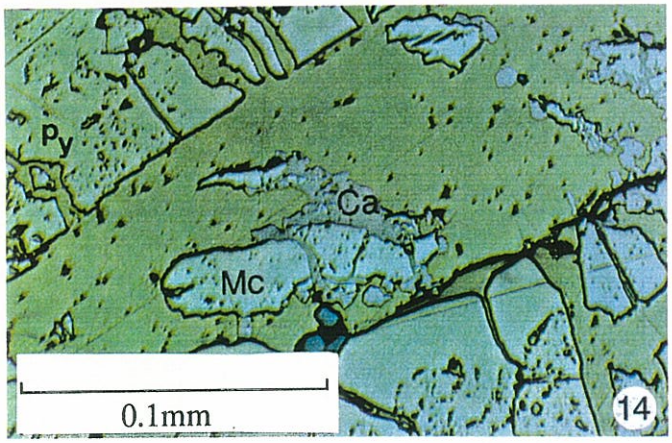
Py
Ca
Mc
0.1mm
14

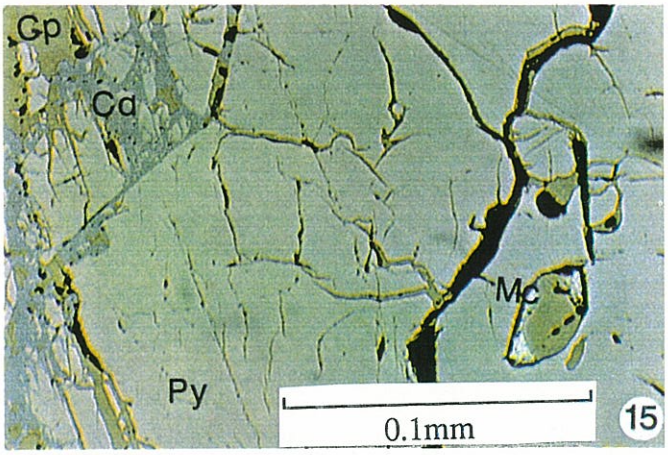
Cp
Ca
Mc
Py
0.1mm
15

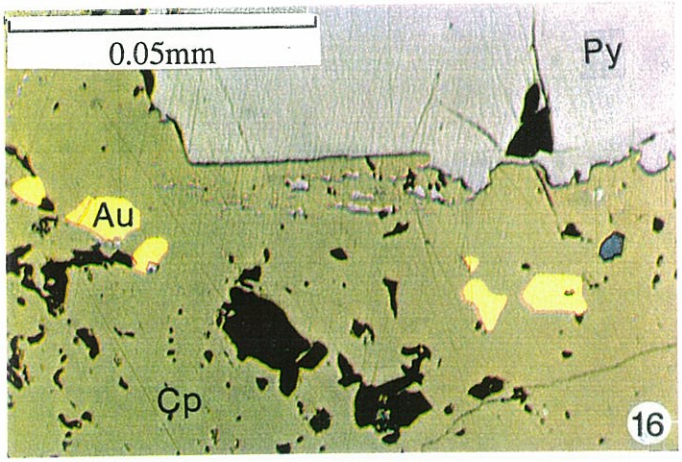
0.05mm
Py
Au
Cp
16

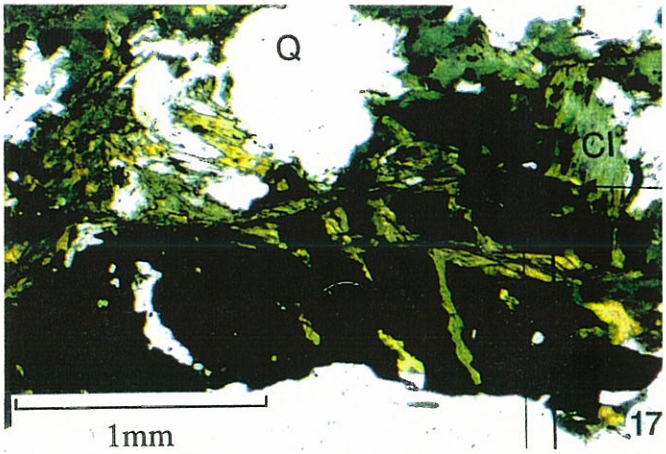
Q
Cl
1mm
17

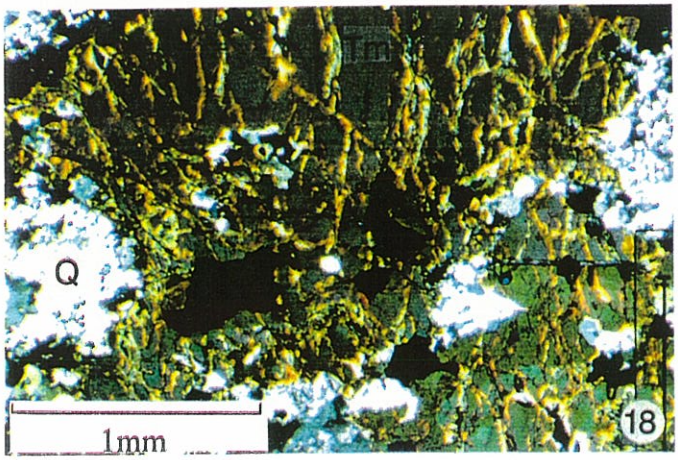
Hm
Q
1mm
18

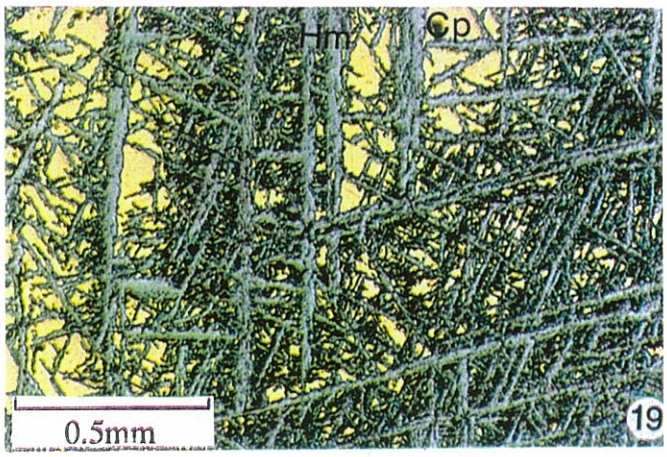
Hm
Cp
0.5mm
19

5.2.5 PARAGENESIS

From the observed textural relationships magnetite was the first mineral precipitated from the ore fluids. Hydrothermal alteration of the magnetite to hematite followed soon after, as can be seen from remnant magnetite within the massive hematite. Following a fracturing event pyrite was deposited within the fractures of hematite and quartz grains, marcasite was co-precipitated with the pyrite. A further fracturing event followed the precipitation of pyrite. Chalcopyrite was deposited within the fractures along with bornite, carrollite and gold. A minor fracturing event followed, which enhanced the subsequent supergene enrichment of the chalcopyrite to covellite (Fig. 9).

5.3 POONA

5.3.1 MORPHOLOGY OF MINERALISATION

Mineralisation at Poona consists of a single lode which is an en échelon extension of the original Poona lode. It closely resembles the Leighton's lode at Wheal Hughes, having the morphology of a single tabular body with small scale wallrock alteration.

5.3.2 MINERALOGY AND TEXTURES OF PRIMARY ASSEMBLAGES

The primary mineral assemblages at Poona are similar to the assemblages found at Wheal Hughes, but in different proportions. The dominant assemblages include chalcopyrite, pyrite and hematite, with minor magnetite, bornite and traces of carrollite, gold and marcasite.

Two generations of hematite are observed at Poona; the first generation predated the sulphide minerals and hosts small magnetite remnants (ie. magnetite altered to hematite). This hematite is fractured and replaced by quartz, pyrite and chalcopyrite. The second generation of hematite appears to have post-dated the pyrite and consists of thin tabular hematite lamellae networks within an open fracture system (Plate 19).

Following the deposition of the second generation hematite, chalcopyrite was precipitated from the mineralising fluids and the resulting textural relationships are similar to the relationships observed at Wheal Hughes. The chemistry of the fluids and/or the conditions under which chalcopyrite was precipitated at Poona differed with respect to Wheal Hughes, as the co-precipitates of chalcopyrite (ie. carrollite, bornite and gold) occur in different proportions.

Massive aggregates and small inclusions of bornite, carrollite and marcasite are observed to occur in greater proportions relative to the Wheal Hughes mineral assemblages (Plate 20, 21).

5.3.3 WALLROCK ALTERATION

Hydrothermal alteration of the country rock (Moonta Porphyry) at Poona is similar to the intensity and extent of alteration observed for the Leighton's lode at Wheal Hughes. Similar alteration assemblages are observed at the Poona and Wheal Hughes mines, although the Wheal Hughes country rock has undergone a greater degree of metasomatism, with a greater abundance of tourmaline.

5.3.4 OXIDISED AND SUPERGENE ASSEMBLAGES

Supergene enriched assemblages at Poona includes chalcocite, covellite and digenite. Digenite is only observed as an alteration product of massive bornite and consequently is not found at Wheal Hughes (Plate 22). The extent of enrichment of the Poona lode is similar to the Leighton's lode, though to a much lesser extent relative to the Wheal Hughes' lode.

Plate 20: Reflecting light photomicrograph of sample 953-069a from Wheal Hughes. Small inclusion of bornite (Bn) in supergene enriched chalcopyrite (Cp), covellite (Cov) is the alteration product.

Plate 21: Reflecting light photomicrograph of sample 953-124 from Poona. Carrollite (Ca) association with pyrite (Py) and its contacts with chalcopyrite (Cp) and bornite (Bn).

Plate 22: Reflecting light photomicrograph of sample 953-124 from Poona. Bornite (Bn) and its supergene alteration product, blue/geen digenite (Di).

Figure 8: Paragenetic sequence of the mineralisation at Poona and Wheal Hughes.

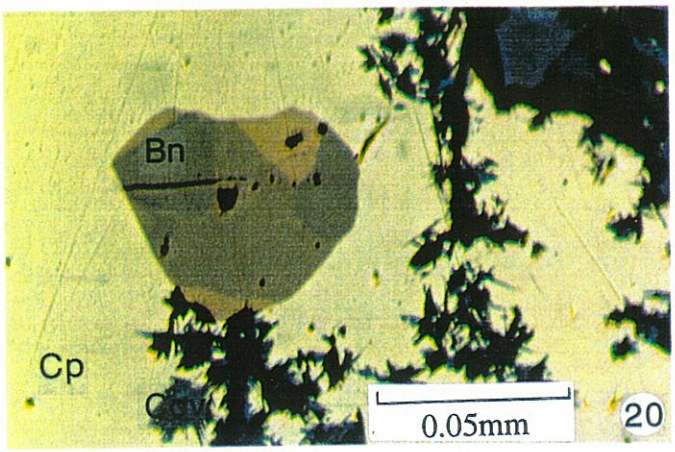

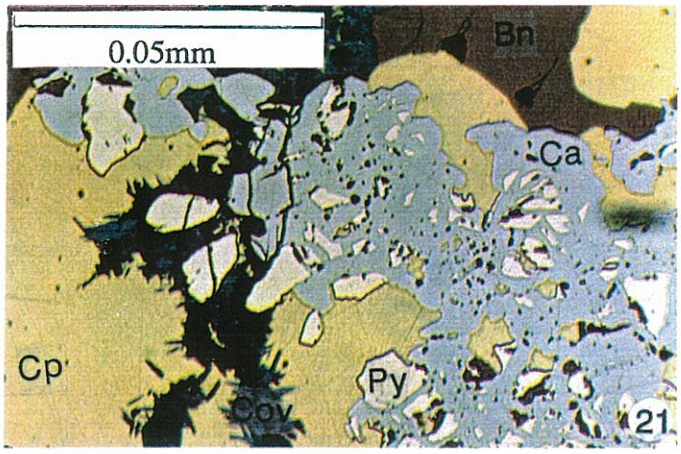

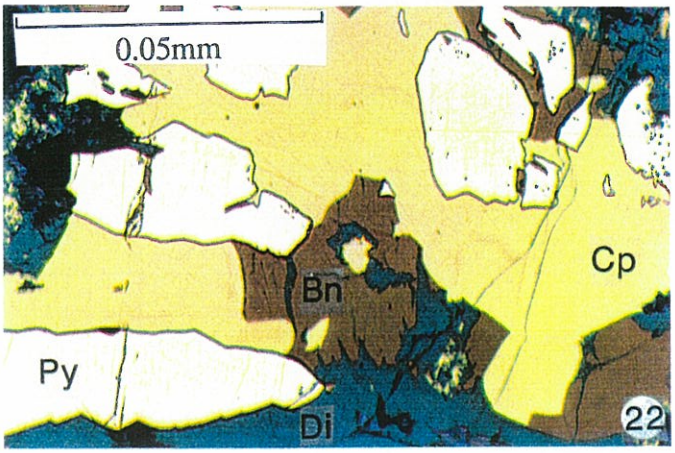

Figure 8

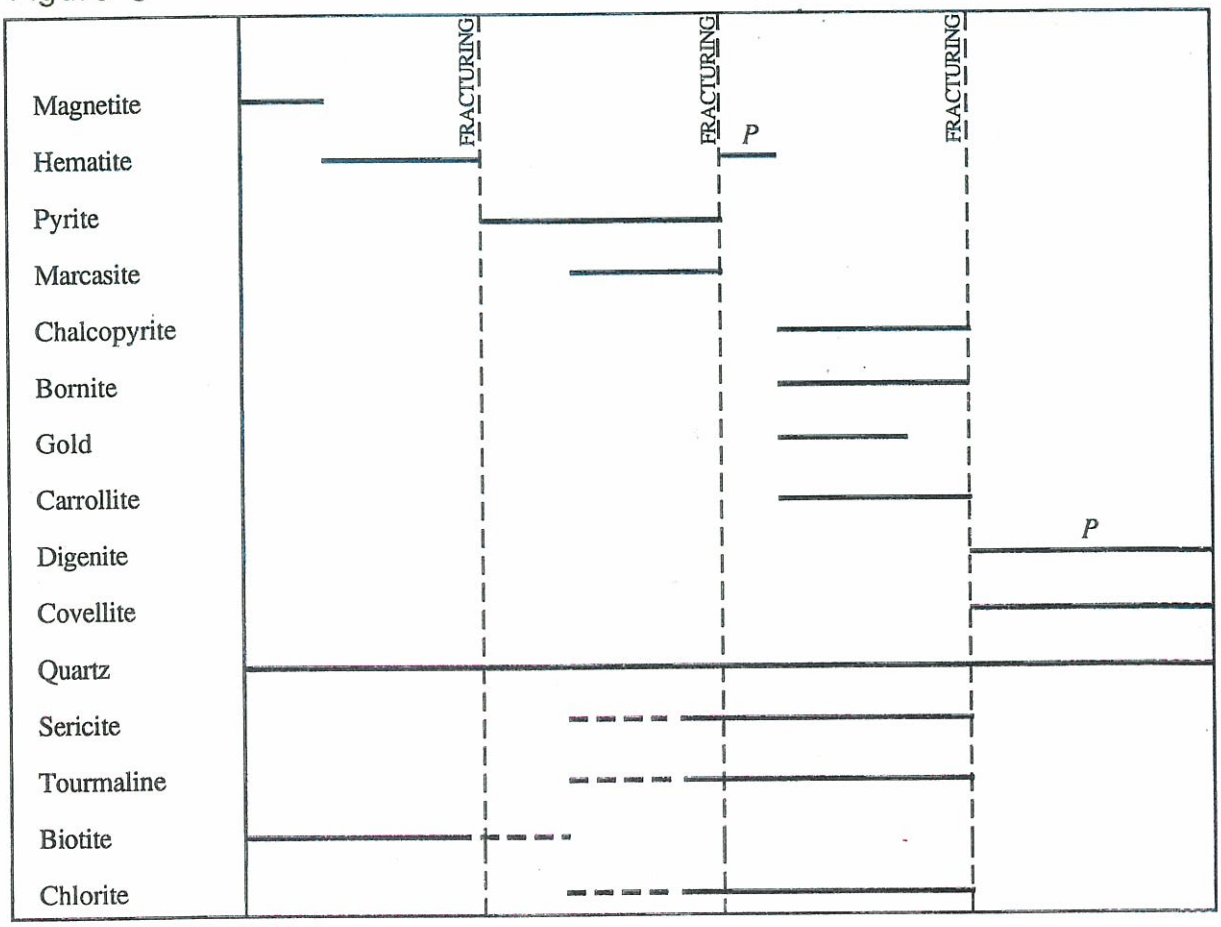

*P - relationship only observed at Poona

5.3.5 PARAGENESIS

The sequence of mineralisation described for Wheal Hughes also applies for Poona, with the exceptions of a second generation of hematite and the occurrence of digenite. Two generations of hematite are observed at Poona, compared to only one at Wheal Hughes. Janz (1990) places the second generation hematite after the chalcopyrite in the paragenetic sequence. On the basis of the present examination of the ore textures, a revision of this interpretation has been made, with the hematite following pyrite but preceding the chalcopyrite. Digenite is an alteration product of massive bornite (Fig. 9).

6. FLUID INCLUSION STUDY

6.1 INTRODUCTION

Thermometric analysis of fluid inclusions has provided valuable information of the physico-chemical conditions and compositions of the fluids, under which the minerals in the Moonta Porphyry formed.

6.2 SAMPLE PETROGRAPHY

Transparent quartz samples closely associated with mineralisation were selected, and doubly polished thin sections were made. The sections were examined petrographically and selected fragments were heated and cooled upon a Reynolds Fluid Inclusion stage. Microthermometric measurements were made on 154 inclusions in 6 samples from Wheal Hughes and 5 samples from Poona.

The fluid inclusions were classified using the scheme of Shepherd et al. (1985) in the following table (Table 1).

Table 1: Fluid inclusion classification scheme

Type	Components	Phases	No. of analyses
1	Monophase Liquid	L	none undertaken
2	Liquid-rich, two phase	L + V	138
3	Vapour-rich, two phase	V + L	10
4	Monophase Vapour	V	none undertaken
5	Multiphase solid	S + L ± V	6

V- dominantly H_2O but CO_2 and N_2 may be present although not observed.

L- aqueous saline solution of NaCl and possibly $CaCl_2$ and/or $MgCl_2$.

S- solid crystals of yellow cubic salt crystals and red tabular hematite crystals.

Inclusion sizes varied from 3.0 x 1.50μm to 18 x 13μm with no apparent relationship between the L/V ratios and fluid inclusion sizes. The general criteria defined by Shepherd et al. (1985) were used for distinguishing between primary, secondary and pseudo-secondary inclusions. Specifically, the main criteria in the case of the Wheal Hughes and Poona samples were as follows;

(1) Primary: formed during crystal growth and identified as large, isolated and randomly distributed inclusions.

(2) Secondary: formed during healing of post-crystallisation fractures and distinguished as irregular and planar groups healing fractures.

(3) Pseudo-secondary: developed during healing of fractures, similar to secondary but with fractures terminating at growth zones.

Yellow and red cubic and tabular solids found within the fluid inclusions have been identified as possible salt and hematite crystals, respectively. The relative abundance of salt and hematite daughter crystals indicate that the hydrothermal fluid was a concentrated brine with a high iron concentration.

6.3 MICROTHERMOMETRY- COOLING

Microthermometric cooling involves the cooling of fluid inclusions until solidification occurs, whereupon the system is heated and the phase changes of the inclusions are recorded. The temperature at which first (T_m) and/or final (T_{fm}) melting occurs can be used to determine the components of the fluid phase, if the phase changes are matched with experimentally determined phase transitions within known systems (eg. Crawford, 1981). Final melting temperatures may be used to determine salinities of the fluid inclusions.

Difficulties in differentiating between the primary,secondary and pseudo-secondary fluid inclusions led to a considerable overlap in data. First melting temperatures (Fig. 9) less than the $NaCl-H_2O$ eutectic of -21.1°C suggest the presence of salts in addition to NaCl, possibly $CaCl_2$ and/or $MgCl_2$. The final melting temperatures (Fig.10) were used to calculate the salinities in terms of NaCl equivalent, using the linear least squares regression method of Potter et al. (1978).

Salinities for type 2 and 3 primary and pseudo-secondary inclusions ranged from 0.2 to 27.9wt.% NaCl equivalent, with a mean of 14.3wt.%.

6.4 MICROTHERMOMETRY-HEATING

The temperature of homogenisation (T_{hom}) is representative of the minimum temperature of fluid entrapment. Microthermometric heating involved the heating of type 2, 3 and 5 inclusions until homogenisation occurred.

Difficulties in identifying between primary, secondary and pseudo-secondary fluid inclusions are reflected in the considerable overlap of the T_{hom} data when plotted upon T_{hom} v.s. frequency graphs (Fig. 11). The homogenisation temperatures suggest a bi-modal distribution, between 480°-280°C, peaking at 380°-320°C, and at 250° to 110°C. Two groups are also distinguished by T_{hom} versus T_{fm} graphs (Fig. 12), with Group 1 data distributed about 265°-110°C and Group 2 about 380°-250°C. The above data suggests that the temperatures between 480°-265°C represents syn-crystallisation fluid entrapment (as indicated by chlorite data), whereas 250°-110°C reflects the temperatures of post-crystallisation fluid entrapment.

The presence of daughter minerals not enclosed by fluid inclusions, liquid-rich monophase inclusions and necking-down of inclusions is indicative of continued healing of inclusions at low temperatures, after the nucleation of the vapour bubble. Primary vapour-rich fluid inclusions coexisting with liquid-rich inclusions are an indication of fluid inclusion entrapment in boiling hydrothermal fluids (Bodnar et al. , 1985).

6.5 DEPTH AND PRESSURE CALCULATIONS

Boiling point curves for water and brines of constant composition (Haas, 1971) enable the estimation of the minimum depth of entrapment of type 2 and 3 fluid inclusions. The model assumes an open vein system of deposition with an associated brine at constant composition. Group 2 and 3 fluid inclusions were trapped in the range 480°-280°C, with a modal distribution

Figure 9: Histogram of first melt temperatures of NaCl-H_2O ice (T_m) from quartz fluid inclusions.

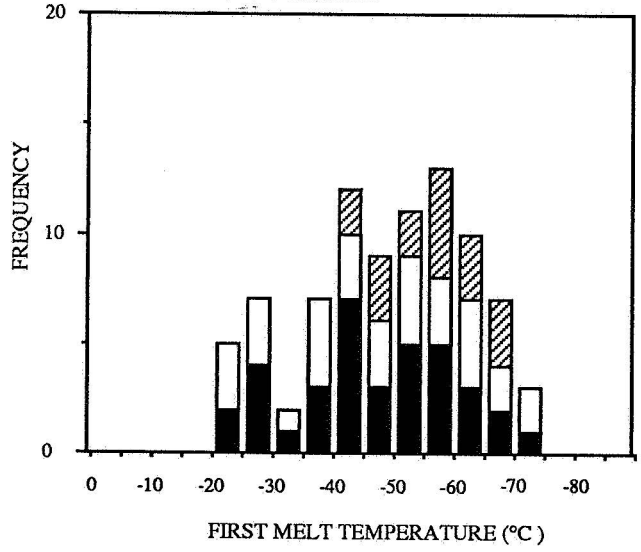

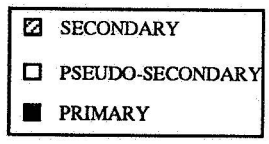

Figure 10: Histogram of final melt temperatures of NaCl-H_2O ice (T_{fm}) from quartz fluid inclusions.

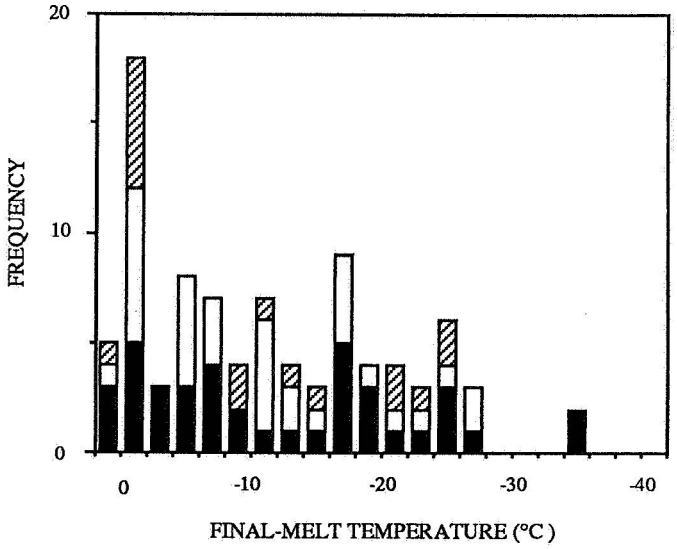

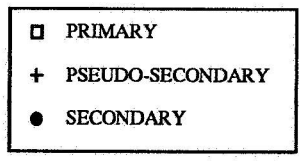

Figure 11: Histogram of the temperature of homogenisation (T_{hom}) data from quartz fluid inclusions

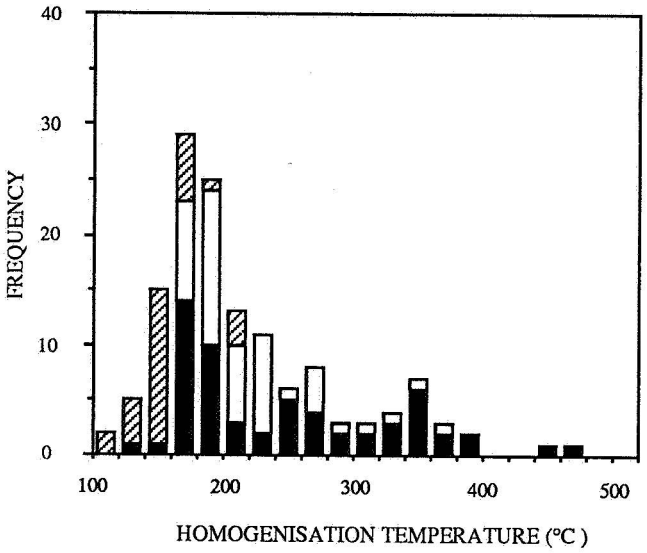

Figure 12: Plot of T_{hom} vs T_{fm}. Two overlapping groups can be differentiated.

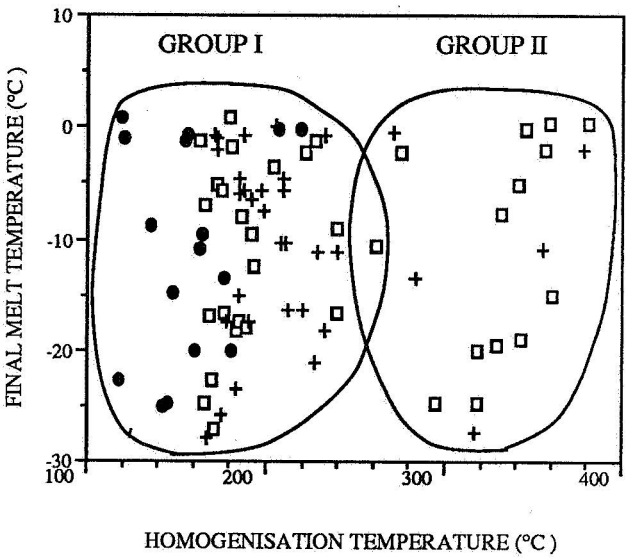

about 380°-320°C. The boiling point curves for 15wt.% NaCl, at 380°-320°C, indicate a minimum depth of boiling in the range of 620 to 1850m.

The hydrostatic and lithostatic pressures can be calculated for the hydrothermal system at the minimum depth of boiling by using the following formula (Shepherd et al., 1985):

$P = H \rho g$

H= depth

P= pressure

ρ= density (hydrostatic = 1.0 gcm^{-3})

(lithostatic = 2.70 gcm^{-3})

g= gravity (= 981 dynes cm^{-2})

The minimum hydrostatic pressure of the fluid so calculated is 61 - 182 bars and the calculated lithostatic pressure is 165 - 490 bars. The minimum hydrostatic pressure of 61 - 182 bars is considered representative of the hydrothermal system, as the mineralisation is a fissure filling/ open vein style deposit.

7. SULPHUR ISOTOPE ANALYSES

7.1 INTRODUCTION

Sulphur isotope analyses were undertaken in an attempt to determine the source of the sulphur, to estimate the temperature of mineralisation and to supplement the petrological and fluid inclusion data.

Sulphur isotope ratios were analysed on 26 samples of chalcopyrite, 9 samples of pyrite and 1 sample of bornite, using the ^{34}S / ^{32}S analyses method of Robinson and Kusakabe (1975). Samples were collected from Moonta Joint Venture DDH cores and from the Poona underground mine and Wheal Hughes open-pit operations.

7.2 SULPHUR GEOTHERMOMETRY

Sulphur isotope geothermometric calculations are based upon the equilibrium sulphur isotope fractionation between co-existing sulphur species (Rye and Ohmoto, 1974). Isotope fractionation is a function of temperature; it assumes that isotopic equilibrium had been attained between the two sulphur species, no isotopic exchange took place after mineralisation and the isotopic equilibrium constants are accurately known. Consequently the temperature of equilibrium can be calculated. For pyrite-chalcopyrite pairs the following relationship applies (Ohmoto and Rye, 1979):

$$T = \frac{(0.67 \pm 0.04)\times 10^3}{\Delta^{1/2}}, \quad \Delta = \delta^{34}S_{pyrite} - \delta^{34}S_{chalcopyrite}$$

However, analyses of pyrite-chalcopyrite pairs display a wide range of Δ values, confirming textural studies of the ore minerals that suggest that equilibrium was not attained between pyrite and chalcopyrite (section 5).

7.3 RESULTS

$\delta^{34}S$ values of samples from the Wheal Hughes mine (Fig. 13) range from 2.5 to 6.4‰ with an average of 4.9‰, while the $\delta^{34}S$ values of the Poona mine (Fig. 14) range from -1.3 to 5.5‰ with an average of 1.4‰.

Frequency distributions of the sulphur isotope data display a single population of data with a relatively narrow range of $\delta^{34}S$ values for each deposit. Although more than one mineralising stage has been identified within the paragenetic sequence, the narrow ranges of $\delta^{34}S$ values suggest that the mineralising fluids remained relatively constant at each site of deposition in terms of fO_2, fS_2, pH. Wheal Hughes is characterised by a heavier $\delta^{34}S$ relative to Poona, suggesting a slight variation in the chemistry of the ore solutions at Wheal Hughes relative to Poona. $\delta^{34}S$ values close to zero are often interpreted as indicative of magmatic systems (Nielsen, 1979), hence the data for the Poona and Wheal Hughes tend to support a magmatic source for the sulphur. However as these $\delta^{34}S$ values could also be explained by a variety of other possible sources, interpretation for the source of the sulphur must be supplemented with other data (to be discussed further in Section 9).

Figure 13: Histogram of Wheal Hughes sulphur isotope analyses.

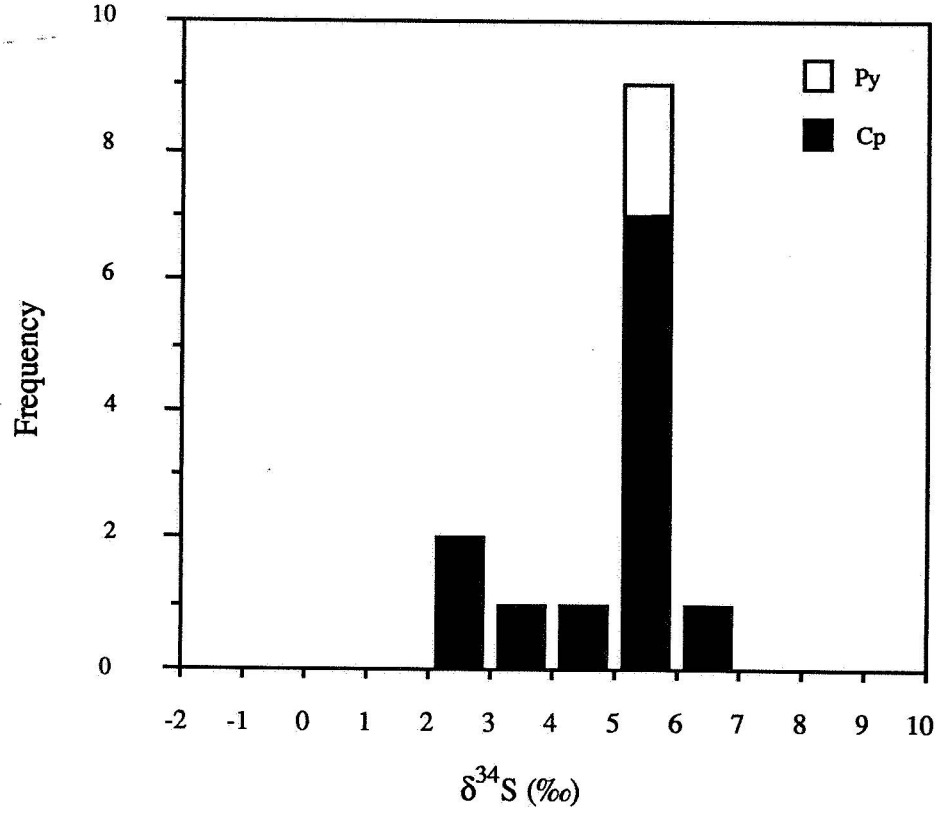

Figure 14: Histogram of Poona sulphur isotope analyses, includes data from Janz (1990).

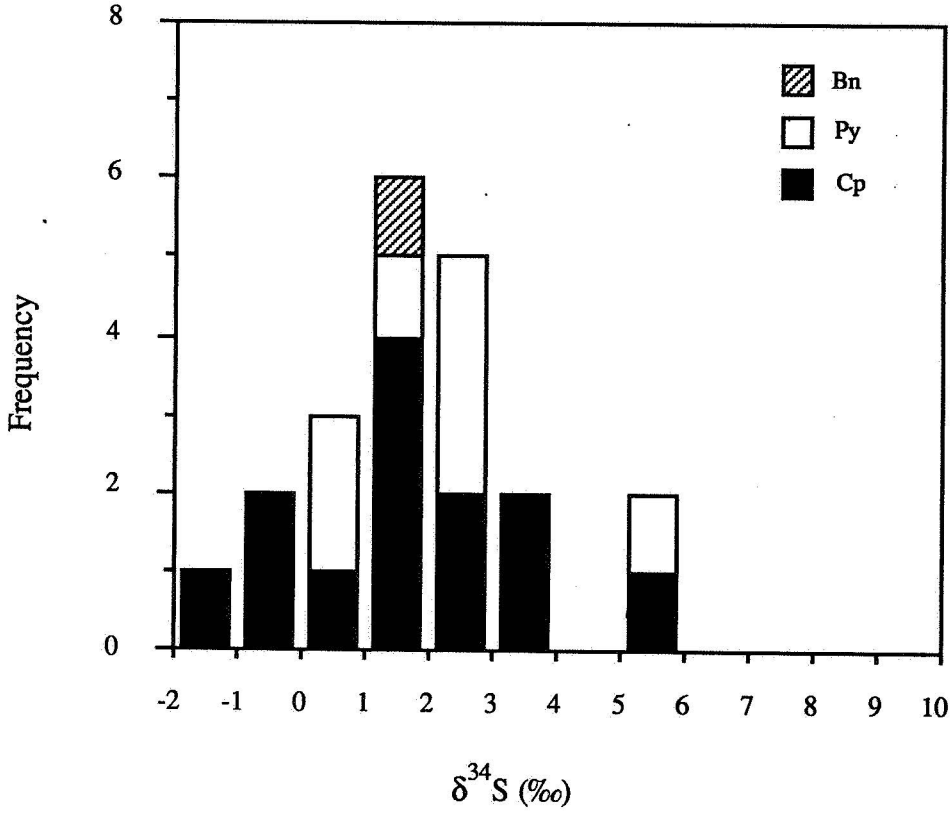

8. ELECTRON MICROPROBE ANALYSIS

8.1 CHLORITE

The fluid-rock interactions of hydrothermal fluids and the host rocks to mineralisation commonly produce the alteration product chlorite. Chlorite's common association with hydrothermal ore deposits and the nonstoichiometry of chlorite enable the physico-chemical conditions of the rock-fluid interactions within hydrothermal systems to be defined, by means of the six-component chlorite solid solution model of Walshe (1986). The model uses electron microprobe analyses to define six thermodynamic components of chlorite and from two geothermometers, together with the constraints defined by the Gibb-Duhem equation, derives the temperature of formation, ferric iron and water content. These parameters then enable the calculation of fO_2 and fS_2.

A total of 137 chlorite analyses from 11 samples were processed at the Australian National University, using the CHLORITE computer program developed by Dr. J. L. Walshe. Calculated temperatures, log fO_2 and log fS_2 at Poona Wheal Hughes are presented in Table 2.

Table 2: Calculated data from chlorite analyses

	POONA	WHEAL HUGHES
Temperature (°C)	163 → 326	187 → 296
log fO_2	-31.4 → -46.8	-34.6 → -46.1
log fS_2	-11.3 → -17.9	-11.6 → -17.3

8.2 SERICITE

Sericite is a fine-grained white mica (muscovite or paragonite) with a composition high in SiO_2, MgO and H_2O and low in K_2O, though not necessarily chemically different from muscovite (Deer et al., 1967). It is a common alteration product in hydrothermal systems. White mica exists as matrix sericite at temperatures ≤ 280°C; at >300°C it is restricted to the alteration of feldspar grains (Hedges and Walshe, unpublished).

A preliminary seven-component solid solution model for muscovite was initiated by Rogers (1983) and expanded upon by Hedges and Walshe (unpublished). This model has been used to calculate temperatures from 46 analyses of sericite from 6 polished thin sections. Calculations were performed using a Macintosh programme written by G. Jenkins. At present only temperatures can be calculated. Calculated temperatures range from 220° to 284°C at Poona and 236° to 258°C at Wheal Hughes (Appendix 11). These temperatures are considerably lower compared with 163°-326°C obtained from chlorite and a modal temperature distribution about 320°-380°C from fluid inclusion analyses.

8.3 TOURMALINE

Tourmaline is a complex borosilicate with the general formula $WX_3Y_6(BO_3)_3Si_6O_{18}(OH)_4$, which allows the substitution of a variety of ions into 3 lattice sites; W = Ca, Na, Mg, K, X = Al, Li, Mg, Fe^{2+}, Fe^{3+}, Mn^{2+} and Y = Al, Fe^{2+}, Fe^{3+}, Cr, Ti, Mg, V^{3+} (Henry and Guidotti, 1985; Plimer, 1988; Deer et al., 1967). The nonstoichiometry means that compositional changes can be related to the bulk composition of the host rock, composition of co-existing minerals and P - T - fO_2 conditions (Henry and Guidotti, 1985). The non-stoichiometry of tourmaline and its close association with copper ore make it a potentially useful supplement for constraining the parameters of the hydrothermal system at Moonta.

Tourmaline compositions, determined from microprobe analyses, are plotted in CaO-FeO-MgO and Na_2O-FeO-MgO ternary diagrams to determine the species type (Fig.17) (Bone, 1988) and in Al -Fe(tot.)-Mg and Ca-Fe(tot.)-Mg ternary diagrams (after Henry and Guidotti, 1985) (Figures 15, 16) to compare with tourmalines from known host rock types. The Poona and Wheal Hughes tourmalines are in the schorl region of the dravite-schorl series. High iron content is normally indicative of a granitic source and a magnesium component is usually associated with metamorphic rocks or metasomatic assemblages (Deer et al., 1965). The Henry and Guidotti (1985) ternary diagrams are based upon the premise that the compositions of tourmaline reflect the bulk rock composition. The Poona and Wheal Hughes tourmalines overlap the field for Li-poor

granitoid pegmatites and aplites and the field for meta-pelites and metapsammites, as defined by Henry and Guidotti.

From the probe analyses of tourmaline calculations have also been made of $Na_2O/(Na_2O+CaO+K_2O)$ and $FeO/(FeO+MgO+MnO)$ ratios for comparison with the compositional fields defined by Ethier and Campbell (1977) (Fig. 18). The Poona and Wheal Hughes analyses plot close to and within Group II, the field of tourmalines associated with altered sediments.

The Moonta tourmaline compositional data do not provide unequivocal evidence for their origin. Tourmaline developed by hydrothermal alteration partially to completely takes on the chemical characteristics of the host rocks, hence the overlap of the data within the magmatic and sedimentary fields may be due to deposition from a hydrothermal fluid (possibly of magmatic origin) that had undergone reaction with the host rocks (ie. the Moonta Porphyry).

Figure 15

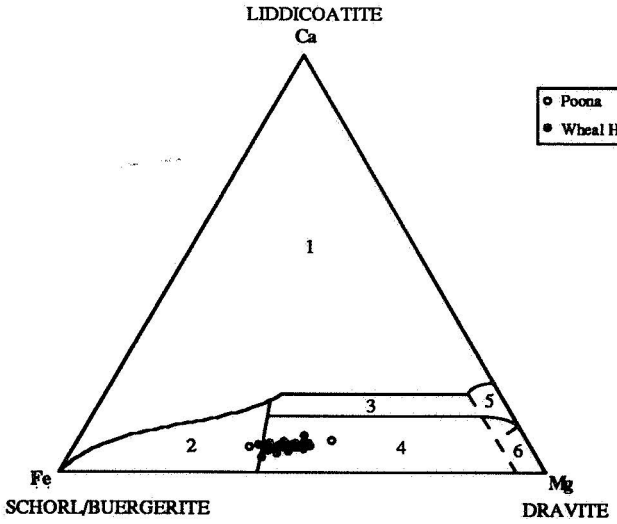

Figure 16

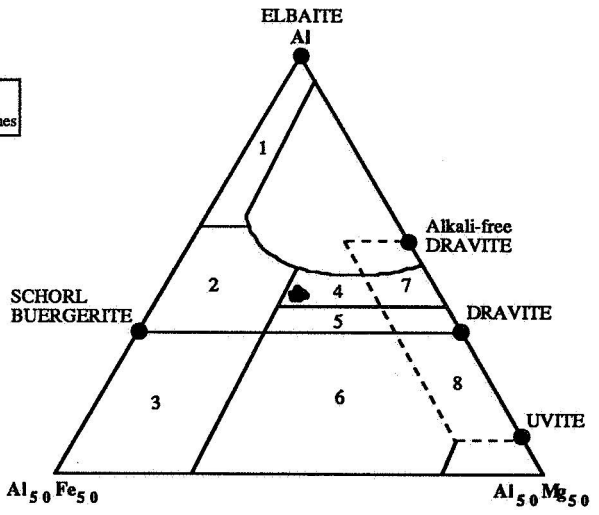

1. Li-rich granitoid pegmatites and aplites
2. Li-poor granitoid pegmatites and aplites
3. Fe^{3+}-rich quartz-tourmaline rocks (hydrothermal altered granites)
4. Metapelites and metapsammites co-existing with Al-saturated phase
5. Metapelites and metapsammites not co-existing with Al-saturated phase
6. Fe^{3+}-rich quartz-tourmaline rocks, calc-silicates and metapelites
7. low Ca-ultramafics and Cr,V-rich metasediments
8. Meta-carbonates and meta-pyroxenites

Figures 15 and 16: Tourmaline analyses from Poona and Wheal Hughes plotted within ternary diagrams adapted from Henry and Guidotti (1985).

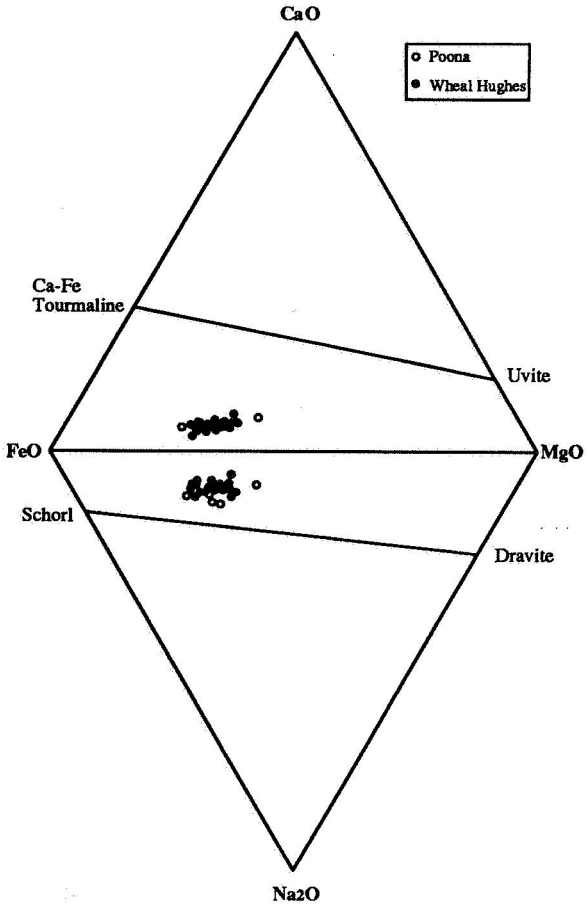

Figure 17: Data plot within the schorl region of the dravite-schorl series. Symbols as in Figs. 15 and 16.

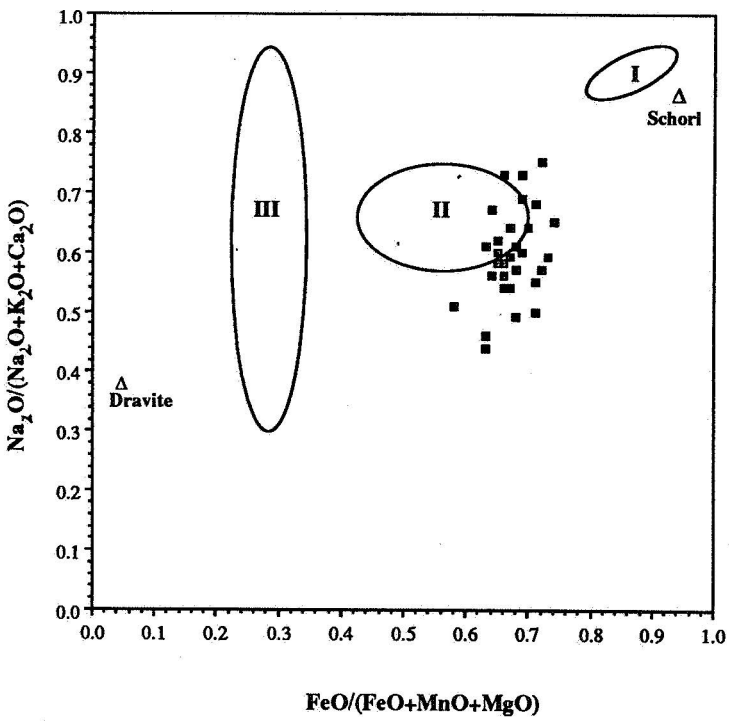

Figure 18: Magnesium and iron rich tourmaline compositional fields are defined by the triangles marked dravite and schorl respectively. Compositional fields for tourmaline are defined by Ethier and Campbell (1977), based upon Proterozoic rocks of southeastern British Columbia; Group I represents tourmalines from the Hellroaring Creek Stock (magmatic source), Group II defines the Aldridge metasediments and tourmalines derived from metamorphism and recrystallisation are defined in Group III, altered zones in the Sullivan mine.

9. GEOCHEMISTRY OF THE MINERALISING FLUID

9.1 GEOCHEMICAL MODELLING

The fluid chemistry for the copper mineralisation at Wheal Hughes and Poona can be modelled by combining the results obtained from fluid inclusion and petrographic studies, sulphur isotope, chlorite and sericite analysis together with thermodynamic data. Temperature, pressure, salinity, log fO_2, log fS_2 and pH are the parameters that can be constrained for the mineralisation.

A log fS_2 vs. log fO_2 diagram (Fig. 19b) for the Fe-S-O system was calculated for 275°C on the basis of the temperatures obtained from chlorite data (Figure 19a). Log fO_2 vs. temperature diagrams (Figs. 19c and 19d) were calculated for $\Sigma S=10^{-1.5}M$ and a pH=4.5. Log fO_2 vs. pH diagrams were calculated for a temperature of 275°C, $a^{K^+}=0.01$ and $\Sigma S=10^{-1.5}M$. Sulphur isotope contours in Figures 19d and 19f were calculated for $\delta^{34}S_{fluid}=0‰$.

Stability fields for the assemblages kaolinite/sericite and sericite/K-feldspar, were calculated after Pisutha-Arnond and Ohmoto (1988). On the basis of the presence of kaolinite and sericite associated with mineralisation, a pH of 4.5 was selected for the calculation of Figures 19c and 19d. Thermodynamic data of Huston and Large (1988) and Barton (1984) were used for calculations in the Fe-S-O system and that of Ohmoto et al. (1983) for the Cu-Fe-S system.

The log fS_2-logfO_2 diagram (Fig. 19b) illustrates a positive linear trend of chlorites, formed in apparent equilibrium with the mineralisation, for the temperature represented (T=275°±10°C). The trend illustrates a decrease in log fO_2 along with log fS_2, a relationship typically found within hydrothermal systems (eg. Hein, 1989). The data points plotting within the pyrite and pyrrhotite stability field show a linear trend with log fO_2-log fS_2, whereas those in the pyrrhotite field and near the pyrite-pyrrhotite boundary are more scattered and lie on a different log fO_2-log fS_2 trend. As no pyrrhotite was observed during petrological studies it can be concluded that the chlorites within the pyrrhotite field were not in equilibrium with sulphides. These chlorites

reflect different conditions of formation to those chlorites in apparent equilibrium with the mineralisation, possibly as a result of post-sulphide fluid mobilisation associated with shearing.

A linear distribution trend for the chlorite data is also illustrated by the log fO_2-temperature diagram (Fig. 19c). The trend is indicative of the tendency for the log fO_2 to decrease with temperature within a cooling hydrothermal system. Although recording higher temperatures fluid inclusion studies show a similar broad range of (homogenisation) temperatures, also reflecting a cooling hydrothermal system. The higher temperatures also possibly reflect paragenetically earlier quartz fluid inclusions associated with magnetite and hematite. The sericite data also display a range of temperatures, with the lower modal temperature distribution possibly reflecting matrix sericite's instability at temperatures >300°C (Hedges and Walshe, unpublished). The chlorite data plot mainly in the pyrite stability field and wholly within the chalcopyrite stability in the 200-350°C temperature range.

The shaded area within the log fO_2-pH diagram (Fig. 19e) constrains the probable fO_2 and pH conditions of the mineralising fluid, from which the bulk of the mineralisation was precipitated. Log fO_2 constraints were based upon the distribution of fO_2 data at 275°±5°C from Figure 19c. The broad pH range is defined by the presence of both kaolinite and sericite in the hydrothermal alteration zone.

The chlorite data and the proposed conditions for the mineralising fluids plot within the $\delta^{34}S_{H_2S}$=0‰ region in Figure 19d, demonstrating that H_2S was the dominant sulphur species and that $\delta^{34}S_{H_2S} \approx \delta^{34}S_{fluid}$. Isotopic fractionations between the sulphide phases and H_2S (Ohmoto and Rye, 1979), at 275°C are -0.2‰ between chalcopyrite and H_2S and 0.3‰ between pyrite and H_2S. The $\delta^{34}S_{cp}$ and $\delta^{34}S_{py}$ values are, therefore, close to $\delta^{34}S_{H_2S}$, which in turn approximates with the $\delta^{34}S_{fluid}$. The average $\delta^{34}S$ values of sulphide minerals for the Poona (1.4‰) and Wheal Hughes (4.9‰) mineralisation can, therefore, be taken as approximating the $\delta^{34}S_{fluid}$ for each deposit.

19a

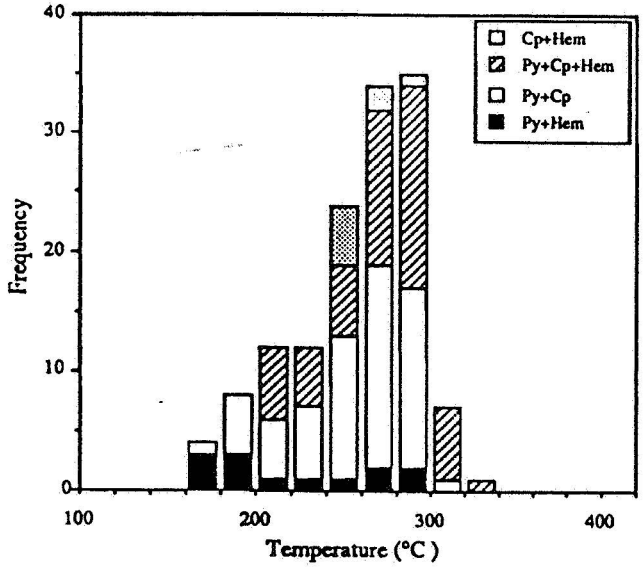

19b

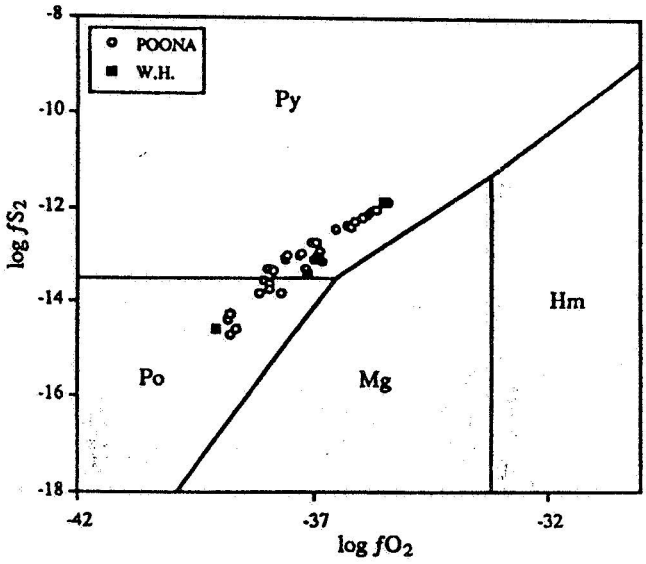

19c

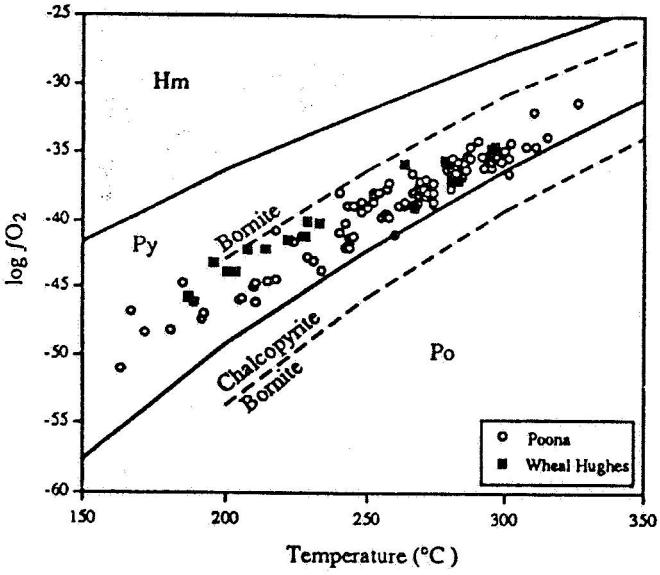

19d

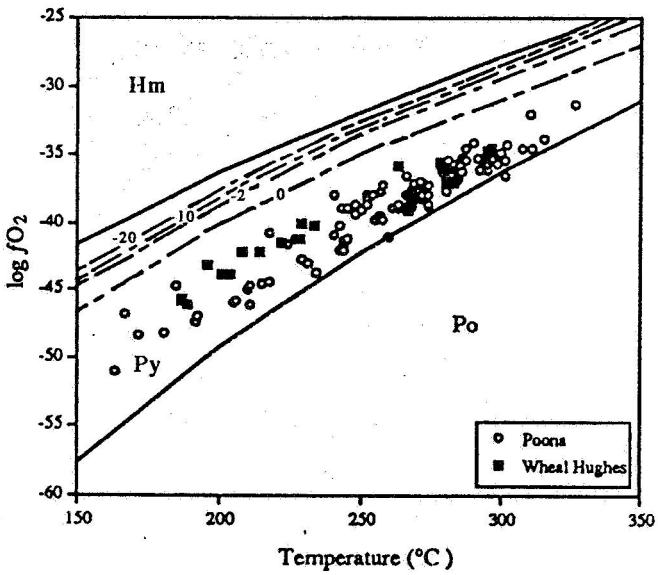

19e

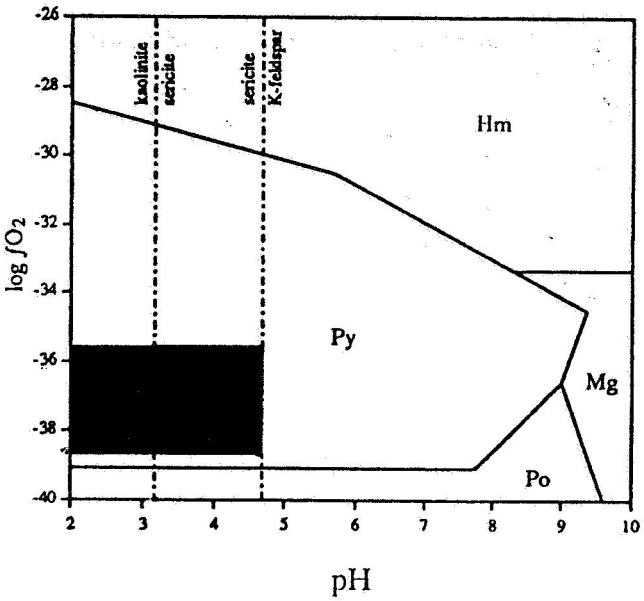

19f

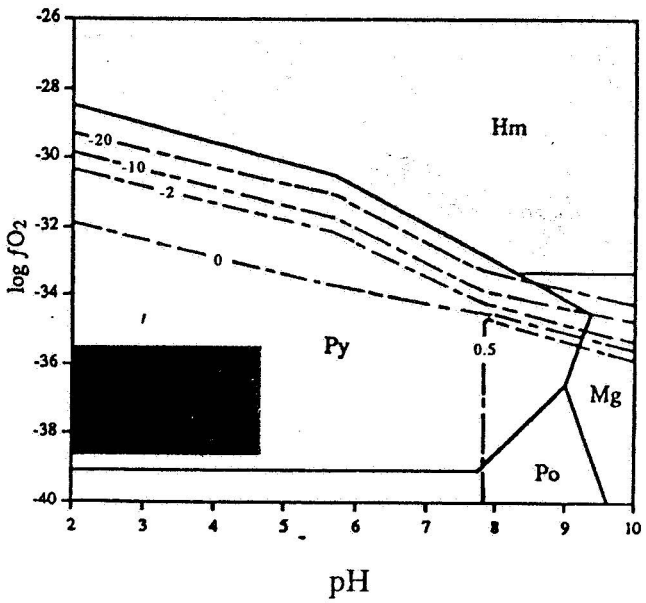

9.2 SOURCE FOR THE SULPHUR

The average $\delta^{34}S$ values for Poona and Wheal Hughes fall within the $\delta^{34}S$ range typical of sulphur derived from a magmatic source, viz. 0±5‰ (Nielsen, 1979). The sulphur associated with mineralisation at Poona is isotopically lighter than that from Wheal Hughes. This variation could be accounted for by a difference in the chemistry of the ore solutions, the chemical environment of the ore fluids (Rye and Ohmoto, 1974; Nielsen, 1979), host rock reactions or timing of the mineralisation (Ohmoto, 1972).

Thermodynamic calculations and geochemical modelling do not differentiate Poona from Wheal Hughes with respect to fO_2-fS_2-temperature-salinity-pH of the ore solutions. Mineralisation at both sites is open-fissure/filling vein style within shear zones, and hosted by the same formation. Consequently the ore fluids transgressed equivalent chemical environments.

Petrographic studies indicate similar ore mineralogies but in different proportions. The Poona lode has a larger component of oxide mineralogy relative to Wheal Hughes. The paragenetic sequence indicates that magnetite/hematite preceded deposition of copper mineralisation, hence the ore fluids at Poona may have reacted with the iron oxides which would have had the tendency to decrease the $\delta^{34}S$ values (Ohmoto, 1972).

The isotopically heavier sulphur content of the Wheal Hughes ore may be the result of reduced hydrothermal fluids mixing with groundwaters, which contaminated the fluids with heavier sulphur. The Wheal Hughes site was topographically lower relative to the Poona site, as indicated by the sedimentary units overlying the country rock at Wheal Hughes. This topographic low may have focussed groundwaters at the site of mineral deposition.

Variation in the $\delta^{34}S$ values can also be related to the timing of the mineralisation. The Poona lode may represent an earlier fractionation of sulphur mobilised from the source, thereby preferentially extracting isotopically lighter $\delta^{34}S$. Later fluid would tend to be isotopically heavier, as observed at Wheal Hughes.

Although the $\delta^{34}S$ values indicate a possible magmatic source for sulphur, the values may also reflect mixing of other hydrothermal fluids which equilibrated at ≈0‰. δD (‰) and $\delta^{18}O$ (‰) analyses of silicate minerals (eg. chlorite, sericite) need to be undertaken to determine if the transporting medium of the ore fluids was definitely magmatic fluid (Ohmoto, 1986).

9.3 GOLD SOLUBILITY

Gold is found in small quantities at Poona and Wheal Hughes and is mined as a by-product of copper. Huston and Large (1989) have shown that gold may be transported either as a $Au(HS)^-_2$ and/or $AuCl^-_2$ complex. The high salinity, low pH, moderate to high temperatures of the Poona and Wheal Hughes fluids, and the close association of gold with chalcopyrite, suggest that $AuCl^-_2$ was the dominant transporting complex of gold. Decreasing solubilities of the gold complex results from increasing pH and decreasing temperature and fO_2, leading to gold deposition. Fluid inclusion studies have shown that boiling occurred within the magmatic hydrothermal system. Boiling, and the associated decrease in temperature and increase in pH, was the most likely factor leading to the deposition of gold at Moonta.

GENESIS OF MINERALISATION

10.1 INTRODUCTION

Based upon the above data, a genetic model can be proposed for the mineralisation at Wheal Hughes and Poona, and possibly applied to all the lodes throughout the Moonta district. A number of questions need to be taken into account in considering the genesis of mineralisation:

(1) Metal/ligand source

(2) Metal transport

(3) Heat Source

(4) Migration of the mineralising fluid

(5) Metal deposition

10.2 METAL/LIGAND SOURCE

Previous investigators of the mineralisation in the Moonta-Wallaroo district have attributed several possible sources for the metals, ie.:

(1) late phase of the porphyry intrusion (Dickinson, 1942).

(2) remobilised from pre-existing submarine exhalative ores in the Doora Schist (Plimer, 1980).

(3) late stage magmatic product of Proterozoic granites (Jack, 1917; Lemar, 1975; Janz, 1990).

Sulphur isotope studies suggest a magmatic source for the sulphur. It is probable that the metal complexing ligands also had a magmatic source. The presence of molybdenite and its characteristic association with magmatic ores also suggests that the metals at Wheal Hughes had a magmatic source.

The evidence for a magmatic component in the ore fluids suggests a genetic association with the Proterozoic granites. Fractures resulting from the intrusion of the Proterozoic granites provided pathways for the migration of the hydrothermal fluids as well as sites for the deposition of the ore bodies.

10.2 METAL TRANSPORT

The fO_2-pH-T conditions outlined in section 9 and the high salinity of the transporting medium suggest that $AuCl^-_2$ was the dominant transporting complex of gold. Cu, Co, Fe and Ni would also have been transported as chloride complexes. Hematite daughter crystals associated with quartz suggest a fluid which was saturated in iron. H_2S was the dominant sulphur species.

10.3 HEAT SOURCE

There are two possible heat mechanisms which could have generated the hydrothermal system in the Moonta district:

(1) intrusion of an igneous body at depth

(2) dilatancy/fluid-diffusion

A granitic batholith, envisaged by Jack (1917) to have reached its maximum altitude near Arthurton, is considered to be one of the possible sources of heat in the Moonta region. The emplacement of a batholith at depth would have disrupted the local geothermal gradient and possibly generated a hydrothermal system involving a significant magmatic component. Cooling and contraction of the batholith after emplacement fractured the overlying country rock. Convection of fluids would have persisted well after the emplacement of the granites, focussing fluids within dilatant fractures and resulting in the deposition of orebodies within the fractures.

Alternatively the dilatantcy/fluid-diffusion model of Sibson et al. (1975) may have provided the mechanism for generating a heat source. The Wheal Hughes' lodes occupy dilatant fractures which localised subsequent deformations, ie. dextral strike-slip shearing and extensional down-dip slips. The principle of the model is based upon fluid migration to zones of lower fluid pressures, to deformation zones that have experienced dilation. With a rise in fluid pressure seismic failure may occur, expelling the fluids upward in the direction of easiest pressure relief. Mineralisation may develop on the fault plane and in connected extension fissures (Sibson et al., 1975).

10.4 METAL DEPOSITION

Metal deposition occurred as a consequence of a two step boiling process during fluid ascent along fracture conduits. Boiling results in the decrease in temperature and a corresponding rise in pH, which causes minerals to precipitate (Reed and Spycher, 1985). A two step boiling process involves the separation of gases (+ steam) from the liquid phase (Heinrich et al., 1989). Condensation and oxidation of the gas phase produces acid waters that trigger argillic alteration of the rocks (Reed and Spycher, 1985), a prominent feature of the Wheal Hughes deposit.

In addition to boiling, the precipitation of metal sulphides from a saline fluid accentuates the decline in reduced sulphur content. Gold deposition will consequently occur over a small temperature interval with adiabatic flashing and will be associated with metal sulphides, although initiation of sulphide deposition precedes that of gold (Heinrich et al., 1989).

Metal deposition proceeded in the sequence: magnetite→ hematite→ pyrite/marcasite→ hematite (Poona only)→ chalcopyrite/bornite/carrollite and gold.

11. CONCLUSIONS

(1) (a) The Moonta Porphyry is a composite igneous rock. Samples from Wheal Hughes and Poona display an ignimbrite texture of a welded tuff. Consequently the Moonta Porphyry has an extrusive origin in the vicinity of Wheal Hughes and Poona.

(b) Geochemical analysis indicates a rhyolite to rhyodacite/dacite composition for the porphyry.

(c) Tectonic discrimination diagrams suggest a within plate setting.

(2) An unmetamorphosed conglomeratic unit interbedded with sandstone unconformably overlies the Moonta Porphyry at Wheal Hughes. This sedimentary unit has been correlated with the Blue Range Beds (Corunna Conglomerate equivalents).

(3) A structural study of the mineralised veins at Wheal Hughes shows that they are structurally controlled by fracturing, which localised later deformation in the form of shearing and extensional dip slips.

(4) The paragenetic sequence of mineralisation is as follows: magnetite, hematite, pyrite+ marcasite, hematite (Poona), chalcopyrite+ bornite+ carrollite and gold. Three fracturing events interrupted mineralisation. The gangue minerals include chlorite, sericite, tourmaline, quartz, biotite and zircon.

(5) (a) The presence of primary vapour-rich fluid inclusions coexisting with liquid-rich inclusions is an indication of boiling of the hydrothermal fluids.

(b) The salinity of the hydrothermal fluid varied between 0.2 and 27.9 wt.% NaCl equivalent with a mean of 14.3 wt.%.

(c) Boiling and the consequent mineral deposition occurred at a minimum hydrostatic pressure of 61 to 182 bars, which corresponds to a depth of 620 to 1850 meters.

(6) (a) Chlorite precipitation occurred over the temperature range of 163° to 326°C at Poona and 187° to 296°C at Wheal Hughes.

(b)Sericite was deposited at temperatures of 220° to 258°C and 236° to 258°C at Poona Wheal Hughes, respectively.

(c) Cooling of the magmatic/hydrothermal fluid systematically lowered the oxidation state of the system, with log fO_2 values ranging from -31.4 to -50.9 and -34.6 to -46.1 at Poona and Wheal Hughes respectively

(d) Log fS_2 of the mineralising fluid declined with decreasing log fO_2 and temperature. Log fS_2 decreased in a linear fashion relative to log fO_2. Two apparent linear associations were detected, with the lower values reflecting different conditions of formation, possibly as a result of later fluid mobilisation associated with shearing.

(e) The pH of the fluid was within the range 2.0 to 4.6.

(f) H_2S was the dominant sulphur species of the fluid.

(7) The sulphur component of the sulphides had a probable magmatic origin. The difference in $\delta^{34}S$ characteristics for Poona and Wheal Hughes are a feature of either contamination from groundwater, timing of mineralisation or reaction of a later mineralising event with iron oxides.

(8) The geological setting, composition of tourmaline, source of sulphur and the presence of molybdenite indicate a magmatic source for the hydrothermal fluid and its component metals and metal complexing ligands.

(9) Two possible heat mechanisms generated the hydrothermal system in the Moonta district: the disruption of the geothermal gradient by the intrusion of an igneous body at depth or a dilatancy/fluid diffusion process. In either case, the heat source generated a hydrothermal system which focussed mineralising fluids into dilatant fractures, effectively localising the mineralisation.

ACKNOWLEDGEMENTS

I would like to acknowledge Moonta Mining Joint Venture for making this project available and in providing me support for the duration of the project. I wish to thank Dennis, Irene, Trevor and Rob for making my stay enjoyable, Brian for his assistance and discussions about the mines, Trish for attempting to make a real Geo out of me, and Chaz and Ron for putting up with me as a room-mate during my stay.

Ross Both receives my sincerest gratitude for his invaluable advice, criticism, humour, patience and understanding throughout the year. He has stoked up my enthusiasm in the pursuit of knowledge. I could not have asked for more of a supervisor, thanks Ross.

I wish to convey my appreciation to the many people who inhabit the Geology department for their help and advice, whose characters and personalities ranged from the strange and unbelievable to friendly and supportive. Special thanks go to the following:

Dr. Keith Turnball for help with the sulphur isotopes

Wayne Mussared and Geoff Trevellyn for thin sections

Rick Barrett for the photography

Sherry Proferes for advice on drafting

John Stanely and Phil McDuie for XRF and XRD

John Willoughby for being John Willoughby

My thanks are also extended to Drs. John Foden, Mike Sandiford, Nick Lemon and Pat James for their advice, and Kathy Stewart and Thomas Flöttman for valuable discussions during the year. Huw Rosser of the Electron Optical Centre receives my special thanks for his advice and allowing me to get off lightly when I crashed his system. Jo Janz's (SADME) continued interest was appreciated during the year.

I would like to thank my fellow Honour students in making this year a most enjoyable and rewarding experience. I would also like to acknowledge Andrew Cooper of the NCPGG and future honour students Kirrilie and Scott who helped break the monotony of the long nights, and reminded me to look at the lighter side of life. Elle McPherson is also acknowledged for her timely appearance, which made me forget about geology for at least a few hours.

Finally, I would like to express my gratitude to my family, particularly to my mother who has had the most traumatic year of her life. I can't say enough to express my gratitude for their support, without which my University career would not have been made possible.

REFERENCES:

Barton, P.B., (1984), Redox reactions in hydrothermal fluids, **In**: Fluid-mineral equilibria in hydrothermal systems, Robertson, J.M.(Ed.). Rev.Econ.Geol., 1, 99-113.

Bates, R.L. and Jackson, J.A., (1984), Dictionary of geological terms. Anchor Press, New York.

Bodnar, R.J., Reynolds, T.J. & Kuelin, C.A., (1985), Fluid inclusion systematics in epithermal systems. **In**: Geology and Geochemistry of epithermal systems. Ed. B.R. Berger & P.M. Bethke. Rev.Econ.Geol., 2, 73-97.

Bone, Y., (1984), The Wardang volcanics, Wardang Island, Yorke Peninsula. S.A.Geol.Surv.Quart.Geol.Notes., 89, 2-7.

Bone, Y., (1988), The geological setting of tourmalinite at Rum Jungle, N.T., Australia- genetic and economic implications. Min. Deposita, 23, 34-41.

Cooke, J., (1990), MMJV- Wheal Hughes: ore reserve calculation. Unpublished company report.

Crawford, A.R., (1965), The geology of York Peninsula. Bull.Geol.Surv.S.A., 39, 13-56.

Crawford, M.L., (1981), Phase equilibria in aqueous fluid inclusions. **In**: Applications to petrology. Ed. L.S. Hollister & M.L. Crawford, Min.Assoc.Can., 6, 75-100.

Creaser, R.A., (1989), The geology and petrology of Middle Proterozoic felsic magmatism of the Stuart Shelf, South Australia. Ph.D.thesis, La Trobe University.

Deer, W.A., Howie, R.A, and Zussman, J., (1967), An introduction to the rock forming minerals. Longmans, London, 528p.

Dickinson, S.B., (1942), The Wallaroo- Moonta copper mining field, part 1, **In:** The structural control of ore deposition in some South Australian copper fields. Geol. Surv. S. Aust. Bull., 20, 7-39.

Dickinson, S.B., (1953), The Moonta and Wallaroo copper mines, **In**: Edwards, A.B. (ed.), Geolgy of Australian Ore Deposits, 5th Emp. Min. Metal. Congr., 1, 487-504. Melbourne: Australasian Institute of Mining and Metallurgy

Ethier, V.G. and Campbell, F.A., (1977), Tourmaline concentrations in Proterozoic sediments of the southern Cordillera of Canada and their economic significance. Can.J.Earth.Sci., 14, 10, 2348-2363.

Fanning, C.M., Flint, R.B., Parker, A.J., Ludwig, K.R. and Blissett, A.H.,. (1988), Refined Proterozoic evolution of the Gawler Craton, South Australia, through U-Pb Zircon geochronology. Precamb.Res., 40/41, 363-386.

Flint, R.B. and Parker, A.J., (1981), The Blue Range Beds, central Eyre Peninsula. Geol. Quart. Notes, 80, 12-15.

Gerdes, R.A., (1983), A geophysical and geological interpretation of the Wallaroo- Moonta province in South Australia. MSc thesis, University of Adelaide.

Gibson, R.G., (1990), Nucleation and growth of retrograde shear zones: an example from the Needle Mountains, Colorado, U.S.A. J.Struct.Geol., 12, 339-350.

Glen, R.A., Laing, W. P., Parker, A.J. and Rutland, R.W.R., (1977), Tectonic relationships between the Proterozic Gawler and Willyama orogenic domains, Australia. J.Geol.Soc.Aust., 24, 3, 125-150.

Goldstein, A.G., (1988), Factors affecting the kinematic interpretation of asymmetric boudinage in shear zones. J.Struct.Geol., 10, 707-715.

Haas, J.L., (1971), The effect of salinity on the maximum thermal gradient of a hydrothermal system at hydrostatic pressure. Econ.Geol, 66, 940-946.

Hedges, M.M. and Walshe, J.L., (1986), Progress in the development of a seven-component solid solution model for muscovite. (Unpublished report), Australian National University.

Heinrich, C.A., Henley, R.W. and Seward, T.M., (1989), Hydrothermal systems (unpublished). AMF, 74p.

Henry, D.J. and Guidotti, C.V., (1985), Tourmaline as a petrogenetic indicator mineral: an example from the staurolite-grade metapelites of NW Maine. Am.Min., 70, 1-15.

Hobbs, B.E., Means, W.D.M. and Williams, P.F., (1976), An outline of structural geology. John Wiley and sons, USA, 571p.

Huston, D.L. and Large, R.R., (1989), A chemical model for the concentration of gold in volcanogenic massive sulphide deposits. Ore Geol.Rev., 4, 171-200.

Jack, R.L., (1917), The geology of the Moonta and Wallaroo mining district, Geol. Surv. S. Aust. Bull., 6, 135 p.

Janz, J., (1990), The Mineralogy and Paragenesis of the Poona Mine Copper Deposit. B.Sc.(Hons) thesis, Flinders University of South Australia.

Jensen, M.L. and Bateman, A.M., (1981), Economic mineral deposits. John Wiley and Sons, USA.

Lemar, R.C., (1975), The origin of the Moonta Porphyry. Grad. Dipl. thesis, South Australian Institute of Technology, 56p.

Lynch, R.E., (1982), An interpretation of the geology and mineralisation of northern Yorke Peninsula, S.A., MSc. thesis, James Cook University.

Martel, S.J., (1990), Formation of compound strike-slip fault zones, Mount Abbot quadrangle, California. J.Struct.Geol., 12, 869-882.

McBriar, E.M., (1962), Primary copper mineralisation at Moonta and Wallaroo, South Australia. MSc. thesis, University of Adelaide.

McClay, K., (1989), The mapping of geological structures. Geological Society of London Handbook, Open University Press, England.

Nielsen, H., (1979), Sulphur Isotopes. **In**: Lectures in isotope geology. Ed: E.Jaeger & J.C. Hunziker. Springer-Verlag publishers, 283-313.

Nicholson, R., (1991), Vein morphology, host rock deformation and the origin of the fabrics of échelon mineral veins. J.Struct.Geol., 13, 635-641.

Ohmoto, H., (1972), Systematics of sulphur and carbon isotopes in hydrothermal ore deposits. Econ.Geol., 65, 551-578.

Ohmoto, H., (1986), Stable isotope geochemistry of ore deposits. **In**: Stable isotopes in high temperature geological processes. Ed: J.W. Valley, H.P. Taylor & J.R. O'Niell. Rev.Min., 16, Min.Soc.Amer., 491-559.

Ohmoto, H., Mizukami, M., Drummond, S.E., Eldridge, C.S., Pisutha-Arnond, V. & Lenagh, T.C., (1983), Chemical processes of Kuroko formation. Econ.Geol., Mon.5, 570-604.

Ohmoto, H. & Rye, R.O., (1979), Isotopes of sulphur and carbon. **In:** Geochemistry of hydrothermal ore deposits. H.L. Barnes (Ed.). John Wiley & Sons publishers, 509-567.

Olson, J.E. and Pollard, D.D., (1991), The initiation and growth of en échelon veins. J.Struct.Geol., 13, 595-608.

Parker, A.J., (1990), Gawler Craton and Stuart Shelf-regional geology and mineralisation. **In:** Geology of the mineral deposits of Australia and Papua New Guinea, Mon 14. Hughes F.E. (Ed.), Australasian Institute of Mining and Metallurgy.

Pearce, J.A., Harris, N.B.W. and Tindle, A. G., (1984), Trace element discrimination diagrams for the tectonic interpretation of granitic rocks. J.Pet., 25, Part 4, 956-983.

Pisutha-Arnond, V. & Ohmoto, H., (1983), Thermal history, and chemical and isotopic compositions of the ore-forming fluids responsible for the Kuroko massive sulphide deposits in the Hokuroku District of Japan. Econ.Geol.Mon., 5, 523-558.

Plimer, I.R., (1980), Moonta-Wallaroo District, Gawler Block, South Australia: A review of the geology, ore deposits and untested potential of EL 544. . North Broken Hill Report, S.A.D.M.E. (unpublished report).

Plimer, I.R., (1988), Tourmalinites associated with Australian Proterozoic submarine exhalative ores. Base metal sulphide deposits, 255-283.

Potter, R.W., (1978), Freezing point depressionof aqueous sodium chloride solution. Econ.Geol., 73, No 2, 284-285.

Pring, A., (1988), Minerals of the Moonta and Wallaroo mining districts, South Australia. Min.Rec., 19, 407-416.

Pryor, O., (1962), Australia's little Cornwall. Rigby, Adelaide.

Reed, M.H. and Spycher, N.F., (1985), Boiling, cooling and oxidation in epithermal systems: a numerical approach. **In:** Geology and geochemistry of epithermal systems, B.R. Berger and P.M. Bethke (Ed.). Rev. Eco. Geo., 2, 249-272 p.

Robinson, B.W. and Kusakabe, M., (1975), Quantitative preparation of sulphur dioxide, for $^{34}S/^{32}S$ analyses, from sulphides by combustion cuprous oxide. Anal.Chem., 47, 1179-1181.

Rye, R.O., and Ohmoto, H., (1974), Sulfur and carbon isotopes and Ore Genesis. Econ.Geo., 69, 826-842 pp.

Segall, P. and Simpson, C., (1986), Nucleation of ductile shear zones on dilatant fractures. Geol., 14, 56-59.

Shepherd, T.J., Rankin, A.H. & Alderton, D.H.M., (1985), A practical guide to fluid inclusion studies. Blackie & Sons publishers, 232p.

Sibson, R.H., Moore, J. McM. and Rankin, A. H., (1975), Seismic pumping - a hydrothermal fluid transport mechanism. J.Geol.Soc.Lond., 131, 653-659.

Simpson, C., (1986), Fabric development in brittle-to-ductile shear zones. PAGEOPH, 124, Nos 1/2, 269-287.

Walshe, J.L., (1986), A six-component solid solution model and the conditions of chlorite formation in hydrothermal systems. Econ.Geol., 81, 681-703.

Ward, L.K. and Jack, R.L., (1912), The Yelta and Paramatta Mines. Rep. Geol. Surv. S. Aust., 1, 18p.

Webb, A.W., (1979), A geochronological investigation of the tectono-magmatic history of the Gawler Craton. Geol.Soc.Aust.Abs., Symposium to the Gawler Craton-extended abstracts.

Webb, A.W., T. B. P., Blissett, A.H., Daly, S.J., Flint, R.B. and Parker, A.J.,. (1986), Geochronology of the Gawler Craton, South Australia. Aust.J.Earth.Sci., 33, 119-143.

Winchester, J.A. and Floyd, P.A., (1977), Geochemical discrimination of different magma series and their differentiation products using immobile elements. Chem. Geol., 20, 325-343.

W.M.C., (1987), Moonta Joint Venture, South Australia. Project information brochure, Western Mining Corporation- exploration division.

SAMPLE LOCATION MAP - WHEAL HUGHES

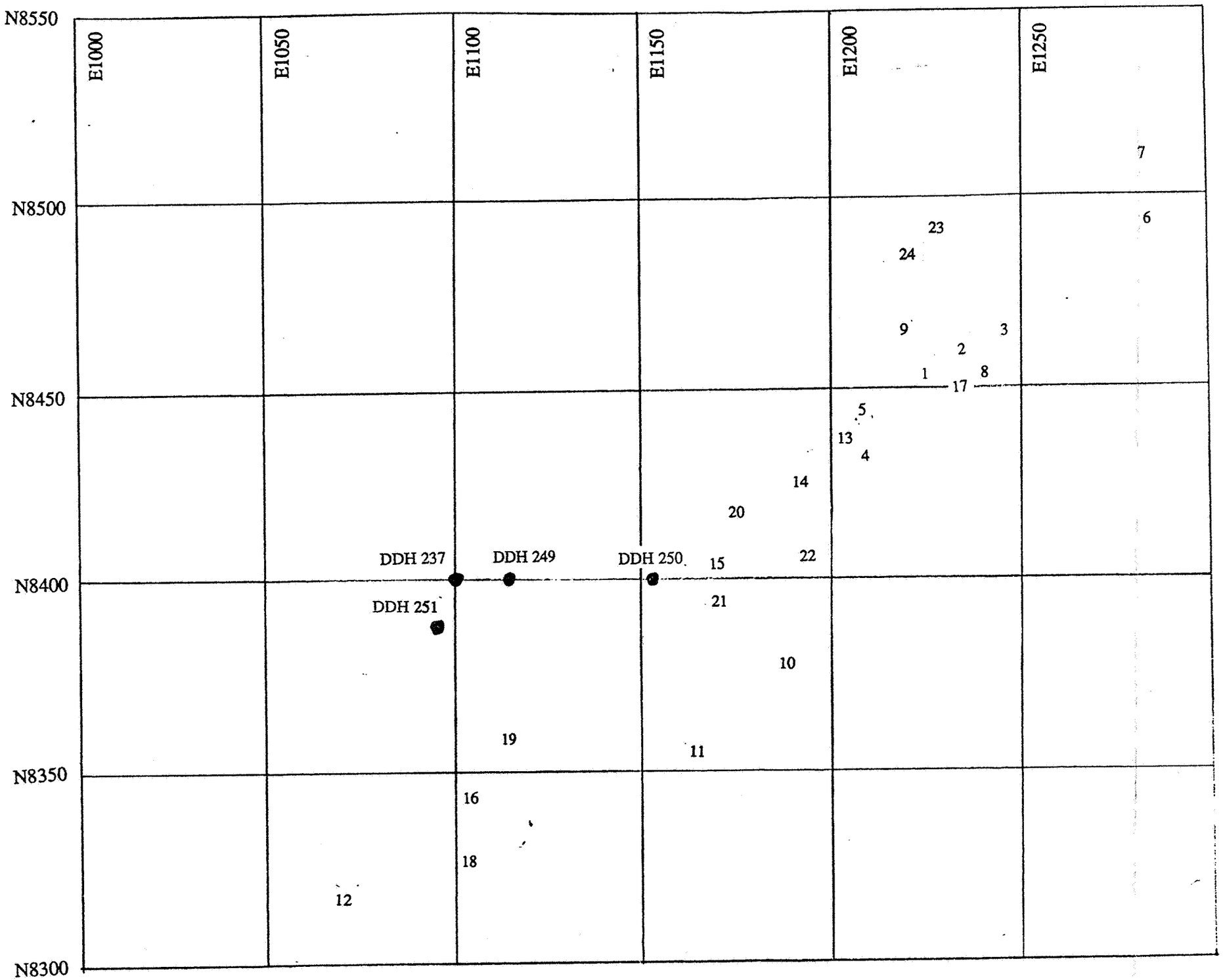

R.L. 14.7 - 15.9

Location	Sample (953-)
1	7, 8
2	10, 11, 12, 13, 38
3	15, 16, 17, 19
4	2
5	2
6	3
7	40, 41, 43, 45, 48, 118
8	5
9	5
10	5
1	62, 63
12	55, 56
1	6
1	6
1	69
16	8
1	116
1	117

R.L. 15.7 - 19.7

Location	Sample (953-)
19	119, 120
2	121
2	12
2	123
2	125
2	12

DDH 237

Depth (m)	Sample (953-)
64.6	128
66.6	129

DDH 249

Depth (m)	Sample (953-)
68.8	131

DDH 250

Depth (m)	Sample (953-)
51.4	130

DDH 251

Depth (m)	Sample (953-)
52.3	133
63.5	132

POONA ORE AND PORPHYRY SAMPLES

Samples located within the Poona underground mining operations

953-	
	DDH 233
100	953-145 → 147.8m
	DDH 239
102	
104	953-146 → 113.1m
	DDH 238
105	
106	953-147 → 111.1m
	DDH 240
107	
108	953-148 → 92.9m
114	953-149 → 91.9m
	DDH 236
121	
122	953-150 → 85.5m
	DDH 234
123	
124	953-151 → 124.6m
	DDH 248
154	
155	953-152 → 30.2m
	DDH 245
156	
157	953-153 → 73.3m

APPENDIX 1

MOONTA-WALLAROO LODE DISTRIBUTION

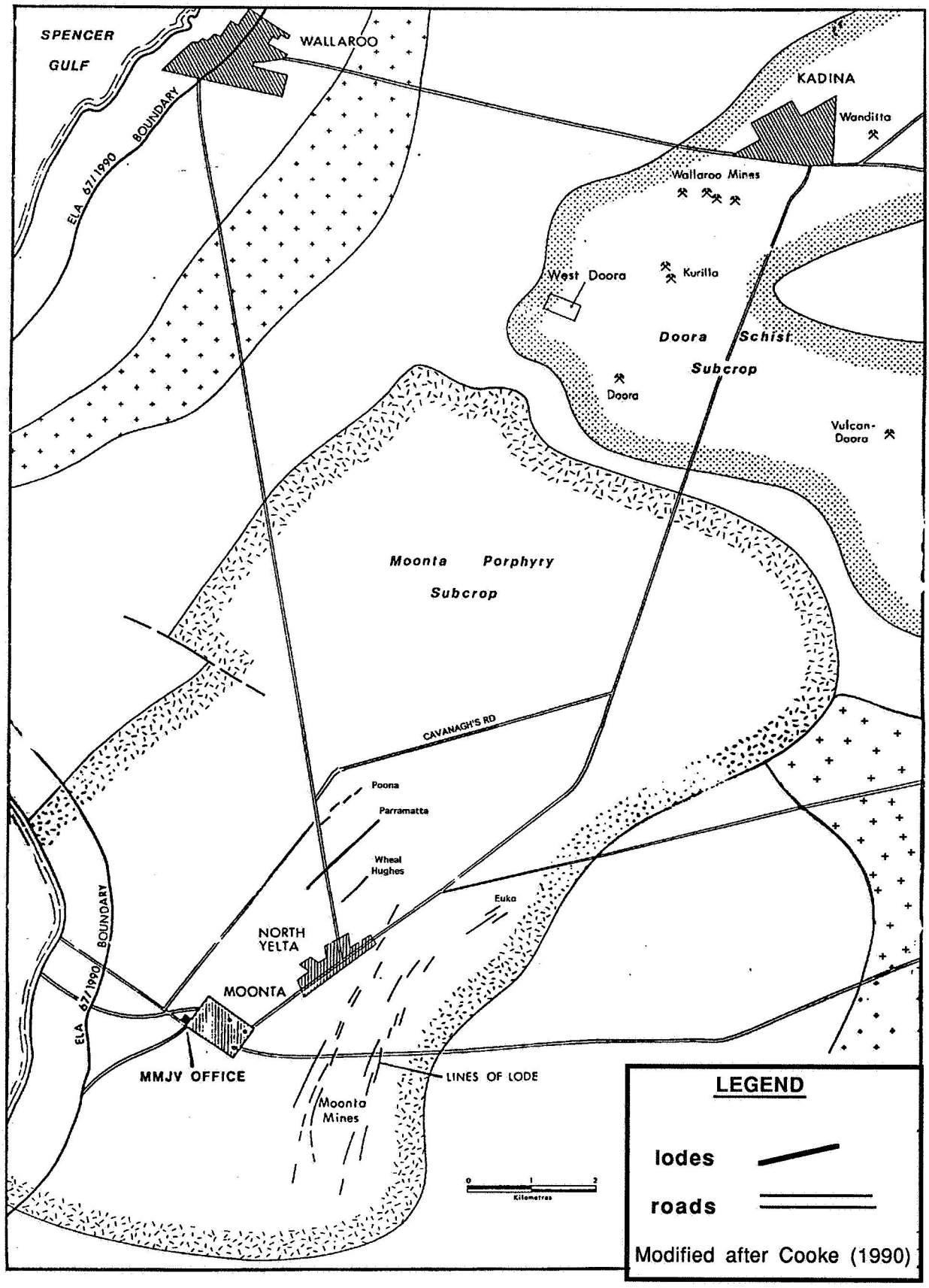

WALLAROO - MOONTA LODE DISTRIBUTION MAP

APPENDIX 2

SELECTED NORMAL THIN SECTION DESCRIPTIONS

SAMPLE- 953-051

LOCATION: Wheal Hughes open-pit

HAND-SPECIMEN: Pink to red/brown fine grained matrix, with sub- to euhedral phenocrysts, white to pink in colour. Green to black aligned, discontinuous lenticles are found wrapped around feldspar phenocrysts. The lenticles range up to 0.4 x 1.5cm in dimension and give the specimen an ignimbrite texture of a welded tuff.

THIN-SECTION: Phenocrysts of plagioclase (up to 5mm) composition predominate within the aphanitic matrix as isolated (resorbed) and glomeroporphyritic grains. The phenocrysts are fractured and these fractures have been infilled by quartz and chlorite. Alteration of the feldspar porphyry involved moderate sericitisation of the phenocrysts and chlorite alteration. Linear and serrated quartz grains are found transgressing the matrix and wrapped around phenocrysts, these resemble flattened pumice fragments-relic primary igneous texture. 1.5x10mm linear aggregates of quartz, k-feldspar and clots of chlorite may represent infilling of a vesicle which was subsequently flattened.

Phenocrysts-10%
- plagioclase 80%
- k-feldspar 20%

Aphanitic groundmass-90%
- feldspars and quartz 80%
- chlorite 10%
- opaques (hematite) 5%
- sericite 4%
- biotite ..... tr

Interpretation: The rhyolite/rhyodacite is possibly an ignimbrite displaying eutaxitic textures.

SAMPLE- 953-025

LOCATION: Wheal Hughes open-pit

HAND-SPECIMEN: A dark brown porphyritic rhyolite. Grey-brown linear lenticles are found defining a foliation and wrapping around pink, randomly distributed feldspar phenocrysts, within an aphanitic groundmass

THIN-SECTION: The extremely fine groundmass contains subhedral, granoblastic and isolated alkali feldspars. The feldspars are up to 4 mm in diameter and have been moderately

sericitised. Aligned chlorite grains and disseminated opaques are distributed throughout the groundmass. Possible relic primary igneous textures are distributed within the granophyric groundmass as; large clots of chlorite, quartz and opaques resembling infilled vesicles, and serrated edged linear quartz grains wrapping around the phenocrysts, resembling flattened pumice fragments. A red colouration is observed, possibly due to the oxidation of iron within the feldspars distributed throughout the groundmass.

Phenocrysts-10%
- plagioclase.....70%
- k-feldspar.....30%

Aphanitic groundmass-90%
- feldspars and quartz.....92%
- chlorite.....5%
- opaques (hematite).....2%
- zircons.....tr
- sericite.....tr

Interpretation: Relic primary structures possibly define an extrusive origin for the rhyolite/rhyodacite

SAMPLE- 953-063

LOCATION: Wheal Hughes open-pit

HAND-SPECIMEN: Fresh, light brown rock that has undergone very little alteration. Euhedral to subhedral coarse phenocrysts are randomly scattered within an extremely fine grained matrix. Dark discontinuous lenticles are aligned within the groundmass, wrapping around pink to white feldspar phenocrysts.

THIN-SECTION: Phenocrysts range from 1 to 5mm in diameter, of predominantly sodic to potassic compositions. They occur as glomeroporphyritic and isolated embayed grains, which have undergone minor sericitisation. Quartz and chlorite are found infilling fractures of the phenocrysts. A relatively high component of opaques are randomly distributed in the matrix and associated with chlorite and quartz aggregates.

Phenocrysts-4%
- plagioclase.....85%
- k-feldspar.....15%

Aphanitic groundmass-96%

feldspars and quartz	86%
opaques (hematite)	10%
chlorite	3%
sericite	tr

Interpretation: Textures indicate an extrusive origin of the countryrock, the feldspar porphyry.

SAMPLE- 953-666

LOCATION: Wheal Hughes open-pit

HAND-SPECIMEN: Relatively fresh pink/brown rhyolite, pink phenocrysts ranging from 1-7mm in diameter are randomly distributed throughout the matrix. A chalcopyrite and minor pyrite vein associated with tourmaline transgresses the porphyry, with minor disseminations adjacent to the mineralised vein. The reddish colouration is possibly due to the oxidation of iron within the feldspars of the matrix.

THIN-SECTION: The phenocrysts are relatively pristine euhedral to subhedral grains of potassic to sodic compositions. The phenocrysts are predominantly plagioclases occurring as isolated and glomeroporphyritic clusters. Fractured tourmaline grains are closely associated with the opaque mineralisation. Chlorites are distributed within the matrix with a preferred orientation and are found to be closely associated with the opaques and infill fractures of the phenocrysts and tourmalines.

Phenocrysts-5%

plagioclase	85%
k-feldspar	15%

Aphanitic groundmass-95%

feldspars and quartz	80%
opaques	12%
chlorite	5%
tourmaline	2%
zircons	tr
sericite	tr

Interpretation: Feldspar porphyry that has been transected by a mineralised vein displays hydrothermal alteration, as chloritisation and tourmalinisation (metasomatism).

APPENDIX 3

SELECTED POLISHED THIN SECTION DESCRIPTIONS

SAMPLE: 953-124

LOCATION: Poona Mine, underground

MACROSCOPIC: Black coated (covellite) massive ore, impregnated with quartz. The sample is composed of chalcopyrite, bornite and minor pyrite. The massive bornite results in a brittle texture and fresh surfaces are readily tarnished.

MICROSCOPIC: The copper ore consists predominantly of massive and disseminated chalcopyrite and bornite distributed in approximately equal proportions throughout the section. Chalcopyrite and bornite are closely inter-related, with smooth continuous boundary contacts suggesting contemporaneous precipitation. Subhedral to anhedral pyrite grains are disseminated throughout the section and have been fractured and replaced by a later mineralisation phase; chalcopyrite, carrollite and bornite infill these fractures. Light gray carrollite is observed to occur along boundaries and fractures of pyrite grains, possibly reflecting reaction fronts (?) of a later sulphide phase (which precipitated chalcopyrite) with the pyrite grains. Dark blue radiating covellite and gray/blue digenite are the main supergene alteration products of the mineralisation. Digenite is found to preferentially alter the bornite and covellite the chalcopyrite, along fractures and grain boundaries. Quartz and tourmaline are found associated with the mineralisation.

Quartz.....44%
Chalcopyrite.....18%
Pyrite.....12%
Bornite.....9%
Covellite.....7%
Digenite.....6%
Carrollite.....2%
Tourmaline.....1%

SAMPLE: 953-013

LOCATION: Wheal Hughes, open-pit (Leighton's lode)→~18m R.L.

MACROSCOPIC: Ore sample dominated by chalcopyrite, supergene covellite upon the surfaces, with randomly distributed pyrite crystals. Mineralisation is associated with an abundance of quartz and medium to coarse grained tourmaline.

MICROSCOPIC: Tourmalinisation accompanied and preceded mineralisation, as pyrite and chalcopyrite are observed to occur within fractures of the silicates and possessing continuous boundaries with the chalcopyrite. Blue/gray laths and subhedral, fractured hematite crystals are replaced by chalcopyrite. Euhedral to subhedral fractured pyrite grains, up to 4mm in size, are found scattered throughout the massive chalcopyrite, with chalcopyrite, quartz and tourmaline infilling the fractures. Covellite is the supergene alteration assemblage of chalcopyrite, with alteration occurring along fracture boundaries.

Tourmaline.....40%
Chalcopyrite.....25%
Quartz.....18%
Pyrite.....10%
Covellite.....5%
Hematite.....2%

SAMPLE: 953-132

LOCATION: Wheal Hughes-DDH 251,63.45m

MACROSCOPIC: Aggregates of coarse tourmaline crystals are found adjacent to chalcopyrite pods and veins, the country rock has been intensely metasomatised.

MICROSCOPIC: Anhedral chalcopyrite fragments are disseminated throughout the section and subhedral pyrite grains up to 3 mm in diameter are scattered within the chalcopyrite. Anhedral hematite grains are distributed within the gangue, which is comprised of tourmaline, quartz, silicified quartz, chlorite and zircons. Remnant magnetites are present within the hematite, the result of hydrothermal alteration. The hematite has been fractured and replaced by chalcopyrite.

Quartz.....42%
Tourmaline.....30%
Chalcopyrite.....10%
Pyrite.....7%
Silicified biotite.....5%
Chlorite.....3%

Hematite 2%
Covellite 1%
Gold ..... acc
Zircon ..... acc

SAMPLE: 953-114a

LOCATION: Poona underground

MACROSCOPIC: Green, highly chloritised ore associated with quartz veining.

MICROSCOPIC: Chalcopyrite, pyrite and hematite are the principal sulphide and oxide minerals respectively. Continuous grain boundaries between the quartz and hematite minerals are observed. Magnetite remnants are hosted by the hematite as hydrothermal alteration relics. Hematite and pyrite have been intensely fractured with chalcopyrite, chlorite and quartz precipitating within these fractures. The specimen has undergone pervasive chloritisation with chlorite precipitated at all stages of the paragenetic sequence, as evidenced by chlorite occurring in fractures and throughout the matrix.

Chlorite 40%
Quartz 33%
Chalcopyrite 10%
Hematite 9%
Pyrite 6%
Covellite 1%
Magnetite 1%

SAMPLE: 953-017

LOCATION: Wheal Hughes, open-pit (Leighton's lode)→~18m R.L.

MACROSCOPIC: Primary mineralisation, dominantly quartz-rich with stringers of tourmaline and disseminated clots of tourmaline.

MICROSCOPIC: The matrix consists of quartz, tourmaline and fine grained muscovite (sericite). Hematite and pyrite have been fractured and infilled by quartz and chalcopyrite, hematite is found scattered in the chalcopyrite and gangue, indicating intense replacement of the iron oxide. Fibrous biotite textures are found distributed in the

matrix, it has undergone silicification, displaying undulose extinction. In places the silicified biotite has also been sericitised, with birefringent sericite observed along the grain boundaries.

Quartz	65%
Tourmaline	10%
Chalcopyrite	8%
Silicified biotite	6%
Pyrite	4%
Sericite	3%
Covellite	1%

SAMPLE: 953-149

LOCATION: Poona- DDH 240, 92.90m

MACROSCOPIC: Massive ore, consisting of chalcopyrite and fragments of pyrite within the specimen.

MICROSCOPIC: Subhedral to anhedral pyrite grains, up to 1cm in size and traces of marcasite have been intensely fractured and replaced by chalcopyrite and its co-precipitates, consisting of bornite and carrollite. Bornite occurs as small inclusions within the chalcopyrite, with smooth boundaries. The matrix consists largely of quartz, chlorite, tourmaline and sericite, which are closely associated with the mineralisation.

APPENDIX 4

POLISHED BLOCK DESCIPTIONS

SAMPLE: 953-114b

LOCATION: Poona mine-underground

MACROSCOPIC: Massive iron-ore, with minor kaolinitic alteration.

MICROSCOPIC: Hematite is the dominant ore mineral, with minor inclusions of pyrite, chalcopyrite and magnetite. Two distinct generations of hematite are observed:

(1) Massive, hydrothermal alteration product of magnetite, as indicated by randomly distributed remnant anhedral magnetite relics within the hematite. Chalcopyrite, pyrite and gangue infill fractures of the hematite.

(2) A later generation of thin tabular hematite intergrowths, creating a lamellae network within open fracture systems.

The hematite lamellae has "grown" around subhedral pyrite grains, indicating that pyrite preceded the second generation hematite. Chalcopyrite later filled the cavities of the network. Covellite is found surrounding grain boundaries of the chalcopyrite.

Hematite	55%
Chalcopyrite	23%
Gangue	10%
Pyrite	6%
Magnetite	5%
Covellite	1%

SAMPLE: 953-069a

LOCATION: Wheal Hughes open-pit (Wheal Hughes lode)→~14m R.L.

MACROSCOPIC: Highly altered, supergene enriched ore.

MICROSCOPIC: Very intense supergene alteration of the main sulphide, chalcopyrite, with covellite comprising a considerable proportion of the total mineral composition. Covellite is only observed altering the chalcopyrite, with remnant chalcopyrite disseminated within the covellite, with isolated subhedral pyrite grains unaffected by the alteration. Minor inclusions of bornite and carrollite are found within the massive chalcopyrite. Carrollite has a preferential association with pyrite.

Chalcopyrite	40%
Pyrite	20%
Gangue	20%
Covellite	18%
Carrollite	2%
Bornite	acc

SAMPLE: 953-105b

LOCATION: Poona mine-underground

MACROSCOPIC: Massive ore, consisting predominantly of chalcopyrite with disseminations of euhedral pyrite and quartz inclusions.

MICROSCOPIC: Subhedral hematite grains, averaging 0.08mm, are found scattered throughout the gangue assemblages. The gangue is closely associated with the mineralisation, infilling fractures. A mineral whiter and brighter than pyrite is found within the chalcopyrite, which has been tentatively identified as marcasite. The marcasite has been fractured and subsequently filled by carrollite and chalcopyrite, consequently it pre-dates the chalcopyrite. Traces of gold, small inclusions of bornite and carrollite have been identified within the chalcopyrite. Minor covellite alteration of the chalcopyrite has occurred.

Chalcopyrite	50%
Pyrite	35%
Gangue	7%
Marcasite	3%
Carrollite	2%
Hematite	1%
Covellite	1%
Gold	acc
Bornite	acc

SAMPLE: 953-069b

LOCATION: Wheal Hughes mine-underground (Wheal Hughes lode)→~14m R.L.

MACROSCOPIC: Supergene enriched ore.

MICROSCOPIC: Intensely blue/purple radiating and massive coveelite crystals have pervasively altered the copper mineralisation. Brown/orange inclusions are distributed within the chalcopyrite. Carrollite is found closely associated with pyrite, bounding the grain boundaries and filling fractures, possibly a reaction front mineral.

Chalcopyrite	44%
Gangue	20%
Covellite	20%
Pyrite	15%
Carrollite	1%
Bornite	acc

APPENDIX 5

WHEAL HUGHES CROSS-SECTIONS

WHEAL HUGHES: CROSS-SECTION A-A'

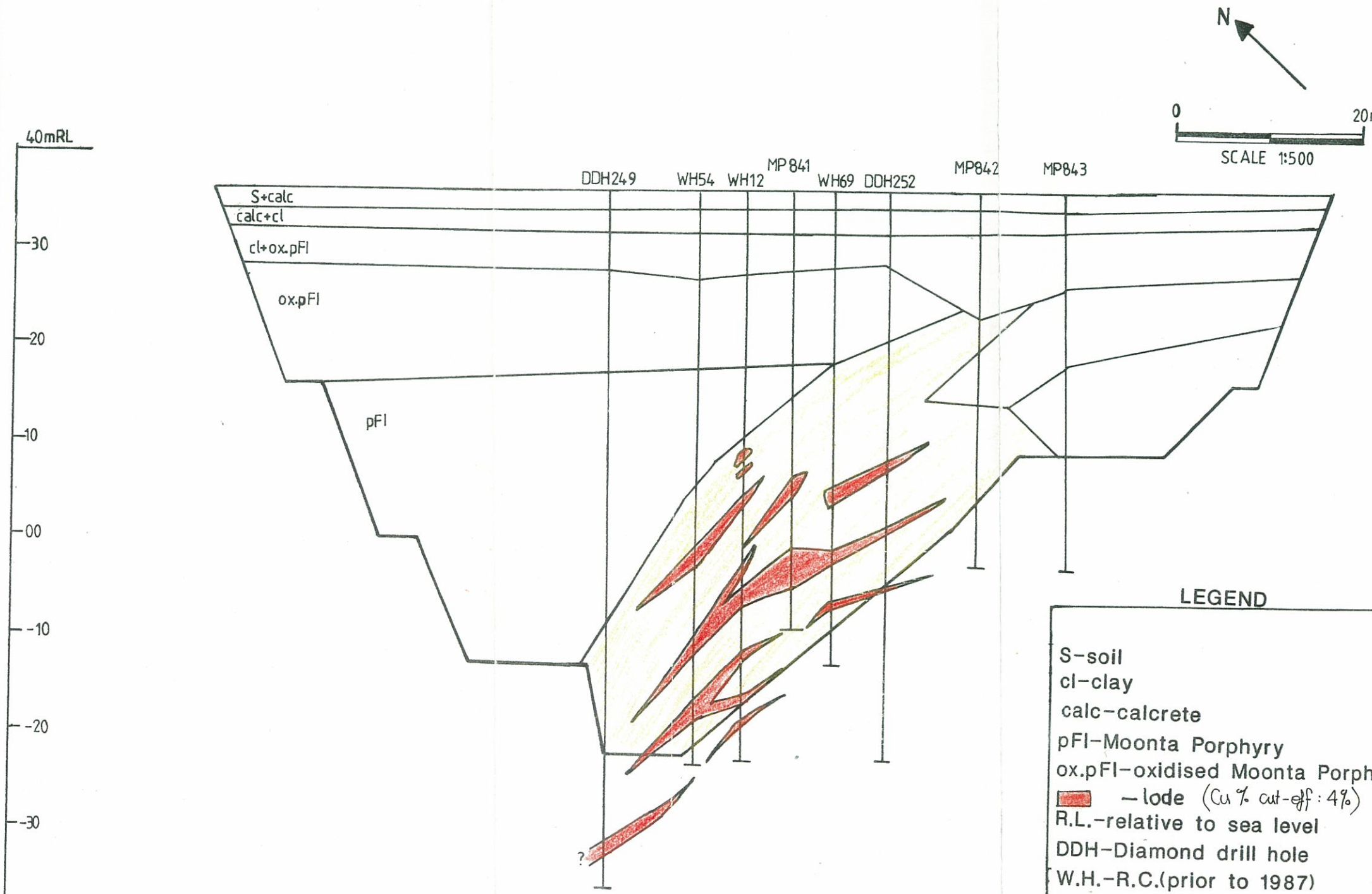

LEGEND

S-soil
cl-clay
calc-calcrete
pFl-Moonta Porphyry
ox.pFl-oxidised Moonta Porphyry
— lode (Cu % cut-off : 4%)
R.L.-relative to sea level
DDH-Diamond drill hole
W.H.-R.C.(prior to 1987)
M.P-R.C.(subsequent to 1987)

Drafted by M.Hafer

Pit outline by B.Kelty 1991

2000mE 2050mE 3000mE

LEIGHTONS: CROSS-SECTION B-B'

N

0 20m

SCALE 1:500

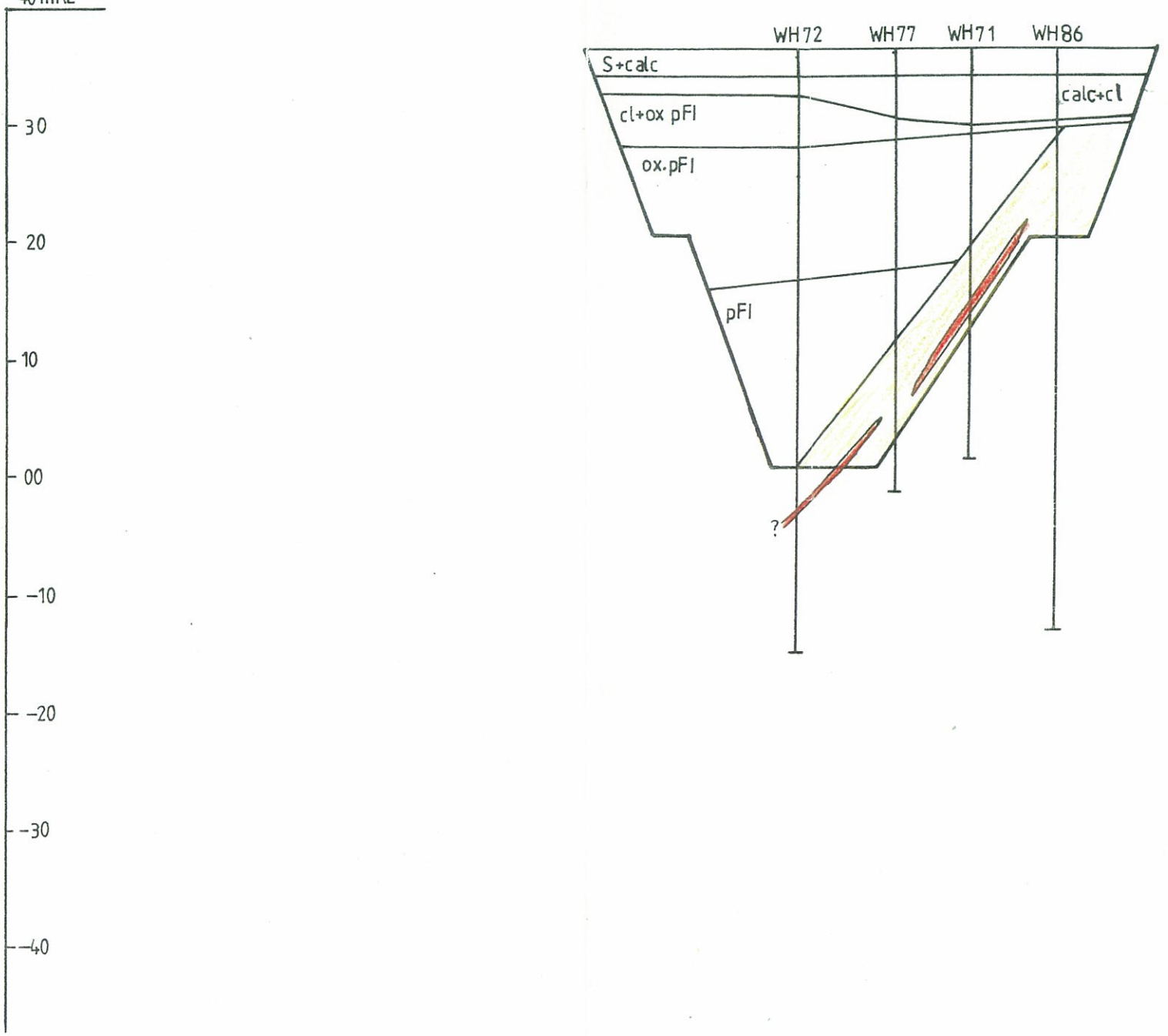

LEGEND

S-soil
cl-clay
calc-calcrete
pFl-Moonta Porphyry
ox.pFl-oxidised Moonta Porphyry
— lode (4% Cu cut-off)
R.L.-relative to sea level
DDH-Diamond drill hole
W.H.-R.C.(prior to 1987)
M.P.-R.C.(subsequent to 1987)

Drafted by M.Hafer

Pit outline by B.Kelty 1991

APPENDIX 6

XRF - WHOLE ROCK ANALYSES

MAJOR ELEMENT ANALYSES OF WHEAL HUGHES MOONTA PORPHYRY SAMPLES

SAMPLE (%)	953-039	953-040	953-045	953-048	953-053	953-056	953-059	953-062	953-C3
SiO2	71.56	75.74	71.78	72.79	72.68	77.80	66.23	71.08	73.60
Al2O3	13.15	12.06	15.79	12.29	12.15	12.66	14.76	12.41	12.29
Fe2O3	3.87	3.32	0.49	4.12	5.28	1.02	5.40	5.35	3.07
MnO	0.01	0.00	0.00	0.01	0.01	0.00	0.01	0.01	0.01
MgO	1.22	0.22	0.37	0.47	0.78	0.34	0.50	1.56	0.91
CaO	0.17	0.10	0.02	0.14	0.16	0.02	0.09	0.21	0.19
Na2O	3.94	4.56	0.57	3.04	4.87	0.30	2.23	4.49	3.56
K2O	3.87	2.89	6.23	4.50	2.92	3.56	8.32	2.48	4.47
TiO2	0.49	0.46	0.53	0.57	0.53	0.39	0.65	0.50	0.50
P2O5	0.07	0.04	0.03	0.07	0.07	0.07	0.09	0.06	0.09
SO3	-0.01	0.00	-0.01	-0.01	-0.01	-0.01	-0.01	-0.01	0.02
LOI	1.37	1.04	3.60	1.35	0.75	3.46	1.27	1.32	1.00
TOTAL	99.70	99.70	100.43	99.40	99.33	100.20	99.62	99.52	99.46

TRACE ELEMENT ANALYSES OF WHEAL HUGHES MOONTA PORPHYRY SAMPLES

SAMPLE (ppm)	953-039	953-040	953-045	953-048	953-053	953-056	953-059	953-062	953-C3
Y	137.1	67.5	91.6	109.4	64.4	109.6	188.6	127.9	122.0
Sr	16.5	3.5	13.4	16.1	2.8	1.3	17.1	11.6	8.8
Rb	105.8	100.7	267.4	132.5	71.7	103.4	191.6	68.0	118.1
Nb	36.9	44.3	48.8	42.1	44.2	36.8	63.9	52.3	46.1
Zr	495.7	484.7	606.6	601.8	558.1	437.3	699.4	572.2	550.8
Th	32.7	36.0	36.9	34.7	40.2	48.6	52.2	39.8	37.6
Pb	2.6	5.9	1.5	4.5	4.4	2.7	1.9	4.6	4.2
U	12.6	17.8	12.0	15.3	8.5	7.4	21.8	14.4	14.6
Ga	22.1	12.6	27.0	21.4	17.4	33.1	18.3	20.4	19.1
Zn	22.4	2.3	0.6	10.0	10.5	-0.1	8.4	18.9	8.6
Ba	791.0	334.0	939.0	1085.0	362.0	245.0	1427.0	453.0	827.0
Sc	9.6	6.1	15.6	13.4	8.8	21.5	11.7	11.1	10.2
Cr	265.0	232.0	82.0	54.0	109.0	161.0	61.0	149.0	178.0
V	12.5	5.7	13.1	13.5	10.2	20.0	16.5	13.5	13.5
Co	22.2	2.6	3.1	5.9	15.0	2.5	6.2	14.2	10.3
Ce	265.0	83.0	40.0	245.0	68.0	447.0	365.0	142.0	198.0
Nd	113.0	36.0	18.0	107.0	27.0	197.0	186.0	59.0	88.0
La	142.0	44.0	19.0	110.0	32.0	230.0	155.0	74.0	97.0
Cu	317.2	142.1	36.6	119.3	375.4	50.9	85.1	93.9	2295.6
Ni	29.7	6.7	4.8	11.4	13.5	9.1	10.1	40.0	18.2

APPENDIX 7

XRD - ALTERATION ASSEMBLAGES

	hematite	pyrite	chalcopyrite	alunite	tourmaline
953-154B.CPI	x	x		x	x
953-121.CPI	x	x		?	x
953-102.CPI		x	x	?	
953-082.CPI		x		x	x
953-065.CPI					x
953-056.CPI			x		x
953-043.CPI				x	x
953-041.CPI					x
953-039.CPI					x
953-031.CPI			x		x
953-022.CPI				x	x
953-008.CPI			x	x	x
953-C3.CPI	x	x	x	x	x
953-106.CPI		x	x		
953-066.CPI				x	x

	chlorapatite	chlorite	dickite	kaolinite	phlogopite
953-154B.CPI	x	x	x	x	x
953-121.CPI				x	
953-102.CPI		x		x	
953-082.CPI		x		?	
953-065.CPI		x		x	
953-056.CPI		x	x	x	
953-043.CPI		x		x	
953-041.CPI		x	x	x	x
953-039.CPI		x		x	x
953-031.CPI		x		x	
953-022.CPI				x	x
953-008.CPI		x		x	x
953-C3.CPI		x		x	
953-106.CPI		x		x	
953-066.CPI					

	covellite	illite	quartz	feldspar	vermiculite
953-154B.CPI			x	x	
953-121.CPI	x	x	x		
953-102.CPI		x	x		?
953-082.CPI		x	x		
953-065.CPI	x	x	x		
953-056.CPI		x	x		
953-043.CPI		x	x		
953-041.CPI		x	x		
953-039.CPI		x	x		
953-031.CPI		x	x		
953-022.CPI		x	x		
953-008.CPI		x	x		
953-C3.CPI		x	x		
953-106.CPI			x		
953-066.CPI		x	x		

	acmite-augite	illite	quartz	feldspar	vermiculite
953-154B.CPI			x	x	
953-121.CPI		x	x		
953-102.CPI		x	x		?
953-082.CPI	x	x	x		
953-065.CPI		x	x		
953-056.CPI		x	x		
953-043.CPI		x	x		
953-041.CPI		x	x		
953-039.CPI		x	x		
953-031.CPI		x	x		
953-022.CPI		x	x		
953-008.CPI		x	x		
953-C3.CPI		x	x		
953-106.CPI			x		
953-066.CPI		x	x		

	acmite-augite	biotite	pyrophyllite	montmorillonite	muscovite
953-154B.CPI					
953-121.CPI					
953-102.CPI					
953-082.CPI	x				
953-065.CPI					
953-056.CPI					
953-043.CPI		x	x		
953-041.CPI				x	x
953-039.CPI			x		
953-031.CPI					
953-022.CPI					
953-008.CPI					
953-C3.CPI					
953-106.CPI					
953-066.CPI					

	hollandite	chalcocite	halloysite	cookeite
953-154B.CPI				
953-121.CPI				
953-102.CPI				
953-082.CPI				
953-065.CPI				
953-056.CPI				
953-043.CPI				
953-041.CPI				
953-039.CPI	x			
953-031.CPI				
953-022.CPI				
953-008.CPI		x	x	
953-C3.CPI		x		x
953-106.CPI		x		
953-066.CPI				

APPENDIX 8

FLUID INCLUSION ANALYSES

Doubly polished thin sections were prepared from quartz samples and examined microscopically for suitability in fluid inclusion analyses. The sections were removed from their mounts by immersion in acetone for 3 to 8 hours. The sections were then broken into pieces small enough to be examined on a heating-freezing stage.

A Reynolds heating-freezing stage attached to a Leitz SM Lux-POL binocular microscope was used for microthermometric analyses. Temperatures were recorded to within $1/10^{th}$ of a degree on a Fluid Inc. 410A Trendicator. Cooling was produced from liquid nitrogen stored in a pressurised dewar. Liquid nitrogen or nitrogen gas was passed to the stage via. an insulated flexible tube, from a copper heat exchange coil inserted into the dewar.

Freezing of the fluid inclusions was achieved by passing liquid nitrogen through to the stage . The inclusions were subsequently warmed with a heating element at a controlled rate, by maintaining a gas flow to the stage. First and final melt of NaCl-H_2O ice and any other significant changes were recorded.

Following the equilibration of the sample to room temperature, a heating procedure was carried out to determine the temperature of homogenisation (T_{hom}) of the inclusions. Heating of the sample was achieved by passing air across an electrical element in the stage into the sample chamber. Heating was slowed to 1°C per minute near the T_{hom} until homogenisation occurred. The results of inclusions that failed to recover a vapour phase upon cooling were rejected.

Wt.% NaCl equivalent was calculated from the final melt temperature (T_{fm}) of NaCl-H_2O ice using the least squares regression method of Potter (1978):

$$w_s = 0.00 + 1.76958\theta - 4.2384 \times 10^{-2}\theta^2 + 5.2778 \times 10^{-4}\theta^3 \pm 0.028$$

WHEAL HUGHES- FLUID INCLUSION TABLE

SAMPLE	Nos. of PHASES	VAPOUR (%)	P, S or PS	SIZE (μm)	T_m	T_{fm}	ThNaCl	T_hTOT	NaCl wt% ± 0.028
953-011, 1	2	30	P	NR	NR	NR	-	258.6	-
,2	2	50	PS	4.5 x 3	NR	NR	-	341.00	-
,3	2	15	P	4.5 x 3	NR	NR	-	337.50	-
,4	2	50	P	3 x 4.5	NR	NR	-	366.80	-
,5	2	10	S	7.5 x 3	-59.00	-22.80	-	117.70	24.57
,6	2	30	P	3 x 1.8	-47.30	NO	-	160.00	-
,7	2	10	P	4.5 x 1.5	NR	NR	-	201.60	-
,8	2	5	PS	7.5 x 6	-26.30	-5.70	-	197.90	8.81
,9	2	5	PS	7.5 x 4.5	-23.40	-5.70	-	209.20	8.81
,10	2	10	PS	7.5 x 7	-23.40	-5.70	-	188.20	8.81
,11	2	30	P	4.5 x 3	NO	-2.20	-	276.00	3.69
,12	2	5	P	7.5 x 4.5	NO	-3.60	-	204.50	5.85
,13	2	10	S	6 x 2.2	-47.20	-24.70	-	145.50	25.80
,14	2	30	P	4.5 x 3	-43.00	-2.40	-	222.20	4.01
953-007, 1	2	5	PS	6 x 3	NO	-1.90	-	172.80	3.21
,2	2	5	PS	7.5 x 6	NO	NO	-	176.60	-
,3	2	10	P	6 x 4.5	NO	-1.30	-	227.80	2.25
,4	2	10	PS	6 x 4.5	NR	NR	-	177.30	-
,5	2	5	PS	7.5 x 4.5	NR	NR	-	193.20	-
,6	2	15	PS	4.5 x 3	NR	NR	-	187.50	-
,7	2	10	PS	17 x 6	-41.50	-1.00	-	172.60	1.73
,8	2	10	P	7.5 x 4.5	-41.60	-22.60	-	169.30	24.44
,9	2	5	S	5.5 x 3	-42.70	NO	-	157.10	-
,10	2	5	P	9 x 3	-54.00	NO	-	139.80	-
,11	2	10	P	18 x 13	NO	-1.20	-	163.30	2.06
953-015, 1	2	10	PS	2 x 3	NO	NO	-	268.00	-
,2	2	30	PS	1.5 x 3	NO	NO	-	258.30	-
,3	2	15	PS	2 x 4	NO	NO	-	268.10	-
,4	2	10	PS	2 x 4	NO	NO	-	235.00	-
,5	2	30	P	4 x 3	NO	NO	-	440.30	-
,6	2	5	S	3 x 3	-67.40	NO	-	143.00	-
,7	2	10	S	3 x 4.5	-67.40	NO	-	152.00	-
,8	2	10	S	12 x 5	-59.00	-25.00	-	142.00	26.00
, 9	2	10	P	9.5 x 8.5	-56.00	-12.60	-	192.70	16.62
,10	2	10	P	6 x 3	-41.70	NO		277.30	-
953-010, 1	2	10	P	3 x 2.5	NO	NO	-	375.70	-
,2	2	5	S	4.5 x 3	NO	-8.80	-	135.60	12.65
,3	2	50	P	4.5 x 3	NO	-5.10	-	341.50	7.99
,4	2	30	P	6 x 6	-69.80	-20.10	-	317.80	22.73
,5	2	10	P	9 x 6	-56.70	-18.00	-	188.60	21.98
,6	2	10	PS	4.5 x 1.5	-52.30	-17.40	-	178.00	20.74
,7	2	5	PS	6 x 4.5	-47.10	-17.40	-	190.70	20.74
953-012, 1	2	20	P	6 x 3	NO	-9.20	-	240.00	13.10
,2	2	5	P	4.5 x 3	-58.00	NO	-	270.10	-
,3	2	10	P	4 x 3	-52.30	-24.70	-	294.80	25.80
,4	2	20	P	3 x 1.8	NO	-15.00	-	359.80	18.79
,5	2	7	PS	3 x 3	-65.00	NO	-	235.50	-
,6	2	10	PS	7.5 x 3	-64.80	-21.00	-	227.00	23.36
,7	2	5	P	6 x 4.5	-52.60	-24.70	-	317.80	25.80
,8	2	7	PS	3 x 3	-69.30	-25.90	-	175.40	26.57
,9	2	10	PS	3.5 x 3	-69.30	-28.00	-	167.00	27.91
,10	2	5	S	4.5 x 1.5	NR	NR	-	134.20	-
,11	2	50	PS	6x4.5	-55.20	-2.00	-	378.20	3.37
,12	2	20	PS	NR	NO	NO	-	264.30	-
953-120c, 1	2	40	S	2.2 x 2.2	NO	-1.10	-	120.00	1.90
,2	2	5	S	4.5 x 1.5	NO	0.90	-	118.60	-
,3	2	10	PS	4.5 x 4.5	-64.00	-27.40	-	316.40	27.52
,4	2	30	PS	6 x 4.5	-57.60	-11.00	-	354.50	15.04
,5	2	15	P	7.5 x 3	-56.8	-7.90	-	330.90	11.59
,6	2	10	PS	7.5 x 6	-45.00	-11.20	-	239.20	15.24
,7	2	15	S	7.5 x 3.5	-46.60	-14.90	-	147.40	18.70
,8	2	10	PS	7.5 x 4.5	-38.00	-11.20	-	229.10	15.24
,9	2	15	S	7.5 x 6.3	NO	-1.20	-	154.30	2.06
,10	2	90	P	6 x 4	NO	-2.00	-	355.80	3.37
,11	2	80	P	8 x 5	NO	NO	-	387.80	-

P= Primary; S= Secondary; PS= Pseudo-secondary; NR= not recorded; NO= not observed; T_m= temp. of first H_2O ice melt; T_{fm}= temp. of final H_2O ice melt; T_hNaCl= temp. of homogenisation of NaCl daughter mineral;

T_hTOT= temp. of complete homogenisation.

POONA-FLUID INCLUSION TABLE

SAMPLE	Nos. of PHASES	VAPOUR (%)	P, S or PS	SIZE (μm)	T_m	T_{fm}	T_hNaCl	T_hTOT	NaCl wt% ± 0.028
953-155b, 1	2	50	P	NR	-49.50	NO	-	244.70	-
,2	2	5	P	9 x 7	-56.50	-17.00	-	168.40	20.43
,3	2	5	P	10.5 x 7	-52.40	-16.60	-	176.20	20.11
,4	2	10	P	12 x 7	NO	NO	-	178.30	-
,5	2	10	PS	11 x 4.5	-30.40	-4.70	-	209.20	7.44
,6	2	10	PS	10 x 6	-30.00	-4.70	-	185.00	7.44
,7	2	10	PS	9 x 7	-23.80	-7.40	-	198.40	10.99
,8	2	10	P	7.5 x 5	-44.20	-8.00	-	186.50	11.71
,9	2	10	P	12 x 9	-30.00	-8.00	-	186.50	11.71
,10	2	10	P	7.5 x 6	-40.00	-16.60	-	240.00	20.11
,11	2	10	PS	7.5 x 3	NO	NO	-	189.40	-
,12	2	15	P	12 x 3	-48.60	NO	-	205.00	-
,13	2	20	PS	7.5 x 7.5	-52.00	-6.00	-	184.50	9.21
,14	2	10	PS	10 x 9	-37.10	-6.60	-	191.50	9.98
,15	2	15	PS	13 x 12	-39.30	-23.50	-	183.60	25.03
,16	2	5	PS	7.5 x 3	NO	NO	-	184.40	-
953-105a, 1	2	10	P	9 x 12	-24.00	-6.90	-	166.00	10.37
,2	2	5	P	NR	NO	NO	-	181.30	-
,3	2	10	P	NR	NO	NO	-	188.70	-
,4	2	5	PS	7 x 6	NO	-0.80	-	187.70	1.39
,5	2	5	PS	15 x 18	-45.40	-0.80	-	170.80	1.39
,6	2	5	PS	7 x 10	-27.60	NO	-	170.80	-
,7	2	5	P	7 x 9	-29.80	-5.20	-	173.10	8.13
,8	2	10	P	13 x 10	-26.70	-1.80	-	180.50	3.05
,9	2	15	P	15 x 12	-23.60	-5.60	-	175.30	8.67
,10	2	5	S	4.5 x 3	NO	NO	-	147.70	-
,11	2	5	S	4.5 x 3	-64.70	NO	-	147.70	-
,12	2	5	S	7 x 3	-58.00	NO	-	147.70	-
,13	2	10	S	6 x 4.5	-58.90	NO	-	138.00	-
,14	2	5	P	9 x 4.5	-60.20	NO	-	140.00	-
953-122, 1	2	5	P	7.5 x 6	-54.80	-18.20	-	183.30	21.35
,2	2	5	P	4.5 x 5	-61.50	-17.40	-	185.50	20.74
,3	3	5	S	12 x 15	-57.00	NO	174.90	150.50	-
,4	4	5	S	9 x 7	-62.30	NO	174.90	158.50	-
,5	3	5	S	NR	NO	NO	177.20	162.30	-
,6	2	7	S	NR	NO	NO	-	161.10	-
,7	2	5	S	NR	NO	NO	-	154.50	-
,8	2	10	S	9 x 4.5	-51.30	-11.00	-	163.40	15.04
,9	2	10	S	9 x 4.5	-47.00	-9.70	-	164.00	13.66
,10	2	5	S	13 x 12	-70.00	-0.70	-	156.10	1.22
,11	2	10	S	7 x 4.5	-52.40	-20.00	-	160.60	22.66
,12	2	5	S	6 x 3.5	-63.20	-20.00	-	181.50	22.66
953-156, 1	2	50	PS	NR	-50.20	-15.20	-	185.40	18.96
,2	2	30	PS	NR	-47.30	-13.40	-	283.70	17.37
,3	2	10	PS	4.5 x 12	-45.00	-10.30	-	208.60	14.31
,4	2	15	PS	NR	-61.10	-10.40	-	211.00	14.41
,5	2	15	PS	2.25 x 2	-51.30	-12.00	-	NR	16.04
,6	3	10	P	7.5 x 14	-30.00	-10.60	NO	261.80	14.62
,7	2	5	P	3 x 4.5	NO	-9.70	-	192.00	13.66
,8	2	5	P	9 x 22	-63.00	0.90	-	179.80	-
,9	2	5	P	3 x 6	NO	NO	-	162.30	-
,10	3	5	P	12 x 10	-40.30	NO	200.30	240.00	-
,11	3	5	P	10 x 11.5	-68.00	-27.00	>260	171.50	27.27
,12	2	5	P	12 x 9	-71.00	NO	-	167.60	-
,13	2	5	P	9 x 10.5	-35.00	-24.70	-	165.80	25.80
,14	2	10	PS	5 x 4.5	-71.70	-16.30	-	220.00	19.87
,15	2	50	PS	3.3 x 3	-71.60	-16.30	-	212.00	19.87
,16	2	10	PS	4 x 4.5	-60.00	-18.30	-	232.70	21.42
,17	2	30	P	14 x 10	-40.70	-18.90	-	342.00	21.87
,18	2	30	PS	7.5 x 3	NO	NO	-	230.20	-
,19	2	20	P	10 x 10	-38.30	-19.60	-	328.40	22.38
,20	2	10	P	11 x 6	NO	NO	-	294.50	-
,21	2	50	P	9 x 7.5	NO	NO	-	474.20	-
953-114a, 1	2	30	P	7.5 x 4.4	NO	0.30	-	358.70	-
,2	2	30	PS	4.5 x 2	-39.90	NO	-	331.20	-
,3	2	50	P	4.5 x 3	-45.00	0.30	-	381.40	-
,4	2	20	P	7.5 x 4.5	-38.50	-0.10	-	344.60	0.18
,5	2	10	PS	3 x 1.5	NO	0.00	-	206.00	-
,6	2	10	PS	3 x 1.5	NO	-0.50	-	271.40	0.87
,7	2	15	PS	3 x 3	NO	-0.70	-	232.80	1.22
,8	2	10	PS	6 x 3	NO	NO	-	218.20	-
,9	2	10	S	7.5 x 3.3	NO	-0.10	-	219.80	0.18
,10	2	20	S	3 x 1.8	NO	-0.10	-	207.40	0.18
,11	2	15	S	3 x 2	NO	-0.10	-	207.40	0.18
,12	2	5	S	6 x 3	-44.20	-13.60	-	176.20	17.55

APPENDIX 9

SULPHUR ISOTOPE ANALYSES:

Sulphide samples were selected for analysis from DDH core and on site from the Poona and Wheal Hughes mines. Sulphides were extracted from coarse specimens with a dental drill. As a result of bornite's brittle texture, alteration and oxidation at normal atmospheric conditions, the specimen was set in epoxy resin and extraction was carried out under a low power microscope from a polished surface. Sulphide species pairs (Py-Cp) exhibiting a common boundary were selected wherever possible to enable the calculation for sulphur isotope geothermometry.

Using the method of Robinson and Kusakabe (1975), sulphur dioxide was obtained from the sulphides by burning an accurately weighed sample, intimately mixed with an oxidant (Cu_2O), in a ceramic boat at temperatures of 900°C to 1000°C for 12 minutes under vacuum. The gas evolved from the combustion of the sulphides was subsequently purified. Non-condensables were separated out and removed by freezing the gas with liquid nitrogen. The carbon dioxide and water vapour was separated from the SO_2 by fractional distillation. H_2O vapour was extracted using ethanol at just above freezing (approximately -80°C). The remaining gas was collected by freezing with liquid nitrogen and CO_2 extracted from the SO_2 using a slurry of n-pentane (-130°C). The purified SO_2 was collected and sealed in a sample tube.

The ^{34}S / ^{32}S ratios were measured on a Micromass VG 602 E Stable Isotope Mass Spectrometer and the sulphur isotope ratios compared to that of the international standard, Canyon Diablo triolite. The results are expressed in per mil (‰) :

$$\delta^{34}S_{sample}\ (‰) = \frac{(^{34}S/^{32}S)_{sample} - (^{34}S/^{32}S)_{standard}}{(^{34}S/^{32}S)_{standard}} \times 1000$$

SULPHUR ISOTOPE ANALYSES- WHEAL HUGHES

SAMPLE	$\delta^{34}S$- Cp (‰)	$\delta^{34}S$- Py (‰)
953-011	5.3	-
953-012	5.6	-
953-013	5.6	-
953-019	5.6	-
953-038	5.6	-
953-120	3.9	-
953-121	-	5.1
953-122b	6.4	-
953-125	5.2	5.6
953-126	5.5	-
953-128	2.6	-
953-129	2.5	-
953-132	4.5	-

SULPHUR ISOTOPE ANALYSES- POONA

SAMPLE	$\delta^{34}S$- Cp (‰)	$\delta^{34}S$- Py (‰)	$\delta^{34}S$- Bn (‰)
953-105b	-1.3	-	-
953-108	3.1	-	-
953-114	-0.2	-	-
953-122	1.3	1.4	-
953-124	-	-	1.7
953-146	1.8	-	-
953-150	1.8	-	-
953-153	-0.7	-	-
953-155	1.3	1.4	-
953-156	1.1	0.9	-
953-157	5.5	-	-

APPENDIX 10

ELECTRON MICROPROBE ANALYSES

CHLORITE

Polished thin-sections of ore samples containing chlorite were selected for electron microprobe analysis. Analyses of the chlorites were carried out on a Jeol 733 Superprobe in the Electron Optical Centre of the University of Adelaide, using the energy dispersive spectrometry (EDS) system. The X-Ray microanalyser is fitted with a Moran scientific control hardware and software running in an ACER 386 P.C. Polished thin-sections were carbon coated in a Denton DV-502 vacuum coating unit and analysed using a 3 nA electron beam current at an accelerating voltage of 15 keV.

The wt.% oxide values were processed using the CHLORITE program developed by Walshe; temperature, log fO_2 and log fS_2 are presented overleaf.

WHEAL HUGHES - CHLORITE ANALYSES

953-	129, 1-1	129,1-2	129, 1-3	129, 1-4	129, 2-1	129, 2-3	129, 4-2	129, 4-3	129, 5-1	129, 5-2	130, 1-2	130, 1-1	130, 2-1	130, 2-2
SiO_2	25.72	26.17	25.64	27.97	28.56	27.79	26.50	28.42	28.04	29.77	24.13	24.07	28.37	28.14
Al_2O_3	20.46	20.01	20.23	17.85	18.89	17.20	19.14	19.18	18.47	18.76	21.46	21.35	17.26	17.8
Fe_2O_3	0.00	0.00	0.00	0.00	0.00	0.00	0.00	0.00	0.00	0.00	0.00	0.00	0.00	0.00
FeO	33.81	34.71	35.11	24.27	20.84	24.38	24.24	26.17	23.54	19.27	33.39	33.98	22.04	22.9
MnO	0.33	0.03	0.18	0.00	0.00	0.18	0.37	0.00	0.15	0.16	0.17	0.24	0.12	0.07
MgO	9.80	9.34	9.07	17.21	19.46	16.47	17.07	16.94	17.73	21.37	8.82	8.41	18.43	18.03
Na_2O	0.00	0.00	0.00	0.00	0.00	0.00	0.00	0.00	0.00	0.00	0.00	0.00	0.00	0.00
K_2O	0.00	0.00	0.00	0.00	0.09	0.00	0.00	0.00	0.11	0.00	0.06	0.07	0.00	0.00
TiO_2	0.04	0.00	0.17	0.00	0.00	0.00	0.00	0.00	0.26	0.17	0.00	0.00	0.05	0.08
Cr_2O_3	0.00	0.00	0.00	0.00	0.00	0.00	0.00	0.00	0.00	0.00	0.00	0.00	0.00	0.00
CaO	0.17	0.25	0.14	0.17	0.09	0.03	0.17	0.07	0.13	0.10	0.19	0.18	0.14	0.12
TOTAL	90.33	90.51	90.54	87.47	87.93	86.05	87.49	90.78	88.43	89.60	88.22	88.3	86.41	87.14
Temp. (°C)	281	267	283	204	208	189	263	222	214	196	296	296	187	201
log fO_2	-36.93	-39.08	-37.13	-43.84	-42.12	-46.14	-35.78	-41.49	-42.13	-43.19	-34.61	-34.73	-45.70	-43.89
log fS_2	-13.08	-14.60	-13.42	-16.12	-15.17	-17.29	-12.01	-14.94	-15.23	-15.67	-11.57	-11.63	-17.02	-16.12
Mg No	34.49	32.45	31.77	55.82	62.46	54.78	55.95	53.56	57.42	66.49	32.24	30.95	59.93	58.44

953-	130, 2-3	130, 3-2	130, 3-5	130, 4-3	130, 4-5	130, 4-6
SiO_2	27.37	26.4	27.96	24.57	24.39	28.91
Al_2O_3	18.17	18.51	18.66	21.67	20.8	17.4
Fe_2O_3	0.00	0.00	0.00	0.00	0.00	0.00
FeO	26.71	25.06	23.74	34.03	33.25	23.03
MnO	0.12	0.37	0.36	0.26	0.00	0.05
MgO	15.82	15.26	17.98	8.9	8.12	18.67
Na_2O	0.00	0.00	0.00	0.00	0.00	0.00
K_2O	0.03	0.07	0.00	0.00	0.00	0.07
TiO_2	0.15	0.13	0.00	0.00	0.00	0.00
Cr_2O_3	0.00	0.00	0.00	0.00	0.00	0.00
CaO	0.11	0.18	0.12	0.19	0.09	0.14
TOTAL	88.48	85.98	88.82	89.62	86.65	88.27
Temp. (°C)	228	233	229	295	278	187
log fO_2	-41.11	-40.14	-40.07	-34.76	-35.48	-45.81
log fS_2	-14.77	-14.26	-14.18	-11.64	-11.91	-17.09
Mg No	51.46	52.38	57.72	32.15	30.32	59.13

POONA- CHLORITE ANALYSES

953-	152, 1-3	152, 1-4	152, 1-5	152, 3-1	152, 3-2	152, 3-4	152, 4-2	152, 4-3	152, 4-4	152, 4-5	152, 5-1	152, 5-2	100, 1-1	100, 1-2
SiO_2	28.58	25.95	27.13	26.83	23.21	27.41	24.43	24.81	25.25	26.01	25.35	26.55	23.87	27.83
Al_2O_3	17.41	19.04	19.38	19.31	20.74	19.07	20.27	20.44	22.01	18.72	20.76	18.37	20.89	18.74
Fe_2O_3	0.00	0.00	0.00	0.00	0.00	0.00	0.00	0.00	0.00	0.00	0.00	0.00	0.00	0.00
FeO	23.34	31.27	26.54	28.97	34.36	27.60	34.21	31.55	32.17	29.15	34.28	25.40	36.36	21.29
MnO	0.23	0.59	0.09	0.35	0.00	0.29	0.67	0.81	1.35	0.95	0.22	0.37	0.17	0.00
MgO	17.09	9.31	14.68	10.68	6.93	11.94	7.61	9.37	8.09	9.31	7.38	10.89	6.94	19.73
Na_2O	0.00	0.07	0.00	0.00	0.00	0.00	0.00	0.00	0.00	0.00	0.00	0.00	0.01	0.00
K_2O	0.04	0.09	0.08	0.20	0.00	0.01	0.00	0.00	0.03	0.09	0.00	0.12	0.00	0.05
TiO_2	0.25	0.00	0.00	0.00	0.00	0.02	0.00	0.27	0.00	0.00	0.00	0.05	0.00	0.05
Cr_2O_3	0.00	0.00	0.00	0.00	0.00	0.00	0.00	0.00	0.00	0.00	0.00	0.00	0.00	0.00
CaO	0.30	0.12	0.12	0.26	0.30	0.39	0.05	0.19	0.15	0.23	0.17	0.22	0.07	0.11
TOTAL	87.24	86.44	88.02	86.60	85.54	86.73	87.24	87.44	89.05	84.46	88.16	81.97	88.31	87.80
Temp. (°C)	172	215	224	193	297	181	281	280	266	192	258	163	299	240
log fO_2	-48.28	-44.51	-41.62	-46.99	-35.31	-48.24	-35.40	-36.87	-36.56	-47.41	-39.70	-50.94	-35.19	-37.99
log fS_2	-18.36	-17.15	-15.02	-18.13	-12.23	-18.54	-11.89	-12.94	-12.44	-18.52	-14.70	-19.89	-12.22	-13.08
Mg No.	56.80	35.47	49.73	40.09	26.44	43.87	29.39	35.70	32.91	37.58	28.06	43.78	25.64	62.28

953-	100, 1-3	100, 1-4	100, 1-5	100, 2-1	100, 2-2	100, 2-3	100, 3-1	100, 3-2	100, 3-3	100, 3-4	104, 1-1	104, 1-2	104, 1-3	104, 2-1
SiO_2	23.35	23.28	24.52	23.53	21.85	24.50	24.59	24.47	23.96	24.15	25.11	24.11	23.42	24.07
Al_2O_3	20.66	20.67	20.52	21.80	22.72	19.84	20.61	20.62	19.49	21.78	21.27	20.64	21.32	21.36
Fe_2O_3	0.00	0.00	0.00	0.00	0.00	0.00	0.00	0.00	0.00	0.00	0.00	0.00	0.00	0.00
FeO	35.87	35.25	35.94	33.86	40.56	33.87	34.64	35.98	34.37	35.65	36.85	36.69	37.08	37.71
MnO	0.23	0.11	0.22	0.28	0.06	0.18	0.27	0.05	0.37	0.00	0.00	0.00	0.05	0.00
MgO	7.22	6.96	7.84	9.26	3.43	8.56	8.08	7.83	8.78	7.38	7.04	6.13	5.46	4.85
Na_2O	0.00	0.00	0.00	0.00	0.00	0.00	0.00	0.00	0.00	0.00	0.00	0.00	0.00	0.00
K_2O	0.00	0.00	0.00	0.00	0.00	0.02	0.00	0.04	0.00	0.00	0.00	0.00	0.02	0.00
TiO_2	0.00	0.00	0.00	0.04	0.00	0.04	0.28	0.11	0.01	0.00	0.00	0.00	0.21	0.00
Cr_2O_3	0.00	0.00	0.00	0.00	0.00	0.00	0.00	0.00	0.00	0.00	0.00	0.00	0.00	0.00
CaO	0.14	0.13	0.16	0.20	0.11	0.12	0.11	0.03	0.07	0.12	0.07	0.30	0.25	0.06
TOTAL	87.47	86.40	89.20	88.97	88.73	87.13	88.58	89.13	87.05	89.08	90.34	87.87	87.81	88.05
Temp. (°C)	302	300	294	310	326	287	290	295	294	298	280	286	301	279
log fO_2	-34.32	-34.88	-35.72	-32.01	-31.35	-34.61	-34.20	-35.67	-35.12	-35.02	-35.79	-35.31	-35.46	-36.29
log fS_2	-11.45	-11.93	-12.52	-10.20	-9.93	-11.48	-11.27	-12.51	-11.86	-11.96	-12.10	-11.87	-12.62	-12.38
Mg No.	26.75	26.20	28.31	33.14	13.21	31.31	29.75	28.02	31.79	26.95	25.40	22.94	20.87	18.65

WHEAL HUGHES - CHLORITE ANALYSES

953-	129, 1-1	129,1-2	129, 1-3	129, 1-4	129, 2-1	129, 2-3	129, 4-2	129, 4-3	129, 5-1	129, 5-2	130, 1-2	130, 1-1	130, 2-1	130, 2-2
SiO_2	25.72	26.17	25.64	27.97	28.56	27.79	26.50	28.42	28.04	29.77	24.13	24.07	28.37	28.14
Al_2O_3	20.46	20.01	20.23	17.85	18.89	17.20	19.14	19.18	18.47	18.76	21.46	21.35	17.26	17.8
Fe_2O_3	0.00	0.00	0.00	0.00	0.00	0.00	0.00	0.00	0.00	0.00	0.00	0.00	0.00	0.00
FeO	33.81	34.71	35.11	24.27	20.84	24.38	24.24	26.17	23.54	19.27	33.39	33.98	22.04	22.9
MnO	0.33	0.03	0.18	0.00	0.00	0.18	0.37	0.00	0.15	0.16	0.17	0.24	0.12	0.07
MgO	9.80	9.34	9.07	17.21	19.46	16.47	17.07	16.94	17.73	21.37	8.82	8.41	18.43	18.03
Na_2O	0.00	0.00	0.00	0.00	0.00	0.00	0.00	0.00	0.00	0.00	0.00	0.00	0.00	0.00
K_2O	0.00	0.00	0.00	0.00	0.09	0.00	0.00	0.00	0.11	0.00	0.06	0.07	0.00	0.00
TiO_2	0.04	0.00	0.17	0.00	0.00	0.00	0.00	0.00	0.26	0.17	0.00	0.00	0.05	0.08
Cr_2O_3	0.00	0.00	0.00	0.00	0.00	0.00	0.00	0.00	0.00	0.00	0.00	0.00	0.00	0.00
CaO	0.17	0.25	0.14	0.17	0.09	0.03	0.17	0.07	0.13	0.10	0.19	0.18	0.14	0.12
TOTAL	90.33	90.51	90.54	87.47	87.93	86.05	87.49	90.78	88.43	89.60	88.22	88.3	86.41	87.14
Temp. (°C)	281	267	283	204	208	189	263	222	214	196	296	296	187	201
log fO_2	-36.93	-39.08	-37.13	-43.84	-42.12	-46.14	-35.78	-41.49	-42.13	-43.19	-34.61	-34.73	-45.70	-43.89
log fS_2	-13.08	-14.60	-13.42	-16.12	-15.17	-17.29	-12.01	-14.94	-15.23	-15.67	-11.57	-11.63	-17.02	-16.12
Mg No	34.49	32.45	31.77	55.82	62.46	54.78	55.95	53.56	57.42	66.49	32.24	30.95	59.93	58.44

953-	130, 2-3	130, 3-2	130, 3-5	130, 4-3	130, 4-5	130, 4-6
SiO_2	27.37	26.4	27.96	24.57	24.39	28.91
Al_2O_3	18.17	18.51	18.66	21.67	20.8	17.4
Fe_2O_3	0.00	0.00	0.00	0.00	0.00	0.00
FeO	26.71	25.06	23.74	34.03	33.25	23.03
MnO	0.12	0.37	0.36	0.26	0.00	0.05
MgO	15.82	15.26	17.98	8.9	8.12	18.67
Na_2O	0.00	0.00	0.00	0.00	0.00	0.00
K_2O	0.03	0.07	0.00	0.00	0.00	0.07
TiO_2	0.15	0.13	0.00	0.00	0.00	0.00
Cr_2O_3	0.00	0.00	0.00	0.00	0.00	0.00
CaO	0.11	0.18	0.12	0.19	0.09	0.14
TOTAL	88.48	85.98	88.82	89.62	86.65	88.27
Temp. (°C)	228	233	229	295	278	187
log fO_2	-41.11	-40.14	-40.07	-34.76	-35.48	-45.81
log fS_2	-14.77	-14.26	-14.18	-11.64	-11.91	-17.09
Mg No	51.46	52.38	57.72	32.15	30.32	59.13

POONA- CHLORITE ANALYSES

953-	104, 2-2	104, 2-3	104, 2-4	104, 2-4	104, 3-4	104, 3-5	104, 4-1	104, 4-2	104, 4-3	104, 4-4	104, 5-1	104, 5-2	104, 5-3	104, 5-4
SiO_2	25.86	24.69	25.03	24.46	25.00	24.48	22.74	24.76	24.11	24.56	24.19	24.39	24.31	24.28
Al_2O_3	19.92	21.27	20.31	21.16	20.93	19.99	22.59	19.36	19.10	21.40	20.01	20.16	20.24	20.88
Fe_2O_3	0.00	0.00	0.00	0.00	0.00	0.00	0.00	0.00	0.00	0.00	0.00	0.00	0.00	0.00
FeO	35.19	36.36	38.94	39.25	38.27	37.83	42.01	37.58	37.22	36.03	35.97	37.71	36.96	38.29
MnO	0.00	0.05	0.23	0.16	0.18	0.17	0.00	0.12	0.24	0.19	0.09	0.06	0.24	0.09
MgO	7.98	7.56	5.30	4.84	5.52	5.00	0.17	6.39	5.85	7.65	6.20	5.53	6.05	5.37
Na_2O	0.00	0.00	0.00	0.00	0.00	0.00	0.00	0.15	0.00	0.00	0.00	0.00	0.00	0.00
K_2O	0.00	0.01	0.10	0.00	0.00	0.00	0.00	0.00	0.00	0.07	0.06	0.00	0.00	0.00
TiO_2	0.01	0.18	0.07	0.00	0.00	0.02	0.00	0.00	0.00	0.09	0.07	0.08	0.00	0.00
Cr_2O_3	0.00	0.00	0.00	0.00	0.00	0.00	0.00	0.00	0.00	0.00	0.00	0.00	0.00	0.00
CaO	0.13	0.23	0.09	0.01	0.20	0.16	0.08	0.07	0.05	0.19	0.16	0.13	0.08	0.04
TOTAL	89.09	90.35	90.07	89.88	90.10	87.65	87.59	88.43	86.57	90.18	86.75	88.06	87.88	88.95
Temp. (°C)	245	295	263	285	266	256	295	269	274	296	268	270	279	287
log fO_2	-41.20	-35.73	-38.66	-35.82	-37.97	-39.53	-36.16	-37.83	-37.29	-35.39	-37.54	-37.59	-36.29	-35.45
log fS_2	-15.52	-12.58	-13.89	-12.15	-13.30	-14.41	-13.03	-13.33	-13.03	-12.26	-13.01	-13.12	-12.38	-11.96
Mg No.	28.78	27.11	19.91	18.29	20.75	19.36	0.72	23.44	22.28	27.73	23.65	20.82	22.97	20.15

953-	145, 1-1	145, 1-2	145, 1-3	145, 1-4	145, 1-5	145, 2-1	145, 2-3	145, 2-4	145, 3-1	145, 3-2	145, 3-3	145, 4-1	145, 4-2	145, 5-1
SiO_2	27.22	26.05	27.41	26.84	30.55	24.86	26.17	28.80	29.79	27.67	25.86	26.69	26.84	26.42
Al_2O_3	18.61	19.21	18.27	19.20	15.83	20.29	19.61	18.61	17.31	18.96	18.26	19.17	18.38	18.77
Fe_2O_3	0.00	0.00	0.00	0.00	0.00	0.00	0.00	0.00	0.00	0.00	0.00	0.00	0.00	0.00
FeO	27.40	27.09	26.46	25.60	15.53	30.13	26.18	20.96	18.14	23.72	26.18	27.58	27.00	27.67
MnO	0.20	0.52	0.27	0.22	0.04	0.67	0.41	0.08	0.19	0.14	0.39	0.22	0.35	0.39
MgO	15.76	14.46	15.83	15.81	24.39	11.93	14.61	20.30	22.17	17.57	14.64	14.74	15.47	14.72
Na_2O	0.00	0.00	0.00	0.00	0.00	0.00	0.00	0.00	0.00	0.00	0.00	0.00	0.00	0.00
K_2O	0.00	0.00	0.00	0.04	0.05	0.00	0.02	0.00	0.00	0.00	0.09	0.00	0.00	0.00
TiO_2	0.03	0.00	0.00	0.00	0.00	0.03	0.00	0.01	0.04	0.00	0.01	0.13	0.04	0.00
Cr_2O_3	0.00	0.00	0.00	0.00	0.00	0.00	0.00	0.00	0.00	0.00	0.00	0.00	0.00	0.00
CaO	0.00	0.17	0.09	0.02	0.17	0.13	0.18	0.04	0.03	0.00	0.10	0.10	0.11	0.06
TOTAL	89.22	87.50	88.33	87.73	86.56	88.04	87.18	88.80	87.67	88.06	85.53	88.63	88.19	88.03
Temp. (°C)	245	258	227	243	167	287	252	218	185	229	248	248	245	254
log fO_2	-38.94	-37.25	-41.22	-38.85	-46.78	-34.49	-37.95	-40.74	-44.67	-40.05	-38.57	-38.66	-38.88	-37.91
log fS_2	-13.67	-12.81	-14.82	-13.60	-17.42	-11.44	-13.15	-14.47	-16.41	-14.17	-13.48	-13.53	-13.64	-13.15
Mg No.	50.80	49.25	51.84	52.59	73.69	42.13	50.26	63.37	68.64	57.01	50.29	48.99	50.84	49.04

POONA- CHLORITE ANALYSES

953-	145, 5-2	114, 1-1	148, 1-5	148, 2-1	148, 2-4	148, 3-1	148, 3-2	148, 3-5	148, 3-6	148, 5-3	114a, 1-1	114a, 1-2	114a, 1-3	114a, 2-1
SiO_2	23.35	23.82	25.83	25.37	25.98	25.45	25.97	24.72	25.31	25.29	25.47	25.34	25.23	24.57
Al_2O_3	19.04	19.52	21.61	20.77	22.00	21.41	21.09	20.14	21.41	20.95	18.19	18.32	18.60	19.74
Fe_2O_3	0.00	0.00	0.00	0.00	0.00	0.00	0.00	0.00	0.00	0.00	0.00	0.00	0.00	0.00
FeO	40.39	39.92	30.37	30.36	29.04	29.11	30.47	29.08	30.60	29.76	35.42	36.46	35.26	38.47
MnO	0.21	0.17	0.10	0.00	0.05	0.05	0.22	0.06	0.22	0.13	0.14	0.00	0.18	0.16
MgO	3.33	3.66	10.71	10.08	11.29	10.96	10.89	10.08	11.11	10.74	8.85	7.99	8.37	5.41
Na_2O	0.00	0.00	0.00	0.00	0.00	0.00	0.00	0.00	0.00	0.00	0.00	0.00	0.00	0.00
K_2O	0.00	0.00	0.00	0.00	0.00	0.04	0.00	0.00	0.00	0.00	0.05	0.00	0.00	0.00
TiO_2	0.00	0.07	0.05	0.11	0.09	0.07	0.00	0.00	0.08	0.11	0.00	0.02	0.00	0.00
Cr_2O_3	0.00	0.00	0.00	0.00	0.00	0.00	0.00	0.00	0.00	0.00	0.00	0.00	0.00	0.00
CaO	0.04	0.10	0.09	0.10	0.09	0.16	0.11	0.20	0.10	0.22	0.26	0.13	0.19	0.00
TOTAL	86.36	87.26	88.76	86.79	88.54	87.25	88.75	84.28	88.83	87.20	88.38	88.26	87.83	88.35
Temp. (°C)	284	271	267	250	252	257	252	248	283	269	274	261	274	268
log fO_2	-36.83	-38.16	-37.93	-39.11	-38.28	-37.64	-38.67	-39.39	-35.65	-37.61	-38.65	-38.88	-38.76	-38.06
log fS_2	-13.14	-13.83	-13.30	-13.79	-13.34	-13.00	-13.55	-13.93	-12.05	-13.08	-14.58	-14.02	-14.69	-13.54
Mg No.	13.21	14.36	38.72	37.17	40.99	40.22	39.18	38.26	39.55	39.30	31.00	28.08	29.98	20.31

953-	114a, 2-2	114a, 2-3	114a, 3-1	114a, 3-2	114a, 3-3	114a, 4-1	114a, 4-2	114a, 4-3	114a, 5-3	114a, 5-4	114a, 6-1	114a, 6-2	114a, 6-3	114aFI, 1-1
SiO_2	24.89	24.06	23.80	25.96	26.76	26.56	26.81	24.33	26.43	25.04	25.21	25.49	23.53	22.90
Al_2O_3	17.77	19.66	19.19	18.41	16.59	17.02	17.72	19.55	17.03	18.24	17.77	19.56	19.05	21.09
Fe_2O_3	0.00	0.00	0.00	0.00	0.00	0.00	0.00	0.00	0.00	0.00	0.00	0.00	0.00	0.00
FeO	33.77	38.89	42.45	35.54	32.53	31.09	32.63	39.96	30.90	35.56	37.31	31.00	39.78	41.29
MnO	0.19	0.07	0.18	0.27	0.21	0.44	0.09	0.36	0.00	0.25	0.26	0.05	0.11	0.19
MgO	8.04	5.45	3.15	7.16	11.43	11.82	12.31	4.77	11.89	7.26	6.63	9.34	3.43	2.26
Na_2O	0.00	0.00	0.00	0.00	0.00	0.00	0.00	0.00	0.00	0.00	0.00	0.00	0.00	0.00
K_2O	0.00	0.02	0.00	0.04	0.00	0.04	0.00	0.02	0.00	0.00	0.00	0.00	0.00	0.02
TiO_2	0.03	0.00	0.11	0.00	0.00	0.00	0.06	0.04	0.05	0.07	0.00	0.00	0.07	0.00
Cr_2O_3	0.00	0.00	0.00	0.00	0.00	0.00	0.00	0.00	0.00	0.00	0.00	0.00	0.00	0.00
CaO	0.01	0.13	0.01	0.23	0.12	0.07	0.10	0.07	0.16	0.06	0.12	0.27	0.11	0.08
TOTAL	84.70	88.28	88.89	87.61	87.64	87.04	89.72	89.10	86.46	86.48	87.30	85.71	86.08	87.83
Temp. (°C)	231	295	298	211	205	211	240	286	210	244	244	229	267	307
log fO_2	-43.05	-35.05	-35.73	-46.14	-45.90	-44.72	-40.91	-36.22	-44.96	-41.63	-42.06	-42.70	-38.75	-34.62
log fS_2	-16.67	-11.78	-12.72	-18.64	-17.92	-17.10	-14.94	-12.56	-17.23	-15.98	-16.45	-16.12	-14.25	-11.99
Mg No.	30.07	20.10	12.01	26.83	38.75	40.89	40.30	18.16	40.68	27.06	24.46	35.00	13.53	9.27

POONA- CHLORITE ANALYSES

953-	114aFI, 1-2	114aFI, 2-1	114aFI, 2-2	114aFI, 2-3	114aFI, 3-1	114aFI 3-2	114aFI, 4-1	114aFI, 4-2	114aFI, 5-1	114aFI, 5-2	114aFI, 5-3	149, 1-3	149, 1-4	149, 2-1
SiO_2	22.99	23.52	24.13	25.15	25.71	22.43	24.11	24.58	24.10	22.77	23.92	25.63	24.83	25.87
Al_2O_3	22.27	20.34	21.27	20.85	18.89	21.47	19.47	19.63	19.50	18.80	19.89	20.67	20.06	20.75
Fe_2O_3	0.00	0.00	0.00	0.00	0.00	0.00	0.00	0.00	0.00	0.00	0.00	0.00	0.00	0.00
FeO	42.38	39.92	42.16	39.92	39.04	42.04	39.90	39.07	38.58	39.55	41.71	35.33	34.48	29.87
MnO	0.00	0.18	0.24	0.20	0.04	0.33	0.18	0.27	0.00	0.25	0.21	0.04	0.00	0.00
MgO	1.35	2.85	2.41	3.73	5.50	1.68	4.43	5.60	4.64	3.84	3.79	8.43	8.39	10.76
Na_2O	0.00	0.00	0.00	0.00	0.00	0.00	0.00	0.00	0.00	0.00	0.00	0.00	0.00	0.00
K_2O	0.01	0.00	0.04	0.00	0.00	0.00	0.00	0.07	0.00	0.20	0.00	0.00	0.00	0.13
TiO_2	0.00	0.00	0.00	0.00	0.00	0.16	0.00	0.02	0.00	0.03	0.00	0.00	0.13	0.00
Cr_2O_3	0.00	0.00	0.00	0.00	0.00	0.00	0.00	0.00	0.00	0.00	0.00	0.00	0.00	0.00
CaO	0.09	0.07	0.15	0.08	0.09	0.05	0.21	0.27	0.06	0.27	0.16	0.00	0.13	0.22
TOTAL	89.09	86.88	90.40	89.93	89.27	88.16	88.30	89.51	86.88	85.71	89.68	90.10	88.02	87.60
Temp. (°C)	311	272	281	244	234	315	280	284	263	301	300	269	278	242
log fO_2	-34.58	-37.92	-36.95	-41.33	-43.67	-33.84	-37.01	-36.20	-38.88	-36.50	-34.94	-37.03	-35.85	-40.23
log fS_2	-12.16	-13.63	-13.09	-15.64	-17.55	-11.59	-13.09	-12.42	-14.14	-13.81	-11.95	-12.73	-12.12	-14.36
Mg No.	5.37	11.64	9.72	14.65	20.13	7.34	16.83	20.79	17.65	15.21	14.31	29.89	30.25	39.10

953-	149, 2-2	149, 2-3	149, 3-1	149, 3-4	149, 4-3	149, 4-4	149, 5-1	149, 5-2	114aFI, 1-1	114aFI, 1-2	107, 2-1	107, 2-2	107, 2-3	107, 3-1
SiO_2	23.99	23.79	24.34	22.60	24.09	23.75	24.44	23.94	23.73	25.95	24.82	25.09	25.46	24.08
Al_2O_3	20.85	20.17	21.52	22.46	21.32	20.09	20.94	20.17	21.55	21.49	20.18	19.34	20.42	18.65
Fe_2O_3	0.00	0.00	0.00	0.00	0.00	0.00	0.00	0.00	0.00	0.00	0.00	0.00	0.00	0.00
FeO	39.24	41.13	36.65	40.73	36.07	30.21	35.65	42.14	37.45	40.17	33.65	34.47	31.55	36.54
MnO	0.01	0.37	0.26	0.14	0.08	0.13	0.17	0.14	0.31	0.07	0.31	0.32	0.15	0.00
MgO	3.07	2.63	5.28	0.51	6.42	9.87	6.77	2.17	4.21	4.39	9.78	8.68	11.32	6.49
Na_2O	0.01	0.00	0.00	0.00	0.00	0.00	0.00	0.00	0.00	0.00	0.00	0.00	0.00	0.00
K_2O	0.02	0.07	0.04	0.00	0.00	0.00	0.01	0.00	0.00	0.00	0.00	0.00	0.04	0.00
TiO_2	0.02	0.24	0.13	0.00	0.00	0.01	0.01	0.19	0.00	0.00	0.03	0.01	0.01	0.08
Cr_2O_3	0.00	0.00	0.00	0.00	0.00	0.00	0.00	0.00	0.00	0.00	0.00	0.00	0.00	0.00
CaO	0.00	0.12	0.14	0.15	0.22	0.20	0.08	0.05	0.07	0.13	0.13	0.20	0.17	0.08
TOTAL	87.21	88.52	88.36	86.59	88.20	84.26	88.07	88.80	87.32	92.20	88.90	88.11	89.12	85.92
Temp. (°C)	257	274	271	292	295	287	280	268	280	260	291	280	282	274
log fO_2	-39.53	-37.91	-36.98	-36.14	-36.17	-35.44	-35.70	-38.80	-36.14	-41.07	-35.33	-37.67	-35.94	-37.24
log fS_2	-14.49	-13.75	-12.72	-12.83	-13.05	-11.97	-12.05	-14.38	-12.30	-16.30	-11.94	-13.84	-12.22	-12.99
Mg No.	12.26	10.96	20.88	2.51	24.21	36.97	25.55	8.69	17.27	16.42	34.52	31.42	39.18	24.04

POONA- CHLORITE ANALYSES

953-	107, 3-2	107, 3-3	107, 4-1	107, 4-3	107, 4-5
SiO_2	25.25	25.44	23.18	25.95	26.47
Al_2O_3	17.68	19.11	19.39	17.53	17.44
Fe_2O_3	0.00	0.00	0.00	0.00	0.00
FeO	34.34	36.49	40.00	33.15	32.40
MnO	0.00	0.30	0.05	0.15	0.42
MgO	9.09	6.67	3.15	9.71	10.37
Na_2O	0.00	0.00	0.00	0.00	0.00
K_2O	0.00	0.00	0.00	0.00	0.18
TiO_2	0.00	0.00	0.00	0.06	0.15
Cr_2O_3	0.00	0.00	0.00	0.00	0.00
CaO	0.00	0.22	0.25	0.17	0.14
TOTAL	86.36	88.23	86.02	86.72	87.57
Temp. (°C)	255	242	280	218	206
log fO_2	-39.78	-42.07	-37.19	-44.45	-45.87
log fS_2	-14.64	-16.31	-13.30	-17.31	-17.95
Mg No.	32.05	25.04	12.40	34.49	36.85

APPENDIX 11

ELECTRON MICROPROBE ANALYSIS

SERICITE

Polished thin-sections of ore samples containing sericite were selected for electron microprobe analysis. Analyses of the sericites were carried out on a Jeol 733 Superprobe in the Electron Optical Centre of the University of Adelaide, using the energy dispersive spectrometry (EDS) system. The X-Ray microanalyser is fitted with a Moran scientific control hardware and software running in an ACER 386 P.C. Polished thin-sections were carbon coated in a Denton DV-502 vacuum coating unit and analysed using a 3 nA electron beam current at an accelerating voltage of 15 keV.

From the wt.% oxide values and the hydroxyl component calculated on the basis of 22 oxygen equivalents, crystallization temperature was calculated using the seven component solid solution model for sericite developed by Hedges and Walshe (unpublished). The wt.% oxide and hydroxyl components together with the crystallization temperatures are presented overleaf.

HISTOGRAM-SERICITE FORMATION TEMPERATURE

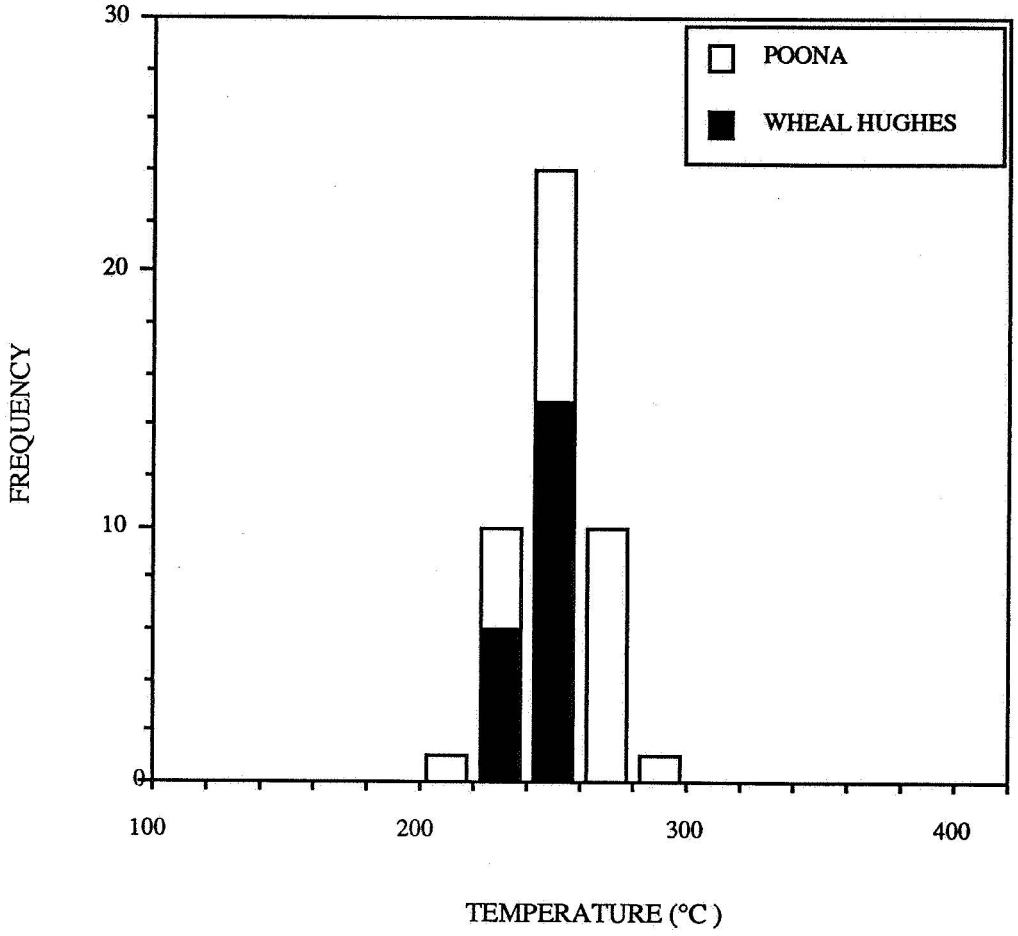

WHEAL HUGHES - SERICITE DATA

W.H.: 953-	130,1-2	130,1-3	130,3-1	130,3-2	130,3-3	130,3-4	130,4-1	130,4-2	130,5-3	130,5-4	130,5-4	130,5-5	120b,1-1	120b,1-2
SiO_2	48.68	46.56	51.74	48.16	50.85	50.80	53.53	51.78	51.11	52.43	52.10	50.80	53.11	50.87
TiO_2	0.55	0.00	0.27	0.00	0.00	0.66	0.00	0.00	0.00	0.36	0.00	0.10	0.05	0.00
Al_2O_3	21.34	18.89	22.36	20.30	20.01	24.10	19.97	19.90	23.50	19.88	22.13	20.39	24.43	23.10
FeO	6.90	2.19	3.56	6.30	6.35	4.85	6.07	6.63	4.31	7.99	4.23	6.66	3.09	3.67
MnO	0.21	0.07	0.17	0.04	0.04	0.00	0.00	0.00	0.06	0.07	0.15	0.00	0.00	0.06
MgO	4.38	4.21	4.40	4.02	3.56	4.27	4.05	4.15	3.59	5.16	4.37	4.02	3.00	2.95
CaO	0.31	0.13	0.37	0.39	0.35	0.18	0.23	0.36	0.27	0.43	0.39	0.28	0.33	0.33
Na_2O	0.00	0.00	0.00	0.00	0.00	0.00	0.00	0.00	0.00	0.00	0.00	0.00	0.00	0.00
K_2O	10.03	7.76	9.49	9.77	9.55	9.36	10.22	9.42	9.81	10.20	10.04	9.96	7.90	8.26
Cr_2O_3	0.11	0.06	0.00	0.28	0.16	0.01	0.10	0.03	0.09	0.00	0.04	0.07	0.10	0.00
TOTAL	92.50	79.88	92.35	89.26	90.88	94.24	94.16	92.26	92.75	96.50	93.45	92.28	92.01	89.25
T(°C)	256	238	250	257	248	249	250	241	258	242	256	252	236	241

W.H.: 953-	120b,1-3	120b,1-4	120b,1-5	120b,2-2	120b,2-3	120b,2-2	120b,2-3
SiO_2	52.85	51.92	52.95	53.29	52.25	53.29	52.25
TiO_2	0.16	0.00	0.09	0.19	0.00	0.19	0.00
Al_2O_3	23.85	24.05	24.53	24.75	23.92	24.75	23.92
FeO	3.45	3.15	3.07	3.50	3.03	3.50	3.03
MnO	0.15	0.13	0.02	0.06	0.11	0.06	0.11
MgO	3.09	3.15	3.07	3.34	3.30	3.34	3.30
CaO	0.45	0.31	0.44	0.27	0.34	0.27	0.34
Na_2O	0.00	0.00	0.00	0.00	0.00	0.00	0.00
K_2O	8.56	8.77	8.64	8.19	8.28	8.19	8.28
Cr_2O_3	0.00	0.16	0.08	0.00	0.07	0.00	0.07
TOTAL	92.55	91.64	92.87	93.59	91.30	93.59	91.30
T(°C)	241	246	243	237	240	237	240

POONA-SERICITE TABLES

POONA: 953-	152 ,1-2	152,2-1	152,2-2	152,2-3	152,3-2	152,3-3	152,4-1	152,4-3	152,4-5	148,1-1	148,1-1	148,1-2	148,1-2	148,1-3
SiO_2	50.31	50.90	50.28	51.44	48.97	50.73	52.33	42.70	46.87	51.32	51.16	39.11	50.93	51.47
TiO_2	0.02	0.09	0.25	0.00	0.06	0.00	0.02	0.46	0.14	0.19	0.09	0.11	0.23	0.14
Al_2O_3	27.19	25.54	26.00	26.42	25.87	26.58	26.34	22.85	25.52	27.66	28.15	22.15	27.64	27.18
FeO	4.17	3.84	4.18	3.90	2.84	2.67	2.75	9.54	6.48	1.76	1.71	1.62	2.19	2.44
MnO	0.12	0.05	0.24	0.00	0.00	0.08	0.06	0.00	0.03	0.01	0.00	0.09	0.16	0.09
MgO	2.20	2.59	2.34	2.28	2.09	2.32	2.93	2.78	2.21	2.07	2.46	2.26	2.60	3.02
CaO	0.29	0.42	0.37	0.50	0.28	0.33	0.40	0.26	0.53	0.45	0.35	0.31	0.34	0.36
Na_2O	0.09	0.00	0.00	0.00	0.00	0.00	0.00	0.00	0.00	0.00	0.09	0.00	0.00	0.00
K_2O	8.74	9.33	9.38	8.58	7.61	7.83	7.39	7.03	7.57	10.36	10.43	8.27	9.76	10.03
Cr_2O_3	0.14	0.02	0.12	0.00	0.16	0.13	0.00	0.20	0.28	0.07	0.00	0.21	0.00	0.04
TOTAL	93.27	92.78	93.14	93.11	87.89	90.67	92.21	85.82	89.63	93.89	94.43	74.12	93.85	94.77
T(°C)	252	256	258	248	244	243	235	228	240	279	279	284	266	267

POONA: 953-	148,3-4	148,3-5	148,5-4	148,5-5	148,5-5	148,5-6	114a,5-1	114a,5-2	149,3-2	149,3-3	149,4-1
SiO_2	48.60	49.13	51.29	49.54	49.54	49.93	51.03	47.63	50.10	48.85	50.94
TiO_2	0.10	0.00	0.17	0.20	0.20	0.02	0.25	0.03	0.00	0.12	0.00
Al_2O_3	32.69	32.46	27.75	26.51	26.51	25.99	25.14	24.74	32.13	32.23	33.52
FeO	1.32	1.35	1.76	1.85	1.85	2.11	4.89	6.86	1.67	1.07	1.17
MnO	0.10	0.06	0.09	0.04	0.04	0.06	0.00	0.19	0.04	0.00	0.00
MgO	0.25	0.04	2.45	2.28	2.28	2.55	3.38	3.96	0.64	0.62	0.48
CaO	0.54	0.37	0.41	0.36	0.36	0.24	0.28	0.41	0.33	0.29	0.39
Na_2O	0.00	0.00	0.00	0.00	0.00	0.00	0.00	0.00	0.00	0.00	0.00
K_2O	9.02	8.84	8.39	9.94	9.94	9.64	7.59	5.99	8.72	8.29	8.60
Cr_2O_3	0.00	0.07	0.01	0.06	0.06	0.14	0.06	0.07	0.01	0.26	0.10
TOTAL	92.61	92.31	92.31	90.78	90.78	90.68	92.62	89.87	93.64	91.71	95.21
T(°C)	270	267	249	276	276	268	234	220	262	260	260

APPENDIX 12

ELECTRON MICROPROBE ANALYSIS

TOURMALINE

Polished thin-sections of ore samples containing tourmaline were selected for electron microprobe analysis. Analyses of the tourmalines were carried out on a Jeol 733 Superprobe in the Electron Optical Centre of the University of Adelaide, using the energy dispersive spectrometry (EDS) system. The X-Ray microanalyser is fitted with a Moran scientific control hardware and software running in an ACER 386 P.C. Polished thin-sections were carbon coated in a Denton DV-502 vacuum coating unit and analysed using a 3 nA electron beam current at an accelerating voltage of 15 keV.

The wt% oxide values, hydroxyl/structural formulae calculated on the basis of 20 oxygen equivalents were recorded together with the calculated $Na_2O/(Na_2O+CaO+K_2O)$ and $FeO/(FeO+MgO+MnO)$ ratios, to evaluate the compositional differences in the probe analyses of dravite-schorl tourmaline (Ethier and Campbell, 1977). Ratios and compositional data are presented overleaf.

TOURMALINE COMPOSITIONS

	POONA: DDH 240; 91.95m			WHEAL HUGHES: DDH-251; 63.45m			WHEAL HUGHES: 20-17 level					
	953-149,2-1	953-149,4-2	953-149,2-2	953-132,4-5	953-132,3-1	953-132,6-3	953-011,1-1	953-011,2-1	953-011,2-2	953-120b,2-1	953-120b,3-1	953-120b,3-2
SiO_2	34.16	35.46	35.90	34.46	34.51	34.58	35.25	34.75	35.44	34.95	34.31	35.15
TiO_2	0.78	0.52	0.37	0.29	0.97	0.86	0.89	0.53	0.74	0.92	0.75	0.68
Al_2O_3	26.63	28.87	28.72	26.38	27.66	26.21	26.82	28.47	26.33	26.16	26.11	27.35
FeO	13.42	12.09	13.51	12.70	14.00	13.44	13.87	12.34	13.65	13.18	15.13	14.18
MnO	0.15	0.13	0.08	0.12	0.00	0.19	0.13	0.00	0.00	0.10	0.06	0.00
MgO	6.45	5.41	6.12	7.26	5.46	6.88	7.05	6.51	6.47	6.20	5.89	5.83
CaO	1.27	0.92	0.94	1.96	0.77	1.31	1.54	1.22	1.68	1.24	1.36	1.08
Na_2O	1.84	2.03	2.80	1.75	2.41	1.82	1.95	1.87	1.61	1.97	1.84	2.26
K_2O	0.00	0.00	0.08	0.14	0.04	0.01	0.00	0.00	0.00	0.00	0.04	0.00
Cr_2O_3	0.06	0.00	0.12	0.16	0.07	0.00	0.00	0.31	0.06	0.13	0.00	0.18
TOTAL	84.76	85.44	88.63	85.21	85.90	85.29	87.50	85.99	85.97	84.84	85.49	86.70
$Na2O/(Na_2O+K_2O+Ca_2O)$	0.59	0.69	0.73	0.46	0.75	0.58	0.56	0.60	0.49	0.61	0.57	0.68
FeO/(FeO+MnO+MgO)	0.67	0.69	0.69	0.63	0.72	0.66	0.66	0.65	0.68	0.68	0.72	0.71
No. of ions (20 0_2 euivalents)												
Si	4.86	4.93	4.87	4.87	4.85	4.88	4.86	4.83	4.96	4.95	4.88	4.90
Ti	0.08	0.05	0.04	0.03	0.10	0.09	0.09	0.05	0.08	0.10	0.08	0.07
Al	4.46	4.73	4.59	4.40	4.58	4.36	4.36	4.67	4.34	4.37	4.38	4.49
Fe	1.60	1.40	1.53	1.50	1.64	1.59	1.60	1.44	1.60	1.56	1.80	1.65
Mn	0.02	0.02	0.01	0.01	0.00	0.02	0.02	0.00	0.00	0.01	0.01	0.00
Mg	1.37	1.12	1.24	1.53	1.14	1.45	.45	1.35	1.35	1.31	1.25	1.21
Ca	0.19	0.14	0.14	0.30	0.12	0.20	0.23	0.18	0.25	0.19	0.21	0.16
Na	0.51	0.55	0.74	0.48	0.66	0.50	0.52	0.50	0.44	0.54	0.51	0.61
K	0.00	0.00	0.01	0.02	0.01	0.00	0.00	0.00	0.00	0.00	0.01	0.00
Cr	0.00	0.00	0.00	0.00	0.00	0.00	0.00	0.00	0.00	0.00	0.00	0.00

TOURMALINE COMPOSITIONS

	POONA: DDH 233; 147.80m			WHEAL HUGHES: 20-17 level							
	953-145,2-5	953-145,2-2	953-145,2-6	953-013,2-2	953-013,6-1	953-013,6-2	953-012,1-3	953-012,2-1	953-012,3-1	953-017,2-2	953-017,4-1
SiO_2	34.52	35.15	35.11	35.26	34.71	35.08	34.05	34.69	34.44	34.88	34.54
TiO_2	1.02	0.59	0.87	0.67	1.01	1.03	0.97	0.45	0.85	1.15	0.34
Al_2O_3	27.15	28.51	27.30	26.12	26.03	26.97	27.73	26.44	25.22	25.50	27.86
FeO	13.18	12.25	13.54	13.24	13.29	13.22	12.44	11.93	14.98	13.74	11.71
MnO	0.02	0.20	0.00	0.06	0.00	0.04	0.12	0.02	0.01	0.00	0.05
MgO	5.94	6.38	6.54	6.87	7.02	6.47	6.97	6.96	6.16	7.19	6.96
CaO	1.30	1.18	1.43	1.54	1.54	1.20	1.19	1.48	1.59	1.66	1.35
Na_2O	1.93	1.94	1.79	1.95	2.14	2.09	2.48	1.16	1.71	1.91	2.08
K_2O	0.00	0.00	0.10	0.09	0.00	0.00	0.03	0.00	0.09	0.00	0.00
Cr_2O_3	0.00	0.14	0.05	0.00	0.00	0.12	0.00	0.00	0.25	0.25	0.05
TOTAL	85.05	86.34	86.74	85.79	85.73	86.21	85.98	83.13	85.31	86.27	84.94
$Na_2O/(Na_2O+K_2O+Ca_2O)$	0.60	0.62	0.54	0.54	0.58	0.64	0.67	0.44	0.50	0.54	0.61
$FeO/(FeO+MnO+MgO)$	0.69	0.65	0.67	0.66	0.65	0.67	0.64	0.63	0.71	0.66	0.63
No. of ions (20 O_2 euivalents)											
Si	4.87	4.86	4.87	4.94	4.88	4.89	4.76	4.96	4.92	4.90	4.85
Ti	0.11	0.06	0.09	0.07	0.11	0.11	0.10	0.05	0.09	0.12	0.04
Al	4.52	4.65	4.46	4.32	4.31	4.43	4.57	4.46	4.25	4.22	4.61
Fe	1.56	1.42	1.57	1.55	1.56	1.54	1.45	1.43	1.79	1.61	1.37
Mn	0.00	0.02	0.00	0.01	0.00	0.00	0.01	0.00	0.00	0.00	0.01
Mg	1.25	1.31	1.35	1.44	1.47	1.34	1.45	1.48	1.31	1.51	1.46
Ca	0.20	0.17	0.21	0.23	0.23	0.18	0.18	0.23	0.24	0.25	0.20
Na	0.53	0.52	0.48	0.53	0.58	0.57	0.67	0.32	0.47	0.52	0.57
K	0.00	0.00	0.02	0.02	0.00	0.00	0.01	0.00	0.02	0.00	0.00
Cr	0.00	0.00	0.00	0.00	0.00	0.00	0.00	0.00	0.00	0.00	0.00

TOURMALINE COMPOSITIONS

	WHEAL HUGHES: 20-17 level				POONA: DDH 240; 92.90m			POONA: underground
	953-017,4-2	953-010,3-2	953-010,1-2	953-010,1-3	953-148,3-3	953-148,3-5	953-148,3-6	953-107,5-1
SiO_2	34.89	34.32	34.66	34.73	34.76	34.95	35.50	35.45
TiO_2	1.08	0.98	0.60	1.38	0.99	0.93	0.59	0.76
Al_2O_3	26.59	25.41	26.75	25.98	26.95	26.50	29.05	26.67
FeO	13.06	15.40	14.04	14.54	14.99	15.20	12.04	11.36
MnO	0.00	0.00	0.00	0.13	0.00	0.25	0.14	0.15
MgO	7.33	5.78	6.15	6.67	5.19	6.10	5.99	8.22
CaO	1.56	1.50	1.20	1.53	1.25	1.54	0.95	1.69
Na_2O	2.10	2.16	2.21	2.09	2.44	1.90	2.65	1.74
K_2O	0.12	0.00	0.05	0.06	0.04	0.00	0.03	0.00
Cr_2O_3	0.07	0.24	0.14	0.00	0.00	0.00	0.11	0.13
TOTAL	86.81	85.79	85.80	87.11	86.60	87.37	87.04	86.17
$Na_2O/(Na_2O+K_2O+Ca_2O)$	0.56	0.59	0.64	0.57	0.65	0.55	0.73	0.51
$FeO/(FeO+MnO+MgO)$	0.64	0.73	0.70	0.68	0.74	0.71	0.66	0.58
No. of ions (20 O_2 euivalents)								
Si	4.84	4.89	4.89	4.84	4.87	4.87	4.86	4.90
Ti	0.11	0.11	0.06	0.14	0.10	0.10	0.06	0.08
Al	4.35	4.27	4.44	4.27	4.45	4.35	4.69	4.35
Fe	1.52	1.84	1.65	1.70	1.76	1.77	1.38	1.31
Mn	0.00	0.00	0.00	0.02	0.00	0.03	0.02	0.02
Mg	1.52	1.23	1.29	1.39	1.08	1.27	1.22	1.70
Ca	0.23	0.23	0.18	0.23	0.19	0.23	0.14	0.25
Na	0.57	0.60	0.60	0.57	0.66	0.51	0.70	0.47
K	0.02	0.00	0.01	0.01	0.01	0.00	0.01	0.00
Cr	0.00	0.00	0.00	0.00	0.00	0.00	0.00	0.00

APPENDIX 13

THERMODYNAMIC EQUATIONS

LOG EQUILIBRIUM CONSTANTS

Reaction	Log K (275°C)	Ref.
$2H_2S + O_2 = S_2 + 2H_2O$	-28.64	3
$HSO_4^- = H^+ + SO_4^{2-}$	-5.68	1
$H_2S^0 = HS^- + H^+$	-7.71	1
$HS^- + 2O_2 = SO_4^{2-} + H^+$	59.6	1
$H_2S^0 + 2O_2 = SO_4^{2-} + 2H^+$	51.94	1
$H_2S^0 + 2O_2 = HSO_4^- + H^+$	57.61	1
$2FeS_2 + 2H_2O = 2FeS + 2HS^- + 2H^+ + O_2$	-57.53	1
$2FeS_2 + 2H_2O = 2FeS + 2H_2S^0 + O_2$	-42.12	1
$6FeS + 6H_2O + O_2 = 2Fe_3O_4 + 6HS^- + 6H^+$	-26.53	1
$6FeS + 6H_2O + O_2 = 2Fe_3O_4 + 6H_2S^0$	-19.7	1
$6FeS + 4O_2 = 2Fe_3O_4 + 3S_2$	105.61	5
$3FeS_2 + 6H_20 = Fe_3O_4 + 6HS^- + 6H^+ + O_2$	-99.56	1
$3FeS_2 + 6H_2O = Fe_3O_4 + 6H_2S^0 + O_2$	-53.33	1
$3FeS_2 + 6H_2O + 11O_2 = Fe_3O_4 + 6SO_4^{2-} + 12H^+$	258.28	1
$3FeS_2 + 2O_2 = Fe_3O_4 + 3S_2$	32.58	5
$4Fe_3O_4 + O_2 = 6Fe_2O_3$	33.18	1
$4FeS_2 + 8H_2O = 2Fe_2O_3 + 8H_2S^0 + O_2$	-60.05	1
$4FeS_2 + 8H_2O + 15O_2 = 2Fe_2O_3 + 8SO_4^{2-} + 16H^+$	355.43	1
$4FeS_2 + 8H_2O + 15O_2 = 2Fe_2O_3 + 8HSO_4^{2-} + 8H^+$	400.83	1
$4FeS_2 + 3O_2 = 2Fe_2O_3 + 4S_2$	54.49	5
$5CuFeS_2 + 2H_2S + O_2 = Cu_5FeS_4 + 4FeS_2 + 2H_2O$	-30.57	2
$5CuFeS_2 + 2H_2O = Cu_5FeS_4 + 2H_2S + O_2 + 4FeS$	-39.60	2
$2FeS + S_2 = 2FeS_2$	-13.49	5
$3KAlSi_3O8 + 2H^+ = KAl_3Si_3O_{16}(OH)_2 + 6SiO_2 + 2K^+$		4
$3Al_2Si_2O_5(OH)_4 + 2K^+ = 2KAl_3Si_3O_{10}(OH)_2 + 3H_2O + 2H^+$		4

1. Huston and Large (1989)
2. Ohmoto et al. (1983)
3. Barton (1984)
4. Pisutha-Arnond and Ohmoto (1983)
5. Calculated from Barton (1984) and Huston and Large (1989)

WHEAL HUGHES-OPEN PIT PLAN

E 1000 E 1050 E 1100 E 1150 E 1200 E 1250 E 1300

N 8550 N 8500 N 8450 N 8400 N 8350 N 8300

DDH 237 DDH 249 DDH 250 DDH 251 DDH 252

A A' B B'

WHEAL HUGHES I S.W. DEPOSIT

LYNTONS N.E. DEPOSIT

SCALE 1:500

0 50

meters

R.L. 14.7-15.9

01.07/91

Drafted by M. Hafer

LOCALITY MAPS

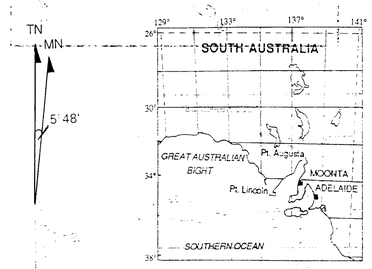

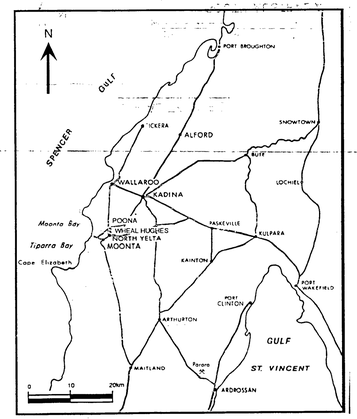

LEGEND

- Calcrete+Soils
- Clays
- Sandstone / Conglomerate
- highly altered M.P.
- Moonta Porphyry (M.P.)
- Cp+Qtz+Tourm±Kaolin
- Cp+Py+Tourm+Qtz±Kaolin
- Cc+Qtz+Tourm+Kaolin
- Cov+Cp+Tourm+Qtz+Kaolin
- Tourm+minor Qtz
- Qtz+minor Tourm
- Limonite
- Pervasive Kaolin flooding

- — ? — Inferred Fault
- q Quartz Vein
- p Pegmatite Vein
- Joint
- Vertical Joint
- ML 35 Mineral Lineation
- 50 Slickenside Lineation
- DDH 2 Diamond Drill Hole
- Antiform
- Synform
- 17.5 R.L.
- B-B' Cross Section

WHEAL HUGHES-OPEN PIT PLAN

E 1000 E 1050 E 1100 E 1150 E 1200 E 1250 E 1300

N 8550 N 8500 N 8450 N 8400 N 8350 N 8300

DDH 237 DDH 249 DDH 250 DDH 251 DDH 252

A A' B B'

LEIGHTONS W.F.I DEPOSIT

WHEAL HUGHES (S.W) DEPOSIT

SCALE 1:500

0 50

meters

R.L. 15.7-19.7

02/05/91

Drafted by M. Hafer

LOCALITY MAPS

TN MN 5° 48'

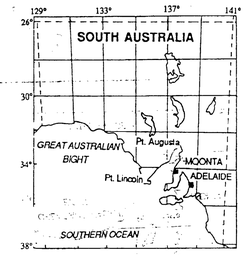

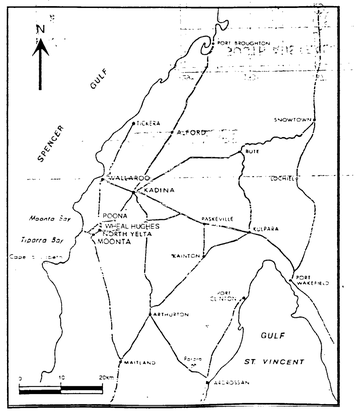

LEGEND

- Calcrete-Soils
- Clays
- Sandstone / Conglomerate
- highly altered M.P.
- Moonta Porphyry (M.P.)
- Cp-Qtz-Tourm-Kaolin
- Cp-Py-Tourm-Qtz-Kaolin
- Cc-Qtz-Tourm-Kaolin
- Cov-Cp-Tourm-Qtz-Kaolin
- Tourm-minor Qtz
- Qtz-minor Tourm
- Limonite
- Pervasive Kaolin flooding

- Inferred fault
- Quartz-vein
- Pegmatite-vein
- Joint
- Vertical Joint
- Mineral lineations
- Slickenside lineation
- Diamond Drill Hole
- Antiform
- Synform
- R.L.
- Cross Section